COMPLEX PULSE FORMING TECHNIQUE USING AM DETECTOR TYPE CIRCUITRY AND THE APPLICATION OF CDMA TO RFID FOR THE SIMULTANEOUS READING OF MULTIPLE TAGS

by

Joshua Y. Maina

B. ENG., University of Maiduguri, Nigeria, 1992

MS, University of Pittsburgh, 1999

Submitted to the Graduate Faculty of

School of Engineering in partial fulfillment

of the requirements for the degree of

Doctor of Philosophy

University of Pittsburgh

2005

UNVERSITY OF PITTSBURGH

SCHOOL OF ENGINEERING

This dissertation was presented

by

Joshua Y. Maina

It was defended on

December 13, 2004

and approved by

James T. Cain, PhD, Professor, Electrical and Computer Engineering

Ronald G. Hoelzeman, PhD, Associate Professor, Electrical and Computer Engineering

Raymond R. Hoare, PhD, Assistant Professor, Electrical and Computer Engineering

Michael R. Lovell, PhD, Associate Professor, Mechanical Engineering

Ming-En Wang, PhD, Assistant Professor, Industrial Engineering

Dissertation Director: Marlin H. Mickle, PhD, Nickolas A. DeCecco Professor, Electrical and Computer Engineering

COMPLEX PULSE FORMING TEACHNIQUE USING AM DETECTOR TYPE CIRCUITRY AND THE APPLICATION OF CDMA TO RFID FOR THE SIMULTANEOUS READING OF MULTIPLE TAGS

Joshua Y. Maina, PhD

University of Pittsburgh, 2005

A novel complex ultra wideband RF pulse forming technique has been developed in this research, using the coefficients derived from discrete Fourier transform of a *virtual pulse train*. Incorporated in this technique is a multiple frequency communication system designed such that transmitter receiver proximity and the fading effect of the individual frequencies make part of a corresponding modulation technique. A code division multiple access (CDMA) application to RFID to greatly reduce read time, while at the same time eliminating inter tag interference, has been investigated with the analysis of a typical cart aisle scenario. With the current rate of growth of inventory world wide there is a tremendous need for a more efficient method of data gathering, data storage, and data retrieval. In this dissertation, the application of the CDMA RFID technology has been analyzed to demonstrate the potentials of integrating the RFID technology to the EPC global numbering system.

DESCRIPTORS

CDMA	DFT
Coefficients	Fading Effect
Correlations	Frequency

Hamming Distance | RFID
Modulation | Transmitter
Receiver | Ultra Wideband
Rectangular Pulse | Virtual Pulse

TABLE OF CONTENTS

LIST OF TABLES

LIST OF FIGURES

ACKNOWLEDGEMENT

I thank the Lord almighty for walking me through this phase of my life which I believe with all the experiences and training undertaken will play a vital roll in the rest of my ensuing endeavor.

I owe a sincere gratitude and appreciation to my advisor Professor Marlin H. Mickle for his honest guidance and expertise advice throughout my graduate program in University of Pittsburgh, without which this dissertation would not have been accomplished. I thank all the faculties who functioned as members of my dissertation committee their input has been of help from the proposal to the completion.

The support from my wife Ladi Y. Maina and children Hyalladjira J. Maina and Galipu J. Maina has been outstanding and I will forever thank them for their sacrifices, and this dissertation is dedicated to them. I appreciate the support from my parents and siblings and thank them for their prayers. I wish to also thank all my friends and other mentors who have influenced me in one way or the other in order for me to get to this point.

1.0 INTRODUCTION

Radio Frequency (RF) has been the primary means of wireless communication in almost all works of human endeavor. Because of its vast application, the RF spectrum has been segregated into bands and channels occupying specific bandwidths with tolerances strictly enforced by the Federal Communications Commission (FCC) and other similar governing bodies around the world.

Currently, the RF spectrum appears to be near exhaustion with respect to channel allocations due to lack of bandwidth within the limits of the RF spectrum. The reuse of bandwidth has recently been applied as a means of overcoming this problem. Multiple frequency communication techniques such as Ultra Wide Band (UWB) and Spread Spectrum (SS) are examples of existing methods applied in a number of currently suitable cases. These techniques have not been found to adequately combat noise because of the inherently low signal power, therefore making detection very difficult. Transmitter power providing signals above the white noise level results in interference with existing channels within the particular bandwidth allocation. Modulation techniques typically employed in UWB technology are either pulse position modulation (PPM) or a derivative of PPM, which does not help in resolving the interference problem though it has other attractive advantages.

While there might be a consensus on the advantages of multiple frequency (wide band) communication techniques, no general agreement exists as to how applications can best take advantage of current multiple frequency methods of communication.

The following topics are chosen for inclusion in this section because they help elaborate on the motivation for this research and lay a proper foundation for the analysis of multiple frequency communication in this dissertation.

1.1 BACKGROUND

Multiple frequency communication was originally proposed for clandestine operations in the military to avoid detection and location by direction finders and to hide the fact that communication was taking place. One result of multiple frequency communication is a spread spectrum technique, which was initially not thought to be possible to apply in wireless telephony because of the many complications in implementing an actual system. This assertion was proven wrong when Qualcom developed Code Division Multiple Access (CDMA), which is a type of SS code for wireless telephony. The main characteristics of CDMA that are of interest to most communications engineers are simultaneous multiple access, interference rejection, security, and robustness.

The application of CDMA in non-telephony systems might not require all the sophistication of the link protocol as in the wireless telephone networks due to learning curve and regulatory aspects. This opens numerous areas of potential application of CDMA as a solution to the problem of simultaneous RFID tag reading multiple access, interference, and security. Multiple geographically dispersed devices communicating simultaneously can connect to a single proper receiver without the possibility of interference from each other. Channel capacity is enhanced by the wide bandwidth occupied by the spread spectrum in CDMA.

1.2 ULTRA WIDEBAND (UWB)

The idea of studying UWB technology is important to this dissertation because one of the contributions in this research is the proposition of *RF pulse formation* using multiple frequency technique, which incorporates a modulation technique involving energy levels of the individual frequencies. UWB provides a good platform for a technology whose low energy level makes it extremely difficult to detect.

Ultra-Wide Band (UWB) is a signal defined as having a fractional bandwidth η larger than 25% or

$$\eta = 2 * \frac{f_H - f_L}{f_H + f_L} \tag{1.1}$$

where, f_H and f_L are the highest and lowest frequencies of interest [25]*. UWB signals are produced by pulse emissions, in which a wide RF spectral bandwidth is related to a specially formed narrow pulse. Base band (repetition rate) pulses are used to encode information for transmission without a specific carrier frequency. Current UWB technology for existing applications range in center frequency from 20MHz to 60GHz with bandwidths from 5MHz to 30GHz.

* Parenthetical references refer to the bibliography

In 1942, Louis De Rosa filed the first UWB patent [26]. The earliest applications of UWB technology are mostly high-powered military radar. The commercial usage of UWB technology was employed in areas such as ground penetration radar (GPR) and for surface investigations for detection of buried objects and geo-technical studies of underground structures. UWB technologies were also used in radar level measurement systems (RLMS) where highly accurate measurements were required in difficult environments.

Gerald F. Ross filed the first patent for UWB Communications in 1973 [27]. Many technical publications and patents have been issued since then. The special attributes of UWB are attracting interest for consumer and commercial implementations of UWB for both ranging and communication. UWB radar devices will be found in; (1) automobiles for occupant sensing or collision warning, (2) industrial process operator proximity safety controls, (3) for inspection of walls and floors, and (4) for finding people during rescue and law enforcement activities. UWB technology offers lower power, multimedia-capable wireless connections within homes, schools, libraries, medical facilities and information dependent businesses.

1.2.1 System Characteristics

Unlike continuous wave signals, UWB signal is said to be immune from the effect of multi path fading because of the ratio of the pulse width over the pulse repetition interval (PRI). A multi path pulse interferes if it overlaps with the arrival of the pulse of interest. If the length of path traveled by a multi path pulse is between 0.3 meters (pulse width times the speed of light) and 300 meters (PRI times the speed of light) longer than the path of the pulse of interest, then the multi path pulse will not affect reception [6].

In an impulse system very particular and rare conditions must persist for multipath effect to take place:

The length of path traveled by the multipath pulse must be less than the pulse width times the speed of light. For example a one nanosecond pulse, that equals 0.3 meters or about 1 foot, i.e., [1 ns] * [300,000,000 meters/seconds].

The multipath pulse that travels a distance that is equal to the interval of time between pulses times the speed of light might interfere times an integral number with the next pulse. For a 1 megapulse per second system that would be equal to traveling an extra 300, 600, 900, etc meters. However, because each individual pulse is subject to the pseudo-random dither, these pulses are decorrelated.

1.2.2 Gaussian Monocycle

Considered as the most basic element of UWB radio technology is the practical implementation of a Gaussian monocycle. The monocycle can be realized both in the frequency and time domains. The monocycle is a wide bandwidth signal, with the center frequency and the bandwidth completely dependent on the monocycle pulse width. In the time domain, the Gaussian monocycle is mathematically similar to the first derivative of the Gaussian function [6]. It has the form:

$$V(t) = \frac{t}{\tau} e^{-\left(\frac{t}{\tau}\right)^2} \tag{1.2}$$

τ is a time decay constant that determines the monocycle's duration, and t is time. In the frequency domain, a Gaussian monocycle's spectrum is of the form:

$$V(f) = -jf\tau^2 e^{-f^2\tau^2} \tag{1.3}$$

The center frequency is then proportional to the inverse of the pulse duration, i.e.

$$F_c \propto \frac{1}{\tau} \tag{1.4}$$

The center frequency of this particular monocycle is the reciprocal of the monocycle's duration, and the bandwidth is 116% of the monocycle center frequency. Thus, for the 0.5ns monocycle, the center frequency is 2GHz and the half power bandwidth is approximately 2GHz.

1.2.3 Pulse Position Modulation (PPM)

Pulse position modulation varies the precise timing of transmission of the monocycle about the nominal position for a constant repetition rate. As an example, a classical PPM system transmits a monocycle nominally every 100ns ($100*10^{-9}$ seconds). During the modulation process in such a system, a "0" digital bit can be represented by a pulse transmitted 100ps ($100*10^{-12}$ seconds) earlier and a "1" digital bit by a pulse transmitted 100ps later than the nominal pulse position. The pulse position modulation distributes the RF energy somewhat uniformly across the band. The spectrum of the signal is smoothed by modulation, thus making the system more difficult to detect. Below is an example of time modulated ultra wideband signal courtesy of Time Domain Inc.

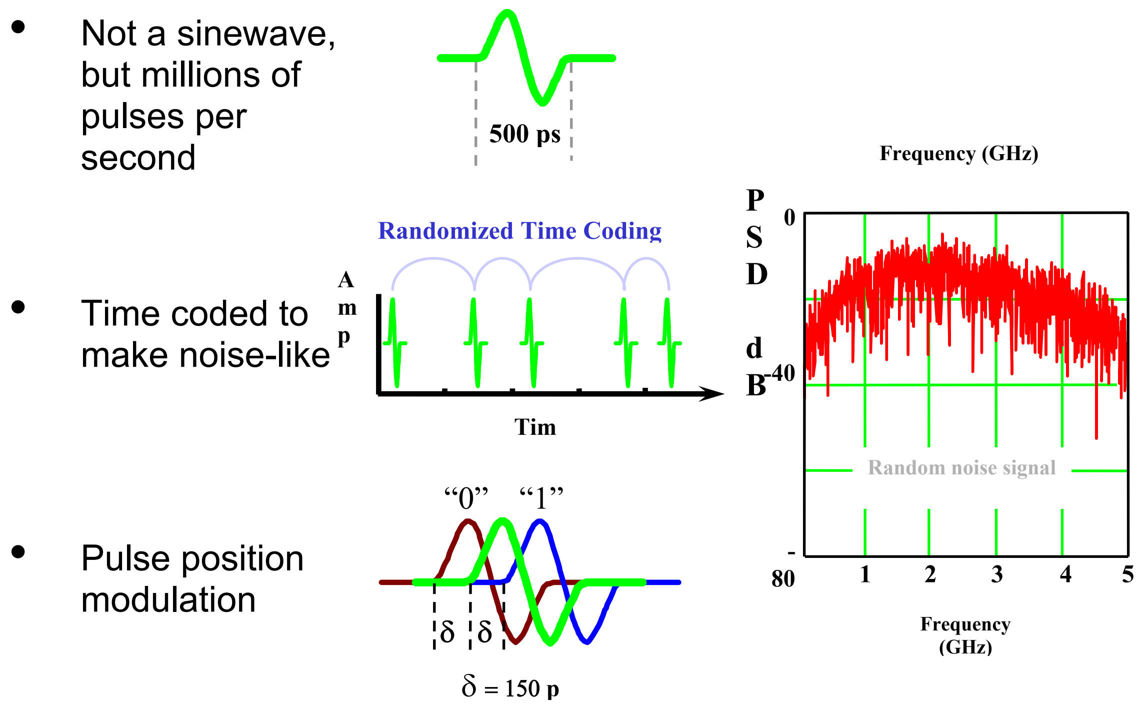

Figure 1.1: Pulse Position Modulation

1.2.4 Multiple Access Technique

One of the benefits of UWB is the ability to use multiple carrier transmitters simultaneously without interference among the various signals. A simple means for spreading the spectrum of these ultra-wide bandwidth low-duty-cycle pulse trains is time hopping with modulation accomplished by additional pulse position modulation at the rate of many pulses per data symbol. A typical time-hopping format employed by an impulse radio in which the k^{th} transmitter's output signal is

$$S_{tr}^{(k)}(t^{(k)}) = \sum_{j=\infty}^{\infty} W_{tr}(t^{(k)} - jT_f - C_j^{(k)}T_c - \partial d_{[J/Ns]}^{(k)}) \qquad (1.5)$$

where $t^{(k)}$ is the K^{th} transmitter clock time and T_f is the pulse repetition time [28]. The transmitted pulse $\omega_{tr}(t)$ is the monocycle as seen in the earlier section of this discussion.

Each user *(K)* is assigned distinctive time shift pattern $\{C_j^{(k)}\}$ called *time-hopping sequence*. This provides an additional time shift of $C_j^k\ T_c$ seconds to the j[th] monocycle in the pulse train where T_c is the duration of the addressable time delay bins. For a fixed T_f, the symbol rate R_s determines the number N_s of monocycles that are modulated a given binary symbol via $R = \frac{1}{N_s T_f} \sec^{-1}$.

The modulation index ∂ can be chosen to optimize performance. The modulation index ∂ specifies the fractional variation of the modulation function about its mean value. When this variation is expressed as a percentage, it is called the *percentage modulation*, and is equal to *m*100%.*

For the purposes of performance prediction the data sequence $\{d_j^{(k)}\}_{j=-\infty}^{\infty}$ is modeled as wide-sense stationary random process composed of equally likely occurring symbols.

1.3 CONCERNS OF UWB

While the numerous excellent characteristics of UWB technology are clear and the large number of possible applications along with the problems it might solve is unquestionable, the technology is not without its dark side which makes research and deployment of the technology difficult at the current state. The following are some of the bottlenecks associated with UWB technology:

- The formation of the unique pulse shape which is related to an ultra wide frequency range has been an issue to almost all UWB promoters.

- Because UWB occupies an extremely wide spectral bandwidth, it overlaps a number currently licensed channels, and this raises great concerns from the license owners for fear of interference.
- The very low power level of UWB signals makes reception difficult and to combat this problem expensive receivers are needed.
- Currently the FCC has not finalized the specific rules and guidelines for the commercial deployment of UWB technology.

In this research, the Industrial Scientific and Medical (ISM) frequencies will be used to introduce an innovative ultra wide band pulse forming technique. The ISM is chosen simply because it has been made available by the FCC for academic and research purposes. Hence, the concept in this dissertation can be analyzed without the additional burden of FCC rules and interference problems.

2.0 PROBLEM STATEMENT

2.1 GENERAL STATEMENT OF THE PROBLEM

Multiple frequency techniques such as spread spectrum and ultra wideband have been known to provide solutions to problems such as intentional signal jamming, inter channel interference, multi-path interference, and the limited bandwidth problem. The methods of forming these techniques is yet to be exhaustively researched, particularly in ultra wideband technology where the shape of the pulses used for communication poses certain difficulties for precise formation. The modulation techniques used in UWB technology, which is either pulse position modulation (PPM) or a derivative of PPM, does not make the implementation of multiple access easy because of the issues of synchronizing all the transmitters to the receivers.

The great advantage of SS and UWB technology has generated great interest in a number of areas of application to solve existing problems. One of these areas is the reading of multiple RFID tags where current technologies are plagued with multiple reads required to be carried out sequentially in order to retrieve information from multiple tags slowing down the reading process and increasing the complexity of the tag logic or processor. Most attempts to implement simultaneous reads meet with problems of collisions, interference, and performance degradation.
In this research, a technique related to RF pulse formation will be implemented using the coefficients from the discrete Fourier transform (DFT) of a *virtual pulse*. The magnitudes of

these coefficients are varied by changing the width of the *virtual pulse* hence, making it possible to modulate the pulse width. The fading effect of RF signals will also be used as a consideration of the modulation process. By computing the magnitude of the multiple frequencies in the RF pulse formation at the transmitter end such that at the receiver end a different magnitude is received as the correct value only if the receiver is at the proper distance from the transmitter. Research is conducted on the application of CDMA in reading RFID tags, in particular the simultaneous reading of multiple tags without the problems of collision and interference.

2.2 SPECIFIC STATEMENT OF THE PROBLEM

Specifically, this research will:

(a) Evaluate the potential use of coefficients from the discrete Fourier transform of rectangular pulse train representing RFID data to individually modulate the magnitude of multiple carrier frequencies, say for example f_1, f_2, f_3, f_4, and f_5. The collective energy level patterns of received signals can represent a "1" or "0". An analysis will be performed of Fourier coefficient magnitude and the power reduction versus distance to determine the number of coefficients (frequencies) required to insure a Hamming distance of 3 between "0" and "1" with some probability that any given coefficient (frequency) will be over or under range by >10%.

(b) Based on the results of (a), the distances between transmitter and receiver will be analyzed for setting the power level of all the transmitted frequencies to cumulatively give a specified range of power value (valid levels as per (a) above) at the correct distance. Signals received before and after the correct range will be invalid due to incorrect received power levels. The analysis will be to determine the sensitivity involved to insure proper reading of tags in one shopping cart aisle without getting a valid read from another cart in a different aisle. Typical aisle distances will be analyzed.

(c) Based on (b), provide a hardware demonstration of the use of signal power levels received at the reader to receive the correct information only at the proper distance from the transmitter. This is achieved by adjusting the output level of the tags such that the fading of the signal provides a method of security and coding. Several transmitters (ISM band) will be powered to show the ability to correctly read the specific codes.

(d) Perform research, analysis and design of the multiple access CDMA technique numbering alternatives for the RFID tag standard EPC global.

(e) Provide a hardware demonstration of the design of (d) for the power level determination using CDMA. This will use commercially off-the-shelf components to transmit multiple signals and using the "Received Signal Strength Indicator (RSSI)" to display the cumulative energy level of the transmitted signals (For demonstration purposes only).

(f) Evaluate the possibility of using one particular alternative coding scheme for multiple simultaneous tag transmissions. Specifically, the technique of "Random Multiple Access Communications without Feedback" will be evaluated.

3.0 COMPLEX PULSE FORMATION

3.1 INTRODUCTION

Ultra Wide Band (UWB) radio signals, sometimes referred to as baseband, impulse, or carrierless radio, incorporates the generation and transmission of an ultra short impulse of radio frequency energy with a characteristic spectrum extending across a very wide range of frequencies. A particular implementation by Time Domain, Inc., [6] extends the bandwidth in excess of 3GHz. The inherent qualities such as low power spectral densities (PSDs), diversity in frequency and immunity to multipath effects has spawned a great deal of interest in this technology for short range high speed indoor radio communication services in addition to other applications such as with GPS [25]. In UWB a wide frequency spectrum extends over a range 10 to 100 times the intelligent bandwidth being transmitted, and maintaining the energy of any single frequency making up the spectrum at a very low level, typically below normal noise levels. While it tends to be obvious that this type of transmission would be essentially non-interfering with other services, implementation has been very difficult so far. The difficulties are largely in the area of generating the extremely short pulses within ultra wide bandwidth, and the formulation of efficient and effective modulation techniques for communications purposes.

In this research a novel technique is proposed, which uses conceptually similar multiple frequency techniques as in UWB and the spread spectrum technique for digital communications. For the purposes of an example, the multiple frequencies are derived from the discrete Fourier transform of rectangular pulses representing information to be communicated in binary form. Each of the frequencies represents an element of a bit being transmitted, and it is the collection of magnitudes of the various energies collected that determine the value of a bit as a "1" or "0".

3.2 FREQUENCY COEFFICIENTS

In this section of the dissertation, the discrete Fourier transform (DFT) of a rectangular pulse train is taken to foster the analysis of the multiple frequencies and the coefficients obtained from the result of the DFT. The value of the frequencies and the magnitude of the coefficients are dependent on the width of the pulse train used in the transform. Appendix A provides an example of the derivation of the DFT of a rectangular pulse train.

The pulse train can now be used to encode information by altering the duty cycle, τ, to represent either a "1" or a "0". Because the coefficient X_K is proportional to τ, different values of X_K can then be used to modulate the amplitude of any available RF carrier. For digital information, two values of τ can be used to achieve X_0 and X_1 for binary "0" and "1" respectively. Figure 3.2 shows the DFT of a rectangular pulse at different sampling frequencies and different values of τ.

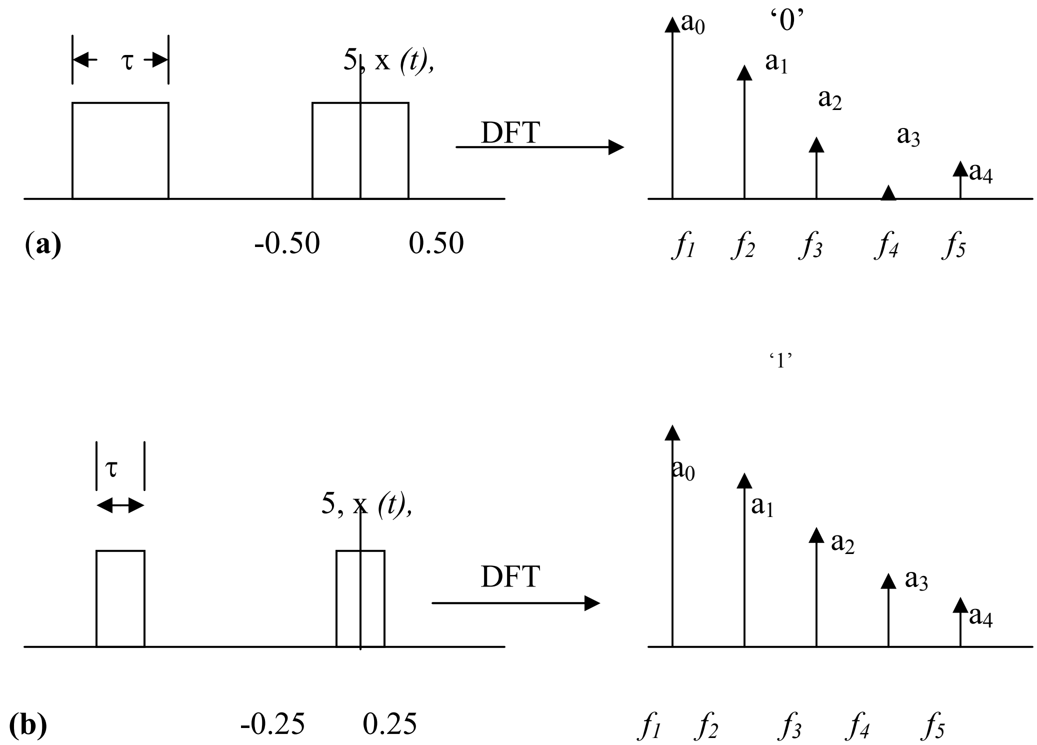

Figure 3.2: Illustration of Reciprocal Spreading Effect

If the pulse duration τ increases or decreases while the period T remains fixed, then the amplitude envelope shrinks or expands relative to the line spacing. Hence, as the pulse gets shorter, the spectrum spreads out and higher frequency components become increasingly important as shown in Figure 3.2.

3.3 FUNDAMENTAL FREQUENCY

When the Fourier Transform is applied on N samples, it is assumed that the signal is periodic over N samples. Therefore, the fundamental frequency of the signal is equal to the inverse of the time T of the N samples. The fundamental frequency is expressed as

$$f_0 = 1/T \tag{3.1}$$

T can be written as a function of sample time, τ, and total number of samples chosen N, to alternately express the fundamental frequency in terms of the sampling frequency f_s and N.

$$f_0 = 1/\tau\,\mathrm{N} = 1/(secs/sample)*Total\ no.\ of\ samples$$

$$f_0 = f_s\,/N \tag{3.2}$$

This frequency, referred to as the *fundamental frequency* of the signal, is really a type of resolution frequency, meaning the target signal components are resolved into multiples of this resolution frequency. For example, sampling the signal at sample time of $1/900*10^6$ sec and observing $1800*10^6$ samples, then the fundamental frequency is

$$f_0 = f_s\,/N = 900*10^6/1800*10^6 = 0.5 \text{ Hz}$$

The Fourier Transform is computed by simply multiplying the fundamental frequency by integer multiples with appropriate magnitudes. With f_0 = 15 MHz, the next harmonic would be f_1 = 30 MHz and so on. An alternate way to view these harmonics of the fundamental frequency as bins, which collect energy. In the DFT they are called cells. Now the n^{th} harmonic can be expressed as n multiplied by f_0.

$$f_n = nf_0$$

this is equal to

$$f_n = n/\tau N = nf_s/N \tag{3.3}$$

The harmonics of the transform are multiplied by the fundamental frequency to produce individual frequencies of the transform. The coefficients of the individual frequencies in turn are the magnitude of the frequencies. The coefficient becomes the item of interest in the modulation technique currently under discussion.

3.4 VIRTUAL PULSE

There is a mechanism by which a repeating square wave can be transmitted when one considers the DFT. If all frequencies of the DFT are transmitted with the corresponding DFT coefficients while accounting for fading, the square wave can be reconstructed from the received frequencies. The analysis and understanding of the square wave reconstruction unveils numerous avenues for investigations and applications. This section deals with one of the investigations and applications.

The DFT of a rectangular pulse provides a spectrum of several frequencies with different amplitudes that are integer multiples of the fundamental frequency, that is, harmonics of the fundamental frequency. If the frequencies are to be transmitted as RF continuous wave (CW), the specific frequencies derived from the DFT might not be available for use for the purpose of this work simply because of FCC regulations. In addition, it is not clear what the FCC will do in the future about multiple frequencies below the noise threshold. For new and innovative purposes, ISM frequencies are used to demonstrate the technique of multiple frequency communication as related to this research work. In addition, ISM frequencies are available for experimentation. Although the spacing between the frequencies that make up the ISM spectrum might not be consistent in ratio compared to a nominal harmonic series, a common denominator derived from the DFT of a *virtual pulse* can be fabricated as the virtual fundamental frequency of the chosen ISM frequencies. In order for this to be feasible, due to the non-integer nature and necessary precision, floating-point numbers must be used to determine the multiples of the fundamental frequency for each of the chosen ISM frequencies. These frequencies are not harmonically related as such but they do represent *some* signal, which has the desired corresponding spectral content. This result is termed *The Virtual Pulse* or *virtual pulse train*.

Consider a *virtual pulse train* having a fixed period T_v and variable pulse duration τ_v. Therefore, because the period is fixed, the fundamental frequency of the DFT is given by:

$$f_{v0} = 1/T_v$$

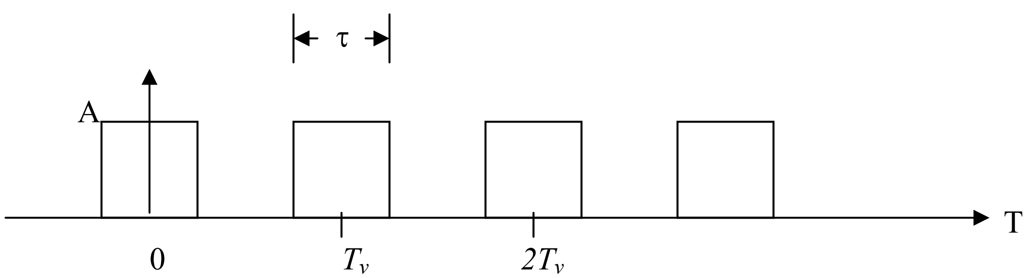

Figure 3.3: Picture of a Virtual Pulse Train

Taking the DFT of this *virtual pulse train* provides a string of frequencies that are hypothetically harmonically related. The spectrum of these frequencies constitutes the chosen ISM frequencies along with potentially many other frequencies. The rest of the frequencies, which are non-ISM, may fall within the spectrum already allocated by the FCC and as such are assumed as not being available for RF communications. This problem is resolved by forcing the non-ISM frequency coefficients to be zero.

3.5 ISM FREQUENCIES

The set of Industrial Scientific and Medical (ISM) frequencies has been determined to be an appropriate candidate for this research because they are free for use within allowed tolerances and restricted power levels. As indicated previously, the set of ISM frequencies are not harmonically related in the RF spectrum. Therefore, what is termed a *virtual pulse* concept will be used to find a common denominator that can be considered the *fundamental frequency* among the chosen ISM frequencies. Consider the following five ISM frequencies, 315MHz, 418MHz, 433MHz, 915MHz, and 2450MHz. A common denominator can be found among these numbers which will provide the means for deriving a fundamental frequency to relate the chosen frequencies and allow modulation by varying the pulse width.

A simple technique is to look at the differences between subsequent frequencies moving from the lowest to the highest. The lowest difference between any two happens to be between 418MHz and 433MHz, which is exactly 15MHz. The fundamental frequency from the DFT of the *virtual pulse train* of period T_v at 0.06µs is given by

$$f_{v0} = 1/T_v = 1/0.06*10^{-6} = 15\text{MHz}$$

Because the fundamental frequency is known, the multiple for each of the five example ISM frequencies can be found using the relationship

$$N_{f_{ISM}} * f_{v0} = f_{ISM} \tag{3.4}$$

Where, f_{ISM} is the ISM frequency and $N_{f_{ISM}}$ is the harmonic number of the ISM frequency.

Hence, for each of the five frequencies the following numbers are the multipliers of the fundamental frequency:

$$N_{315} = \frac{315}{15} = 21$$

$$N_{418} = \frac{418}{15} = 27.867$$

$$N_{433} = \frac{433}{15} = 28.867$$

$$N_{915} = \frac{915}{15} = 61$$

$$N_{2450} = \frac{2450}{15} = 163.333$$

The expressions can now be written in another way as

$$N_{315} * f_0 = 21 * 15 = 315$$
$$N_{418} * f_0 = 27.867 * 15 = 418$$
$$N_{433} * f_0 = 28.867 * 15 = 433$$
$$N_{915} * f_0 = 61 * 15 = 915$$
$$N_{2450} * f_0 = 163.333 * 15 = 2450$$

When the DFT of the *virtual pulse* is obtained, the frequencies spread from the dc component to frequencies beyond 2450MHz. However, for this application, only these five frequencies are utilized, and the remainders of the frequencies within this spectrum are kept at level of zero (switched off). Thus, it is the cumulative energy of these frequencies that represents the information been transmitted.

3.6 RADIO FREQUENCY (RF) PULSES

One of the essential parts of this research is the investigation of the possible implementation of the technique of RF pulse formation for the purpose of communication. When the components of a Fourier transform are known for a particular pulse train, the Fourier series of the components can be used to reconstruct the pulse train.

Figure 3.4 shows the reconstructed rectangular pulse from a series having a fundamental frequency of 15MHz and a period of 0.06μs. Because of the presence of a number of high frequency components, it can be observed that the Gibbs effect [23] is almost eliminated in the reconstructed rectangular pulses. In this case, the interest is in amplitude modulating multiple ISM frequencies (315MHz, 418MHz, 433MHz, 915MHz, and 2450MHz) according to the DFT . These five frequencies are then combined to form an RF pulse sufficiently distinct to be detected by a correlated receiver. It can be seen here that the modulation technique is two fold:

Amplitude modulating the individual ISM frequencies forms a five frequency spreading of the bit energy in the form of digital code. For example in this case, we are transmitting f_{315}, f_{418}, f_{433}, f_{915}, and f_{2450} to represent the code 10011 which can be interpreted as a '0' or '1' depending on the Hamming distance chosen for the reception.

When these five frequencies are combined, an RF pulse is formed whose width can be varied by applying different sets of coefficients to the individual frequencies respectively.

3.6.1 Choice of Coefficients

The choice of the respective coefficients for the individual ISM frequencies was carried out with the goal of creating distinct pulses to represent a "0" and a "1" respectively. The distinction in this instance is the "width" of the pulse in order to perform a pulse width type modulation. For the purpose of having a clear distinction between the two different pulses a minimum ratio of 1:2 for bits "1" and "0" was chosen for this example.

The first pulse is the wider pulse therefore some or all of the coefficients used in generating the pulse could be divided into halves to get the set of coefficients for the second pulse. Most of the effort involved in choosing the coefficients happens during the creation of the wider pulse (first pulse), and the following steps were taken:

- To avoid having an infinite plain a boundary of 0.01 to 10 .0 was set for choosing of coefficients
- Because the effect of some of the frequencies tend to be higher than the others, the frequencies with greater influence on the pulse shape can have coefficients maintained as integer numbers while the frequencies with lesser influence on the pulse shape are maintained as decimal numbers.

For the shorter pulse (second pulse) the coefficients of the pulse with greater influence on the pulse shape is reduced to a value as close to half as possible. This has reduced the width of the pulse to at least half.

The pulse in these cases is the envelope of the function $|\sin \omega_m t| * \sin \omega_c t$ where ω_m is a modulation frequency and ω_c is essentially a set of carrier frequencies. The carrier frequencies are implemented within the ISA bands, and the non-integer frequency is readily available. The method of generating these carrier frequencies relies on a conceptional analogy with a Fourier analysis with floating point coefficients for the "Harmonics" to generate the set of carrier frequencies.

The choice of coefficients is essentially a trial and error process other than possibly the initial choice of the smallest differential between the set of available frequencies although in the described embodiment, these are assumed to be ISM frequencies with no loss to generality.

Obviously, the combination of frequencies is given by:

$$f_{0,1} = \sum_{i=1}^{n} a_i \sin \omega_i t$$

The search process is similar to a combinatorial problem in chemistry. The combinatorial selection in general will be governed by the fading problem at the higher end of the spectrum.

The chosen coefficients are to be based on the distance to the receiver with the transmitter coefficient strengths accounting for the fading of the frequencies. The introduction of fading gives rise to the fixed distance concept presented later in this dissertation.

Figure 3.5 shows the result of combining the five ISM frequencies within the coefficients:

$$\begin{aligned} a_{315} &= 0.10 \\ a_{418} &= 0.10 \\ a_{433} &= 0.05 \\ a_{915} &= 5.00 \\ a_{2450} &= 0.3 \end{aligned}$$

These RF pulses transmit a bit ‘1’ communicated to a receiver.

Figure 3.6 shows a different set of RF pulses constructed by changing the sets of coefficients to:

$$\begin{aligned} a_{315} &= 0.10 \\ a_{418} &= 0.15 \\ a_{433} &= 0.2 \\ a_{915} &= 3.00 \\ a_{2450} &= 0.3 \end{aligned}$$

These RF pulses transmit a bit ‘0’.

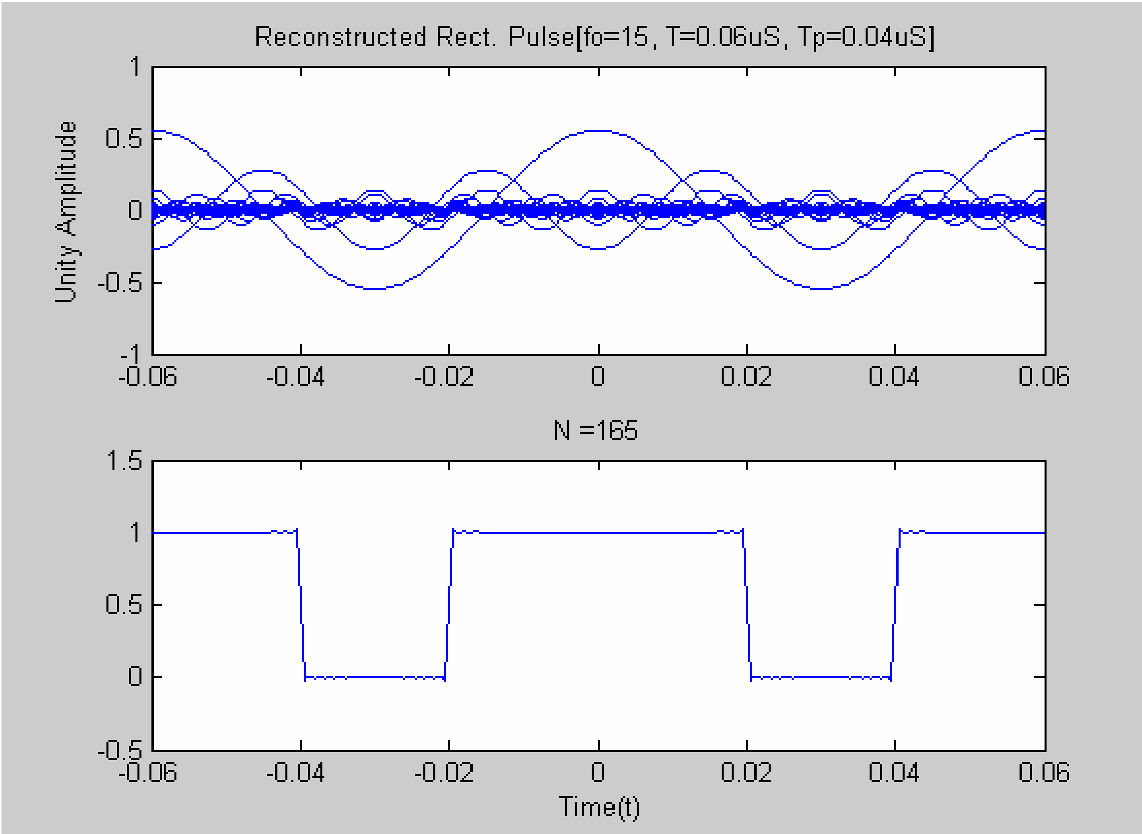

Figure 3.4: Fourier series Reconstruction of Rectangular Pulse Using Frequencies from the Fundamental to the 165 Harmonic.

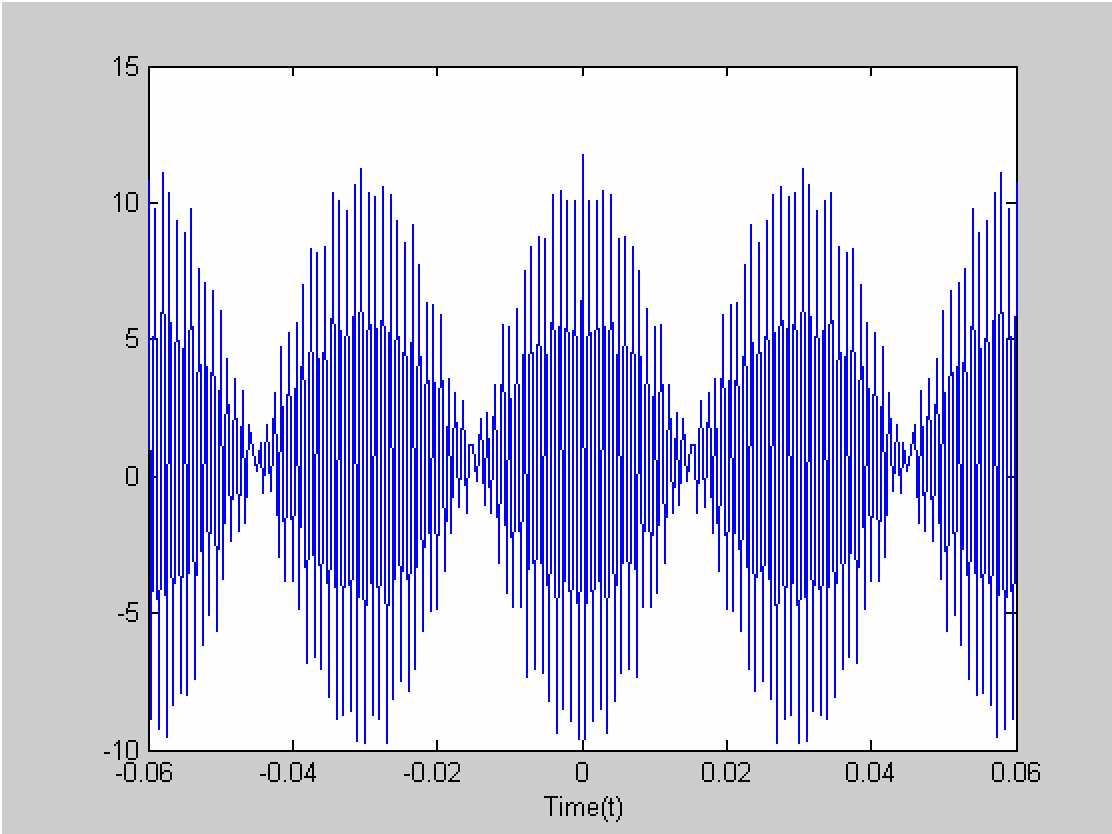

Figure 3.5: Showing the Construction of Pulses using the 21st, 27.867th, 28.867th, 61st, and 163.333rd Harmonics Only with one Set of Coefficients.

By this technique, a type of pulse width modulation is implemented by way of manipulating the coefficients of the individual frequencies whose combination formed the pulses.

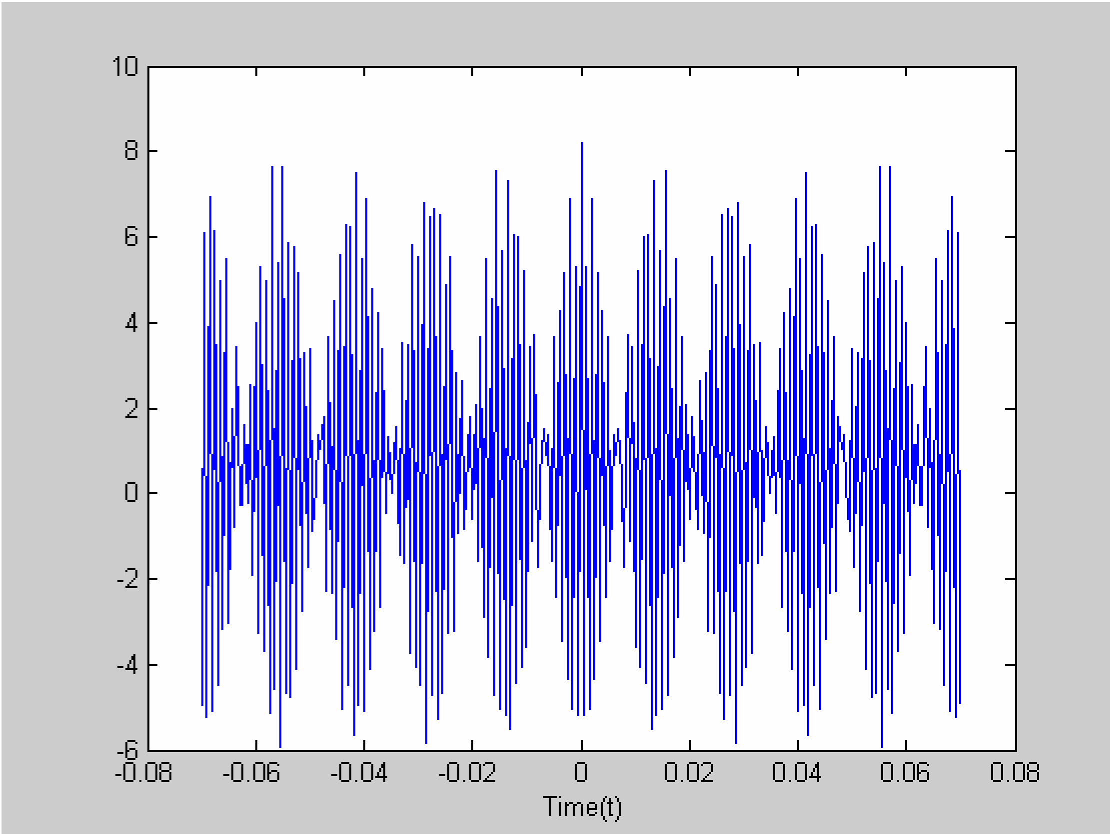

Figure 3.6: Changing the RF Pulse Width by Applying a Different Set of Coefficients

3.7 AM TYPE MODULATION

The goal in this part of the research is to amplitude modulate multiple frequencies, in this case ISM frequencies, collectively representing a single bit of information. Figures 3.5 and 3.6 show two different pulses formed using two different sets of values for the coefficients a_{315}, a_{418}, a_{433}, a_{915}, and a_{2450} resulting in pulses with different widths and amplitudes. The ISM frequencies chosen in this case are the carrier frequencies which constitute the composite frequencies forming the virtual pulse and are represented as

$$f_{315} = a_{315}*cos\theta_{315}t$$

$$f_{418} = a_{418}*cos\theta_{418}t$$

$$f_{433} = a_{433}*cos\theta_{433}t$$

$$f_{915} = a_{915}*cos\theta_{915}t$$

$$f_{2450} = a_{2450}*cos\theta_{2450}t$$

This pulse forming technique stems from the concept of transmitting pulses with short durations whose envelope occupies a wide spectrum of frequencies. In this instance, the ISM frequencies contained in the pulse range between 315MHz and 2450MHz. The coefficients of the individual frequencies are predetermined to maintain a specific pulse shape, duration, and amplitude. The collective energy level of these frequencies is interpreted as a "1" or a "0" according to some preset range of values of the received energy level.

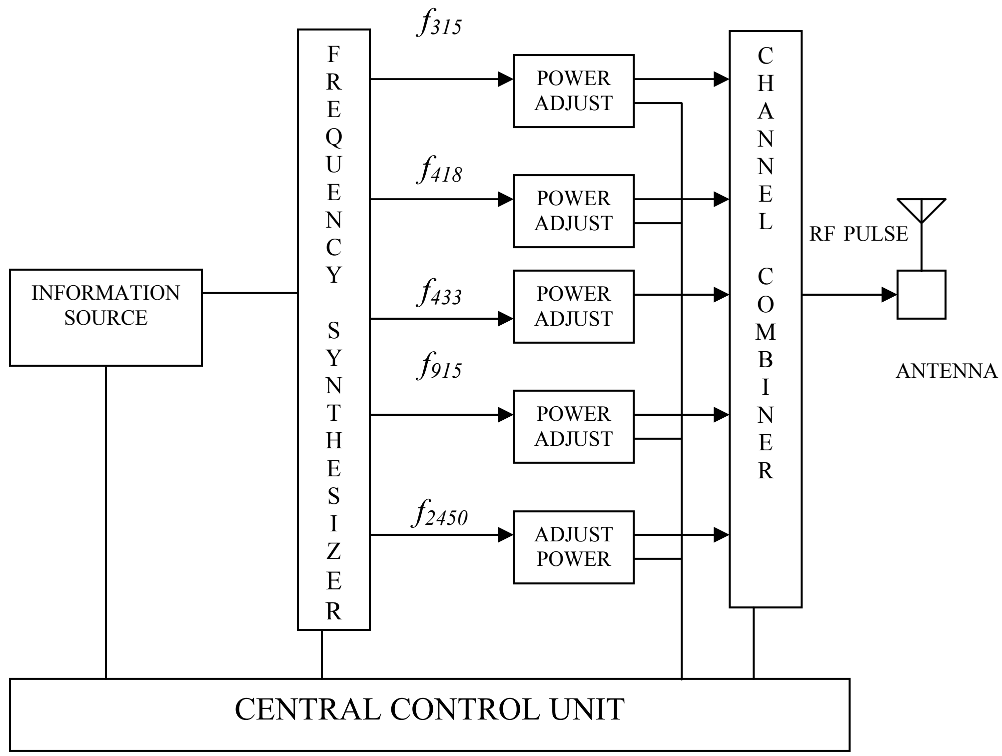

Figure 3.7: A Basic Model of the RF Pulse forming System

A basic model for the RF pulse formation is illustrated in Figure 3.7. In this model, the information source sends the information to be transmitted to the *central control unit* and the *frequency synthesizer*. The frequency synthesizer generates the multiple frequencies which are spread within a wide spectrum as dictated by the central control unit (CCU). The amplitudes of the multiple frequencies are set by the CCU using *power adjust* units connected to all the outputs of the synthesizer. The level adjustment completely depends on whether a bit ‘1’ or bit ‘0’ is being transmitted. The *channel combiner* executes pulse formation by combining the individual multiple frequencies to form an RF pulse of a certain shape. As earlier discussed in Section 3.6, the pulse shape and amplitude is determined by the frequencies being combined and the coefficients (amplitudes) of the respective frequencies.

3.8 SIGNAL FADING

This is the degradation or reduction of energy of a radio frequency (RF) signal as it travels from the transmitter (source) to the receiver (destination). The degradation is normally due to a number of factors such as atmosphere, obstacles or objects, temperature changes and so on. The significance of signal fading to this dissertation is in the modulation technique where transmitted signals arrive at the intended destination with lesser power but are received and decoded as valid signals because the fading effect of the signal has been taken into consideration. There are basically three types of RF signal fading namely free space fading, absorption, and multipath fading.

3.8.1 Free Space Loss

The wavefront radiated signal energy expands as a function of the distance from the transmitter. Signal power at a distance *(r)* from the transmitter can be measured in units of the signal wavelength, and this gives the free space loss *(L_{fsl})* as:

$$L_{fsl} = \frac{r^2 (4\pi)^2}{\lambda^2} \tag{3.5}$$

Using decibels to express the loss and using the frequency 2.45GHz as the signal frequency, the equation can be simplified to:

$$L_{fsl} = 40 + 20 * \log(r) \tag{3.6}$$

where L_{fsl} is in dB and r is in meters.

3.8.2 Attenuation (Absorption)

Some parts of the RF signal are absorbed whenever the signal passes through solid objects. This can conveniently be expressed by adding an "allowed loss" to the free space loss. Attenuation depends very greatly upon the structure of the object the signal is passing through. Metal in the barrier greatly increases the attenuation. Thickness also increases the loss. Some basic rules of thumb on attenuation are:

- Trees account for 10 to 20 dB loss per tree in the direct path. Loss depends upon the size and type of tree. Large trees with dense foliage create greater loss.
- Walls account for 10 to 15 dB depending upon the construction. Interior walls are on the low end and exterior walls, especially those with stucco, create an additional loss.
- Floors of buildings account for 12 to 127 dB of loss. Floors with concrete and steel are at the high end and wood floors are at the low end.
- Mirrored walls have very high loss because the reflective coating is typically conductive.

3.8.3 Multipath Fading

Multipath fading describes phenomena where RF signals are reflected by objects and the reflected signal recombines with the transmitted signal in the opposite direction. This effect is also known as scattering, fading, or Rayleigh fading. When RF signals combine they can be distorted, and the distortion degrades the ability of the receiver to recover the signal in a manner similar to signal loss.

When the free space loss, attenuation and scattering are combined the loss is:

$$L = r^n \frac{(4\pi)^2}{\lambda^2} + L_{allowed} \tag{3.7}$$

Expressed in decibels:

$$L(dB) = 40 + 10 * n * \log(r) + L_{allowed} \tag{3.8}$$

One of the difficulties of using the exponent to model the effect of scattering is that the exponent tends to increase with range in an environment with a lot of scattering.

3.8.4 Link Margin

The performance of any communication link depends on the quality of the equipment being used in addition to environmental factors. Link margin is a way of quantifying equipment performance. An example is the 802.11 communication link, which has an available link margin that is determined by the following four factors:

Transmit power

Transmit antenna gain

Receive antenna gain

Minimum receive signal strength or level

The link margin is:

$$L_{margin} = TX_{power} + TX_{antgain} + RX_{antgain} - RSL \tag{3.9}$$

3.9 GENERAL INVERSE SQUARE LAW

Any point source, which spreads its influence equally in all directions without a limit to its range, will obey the inverse square law. This comes from strictly geometrical considerations. The intensity of the influence at any given radius r is the source strength divided by the area of the sphere for an isotropic radiator. Typically this is expressed as watts per square meter. Being strictly geometric in its origin, the inverse square law applies to diverse phenomena. Point sources of gravitational force, electric field, light, sound or radiation obey the inverse square law [12].

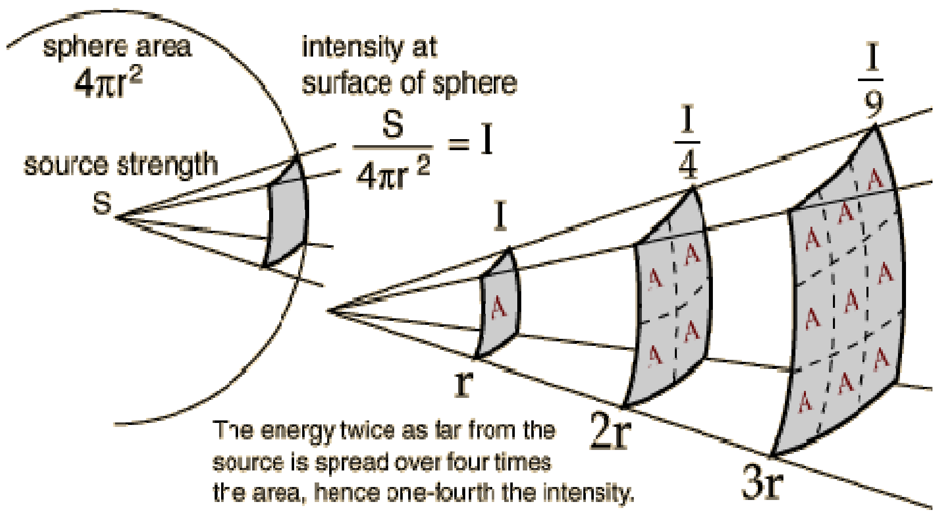

Figure 3.8: Illustration of General Inverse Square Law

3.9.1 Radiation Inverse Square Law

As one of the example fields which obey the general inverse square law, a point radiation source (an isotropic antenna) can be characterized by the relationship below. All measures of exposure will drop off by the inverse square law.

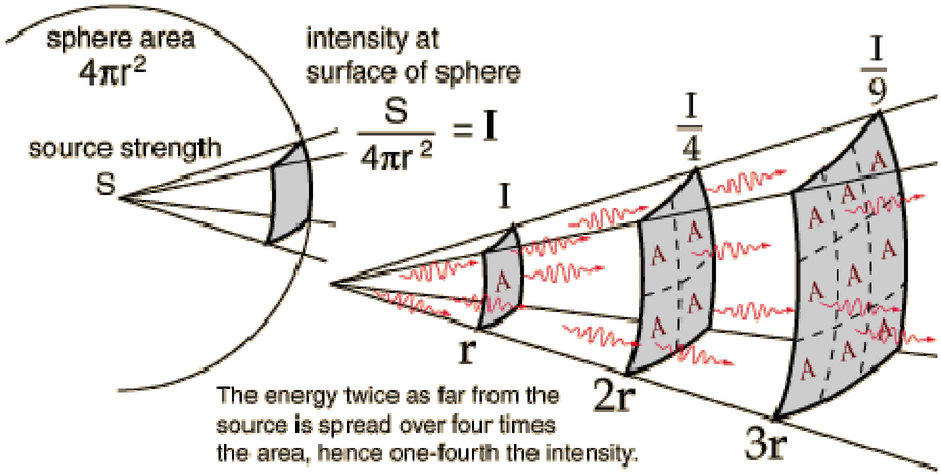

Figure 3.9: Illustration of Radiation Inverse Square Law

3.9.2 Signal Strength and the Inverse Square Law

The "inverse square law" defines how an RF signal would be reduced in power through distance propagated. It must be explained that there are other factors that come into play with respect to signal attenuation. However, the inverse square law has the most dramatic impact. It is known that when measurements are taken at a distance greater than approximately one wavelength away from an electromagnetic radiator (near field/far field boundary), the other influences on the energy level of the radiated wave become essentially insignificant and can be ignored. For example, a 100mW access point actually had 100mW of measured power 1-inch away from the antenna. If the measured power were 100mW at a distance of 1-inch, then the measured power would be 400mW at a distance of ¾-inch, by inverse square law. At ¼-inch, the power would have jumped up to 1600mW.

Obviously, this is not reality because when a transmitter is rated at 100mW, there is an implication that a 100mW signal is present at the last point in the transmitter circuit before the signal enters the antenna. The antenna will introduce some loss or gain, and what comes out will be assumed to be at the power level derived from adjusting the power at the antenna by that gain or loss.

Recognizing that real-world measurements will probably be smaller than those derived in the illustration above, indicates why RSSI values are associated with dBm signal strengths at levels below -10dBm.[RSSI stands for Received Signal Strength Indicator (or Indication): A signal or circuit that indicates the strength of the incoming (received) signal in a receiver. The signal strength indicator on a cell phone display is a common example. RSSI is often done in the baseband signal chain, before the baseband amplifier]. If the measured power at 1-inch from an antenna were 100mW, then we could imagine the following measurements, based on the inverse-square law:

Table 3.1: Illustration of Signal Fading in Accordance with Inverse-Square Law [7]

1” = 100mW = 20dBm

2” = 25mW = 13.9dBm

4” = 6.25mW = 7.9dBm

8” = 1.56mW = 1.9dBm

16” = 0.39mW = -4.08dBm

32” = 0.097mW = -10.1dBm

64” = 0.024mW = -16.1dBm (5.3 feet away)

Table 3.1 (continue)

128” = 0.006mW = -22.2dBm (10.6 feet away)

256” = 0.0015mW = -28.2dBm (21.3 feet away)

Table 3.1 data shows that somewhere between roughly 5 feet and 20 feet away from a 100mW radiator, the signal strength falls to below -20dBm. Consequently, measurements represented by RSSI values that refer to energy levels below -10dBm (or lower) are reasonable and practical.

3.10 TRANSMITTED POWER CONSIDERATION

From the transmitter side, the energy levels of each modulated channel (ISM frequency) are set with respect to the presumed propagation distance and fading effect, such that the correct energy range for the respective information is received at the destination. Figure 3.7 gives a picture of the process of determining the energy level at the transmitter side of the system, and a similar technique is used at the receiver end to collect the cumulative energy received.

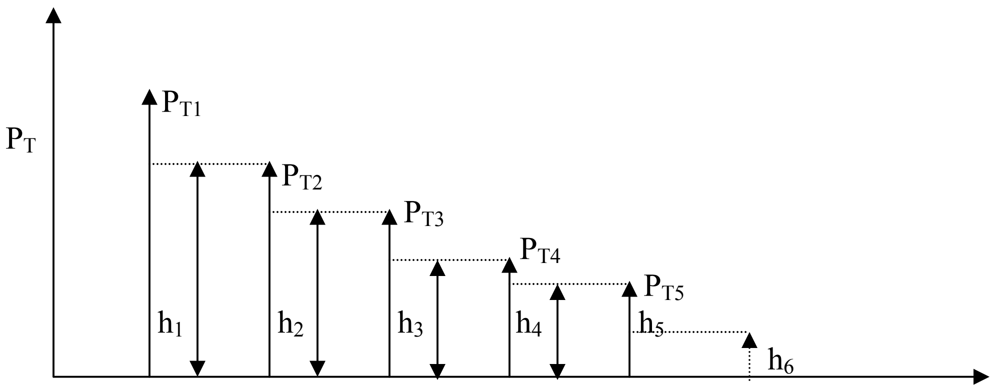

Figure 3.7: Relative Energy Levels of Transmitted Frequencies

Figure 3.7 is a picture of the relative energy levels of multiple frequencies individually transmitted by separate transmitters. The power levels of all the transmitters are set such that the relative powers; P_{T1}, P_{T2}, P_{T3}, P_{T4}, and P_{T5}, of the respective channels are calculated at the transmitters side. The power levels are established bearing in mind the attenuation of the signal before reaching the receiver as it propagates. The expected cumulative power at each of the multiple frequencies is received only when the receiver is at the proper distance. The expressions for the relative power levels are as follows:

$$\left\{\begin{array}{l} P_{T1} = \dfrac{h_1}{h_2} \\ P_{T2} = \dfrac{h_2}{h_3} \\ P_{T3} = \dfrac{h_3}{h_4} \\ P_{T4} = \dfrac{h_4}{h_5} \\ P_{T5} = \dfrac{h_5}{h_6} \end{array}\right\} \tag{3.10}$$

where, h_1, h_2, h_3, h_4, and h_5 are the power levels of f_{315}, f_{418}, f_{433}, f_{915}, and f_{2450} respectively. It is assumed here that the energy ratio of the multiple frequencies remains constant**.**

3.11 RECEIVED POWER CONSIDERATION

The inverse square law can be used to illustrate the relative power levels at the receiver.

Although in practice, the steady fading of P_T might not be realistic because signals having different frequencies fade at different rates due to the difference in wavelengths. A more appropriate relation for the received power in a multiple frequency situation is the *radar equation*, expressed in equation 3.11

$$P_R = P_T \left[\frac{\lambda}{4\pi D} \right]^2 G_T G_R \tag{3.11}$$

where, P_T is the transmit power, G_T and G_R are transmitter and receiver gains respectively, D is the distance traveled by the signal, and λ is the wavelength of the signal and given by

$$\lambda = c/f \tag{3.13}$$

where, c is the speed of light in a vacuum ($3*10^8$), and f is the frequency of the signal. From equation 3.13, it can be seen that λ is a function of the frequency under consideration when it comes to multi-frequency situation. Considering the five ISM frequencies in this case lambda will be as follows:

$$\lambda_{315} = {3*10^8}/{315*10^6} = 0.952m$$
$$\lambda_{418} = {3*10^8}/{418*10^6} = 0.718m$$
$$\lambda_{433} = {3*10^8}/{433*10^6} = 0.693m$$
$$\lambda_{915} = {3*10^8}/{915*10^6} = 0.328m$$
$$\lambda_{2450} = {3*10^8}/{2450*10^6} = 0.122m$$

Because all the frequencies will travel the same distance, λ becomes the variable in this case, hence the fading of the multiple frequencies becomes greater from the lowest to the highest frequencies. Figure 3.8 gives a graphical illustration of the pattern of the five ISM frequencies.

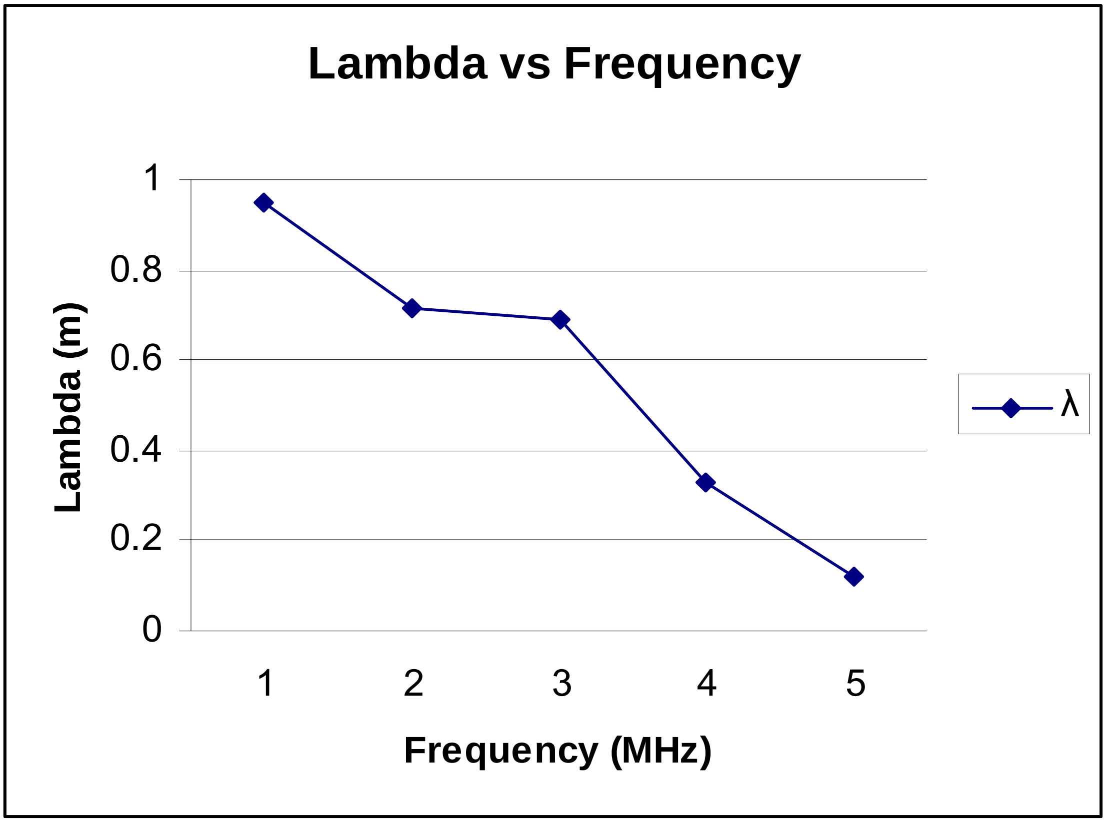

Note: 1, 2, 3, 4, and 5 on the x-axis stand for 315MHz, 418MHz, 433MHz, 915MHz, and 2450MHz respectively.

Figure 3.8: A Graph of the values of λ (Lambda) with respect to Frequencies

The expressions below give the relative power levels P_{R1}, P_{R2}, P_{R3}, P_{R4}, and P_{R5} at the receiver after P_{T1}, P_{T2}, P_{T3}, P_{T4}, and P_{T5} have traveled the distance D from the transmitters.

$$\left\{\begin{aligned} P_{R1} &= f(P_{T1}, D)\alpha P_{T1}\lambda_{315}^2 / [4\pi D]^2 \\ P_{R2} &= f(P_{T2}, D)\alpha P_{T2}\lambda_{418}^2 / [4\pi D]^2 \\ P_{R3} &= f(P_{T3}, D)\alpha P_{T3}\lambda_{433}^2 / [4\pi D]^2 \\ P_{R4} &= f(P_{T4}, D)\alpha P_{T4}\lambda_{915}^2 / [4\pi D]^2 \\ P_{R5} &= f(P_{T5}, D)\alpha P_{T5}\lambda_{2450}^2 / [4\pi D]^2 \end{aligned}\right\} \qquad (3.11)$$

Alternatively power at the receiver can be represented as follows:

$$\left\{\begin{aligned} P_{R1} &= \frac{h_1\lambda_{315} / [4\pi D]^2}{h_2\lambda_{418} / [4\pi D]^2} \\ P_{R2} &= \frac{h_2\lambda_{418} / [4\pi D]^2}{h_3\lambda_{433} / [4\pi D]^2} \\ P_{R3} &= \frac{h_3\lambda_{433} / [4\pi D]^2}{h_4\lambda_{915} / [4\pi D]^2} \\ P_{R4} &= \frac{h_4\lambda_{915} / [4\pi D]^2}{h_5\lambda_{2450} / [4\pi D]^2} \\ P_{R5} &= \frac{h_5\lambda_{2450} / [4\pi D]^2}{h_6\lambda_{418} / [4\pi D]^2} \end{aligned}\right\} \qquad 3.12$$

The values of P_{T1}, P_{T2}, P_{T3}, P_{T4}, and P_{T5} represent bit "0" or "1" and the combination of any three of five bits gives the value, for example 10011.

Due to the difference in fading of the multiple frequencies, the valid power levels of the individual frequencies will be set at different magnitudes. This means the lower value frequencies will be expected to arrive at a higher magnitude than the higher value frequencies. Ranges of the received signals can be categorized as lower boundaries and higher boundaries for the purpose of correct interpretation of the received signal. In the inequality expression below, $1L_{R1}$ and $1U_{R1}$ represent the lower and upper boundaries of received power level which stands for a bit "1" for the first frequency, while $0\ L_{R1}$ and $0\ U_{R1}$ represent the lower and the upper boundaries of the received energy level which stands for a bit "0" for the first frequency. Similarly, the rest of the frequencies have their boundaries based on the anticipated fading.

$$\begin{array}{lcl} 1\ L_{R1} \leq P_{R1} \leq 1\ U_{R1} & & 0\ L_{R1} \leq P_{R1} \leq 0\ U_{R1} \\ 1\ L_{R2} \leq P_{R2} \leq 1\ U_{R2} & & 0\ L_{R2} \leq P_{R2} \leq 0\ U_{R2} \\ 1\ L_{R3} \leq P_{R3} \leq 1\ U_{R3} & \Rightarrow & 0\ L_{R3} \leq P_{R3} \leq 0\ U_{R3} \\ 1\ L_{R1} \leq P_{R4} \leq 1\ U_{R4} & & 0\ L_{R1} \leq P_{R4} \leq 0\ U_{R4} \\ 1\ L_{R5} \leq P_{R5} \leq 1\ U_{R5} & & 0\ L_{R5} \leq P_{R5} \leq 0\ U_{R5} \end{array}$$

Using the *radar equation* the lower and upper boundaries can be set as follows:

$L_{Ri} = R_{Ri} - (P_{Ri} * 0.1)$

$U_{Ri} = R_{Ri} + (P_{Ri} * 0.1)$

where, the subscript i is an integer number from 1 to n with n being the maximum number of frequencies. In this case, it ranges from 1 to 5. These boundaries establish the range for the valid power for the individual multiple frequencies.

3.12 CHANNEL CODING

Shannon's second theorem [23] states that it is possible to signal as closely as desired to the channel capacity rate with an arbitrarily small probability of decoding error the Binary Symmetric Channel (BSC). The maximum amount of information transmitted can at most be equal to the channel capacity, which is [23]

$$C(p) = n[1 - h(p)] = n[1 + p\log p + (1-p)\log(1-p) \tag{3.15}$$

The actual information throughput is less than this because of decoding errors. The aim is to transmit these bits with higher reliability. Without coding, the bits might be received in error with probability *p*. If *p* exceeds the maximum tolerable for the particular application intended, then the channel can be considered useless. However, coding allows for the recovery of the original message with a bit error probability p' that is less than *p*. This means that a certain unavoidable amount of redundancy is needed. Because

$$C(p) = n[1 - h(p)] \leq n \tag{3.16}$$

an n-tuple consists of at most $n[1 - h(p)]$ information bits and at least $nh(p)$ redundant bits, these add up to a total of *n* bits. A linear code over the Galois Field GF(p) for error detection and correction, and for the binary case it is $GF(2)^n$.

A coder maps *k* information symbols into the *n* symbols of n-tuple to form a *code word*. The code words are a subset of all possible q^n n-tuples. This subset is used for signaling purposes. The set of all q^k code words forms a code.

3.13 HAMMING DISTANCE

The Hamming distance is defined as the number of corresponding places (bits) in which two binary n-tuples differ (equal n). Two vectors, *x* and *y* can be compared, and the counts of the number of positions in which they differ will give the respective Hamming distance. Over GF(2), the Hamming distance is simply

$$d_H(x,y)=\sum_{k=1}^{n}(a_k-b_k) \tag{3.17}$$

where x = (a_1, a_2, …, a_n), y = (b_1, b_2, …, b_n), and the subtraction is performed modulo 2.

The Hamming distance between (1, 0, 1, 1, 0, 1) and (1, 0, 0, 1, 1, 0) is 3, because these two 6-tuples differ in three positions, namely, the third, fifth, and sixth. The difference vector can be computed as (0 0 1 0 1 1) and the weight (sum of bits) of the resulting vector is 3.

A block code is expressed as (n, k; d_{min}) where k is the information bits, n is the total number of bits, and d_{min} is the minimum Hamming distance of the code symbols. This distance is frequently used for error correction.

Now, considering the five individually modulated ISM frequencies used in the example cited earlier, the transmission is performed to deliver the correct energy level at the receiver for all five frequencies. Because the frequencies are individually modulated, they individually represent a bit by a code that is of binary form from {00000} to {11111}. Using the block code expression (n, k; d_{min}), a block code can be formed with n = 5, k = 1, and d_{min} = 3 so that the distance between any two code words is large enough for a large error correction capability of a single bit.

The simplest way to encode is by polynomial multiplication such as the product of a data polynomial *d(x)* of degree not exceeding *k-1* and polynomial generator *g(x)* of degree n-k. This will always produce a code word of degree not exceeding *n-1*. This encoding procedure is easily implemented with linear shift register circuitry. For example:

$g(x) = x^3 + x^2 + 1$

$d(x) = [0; 1; x; x+1]$

$d(x)g(x) = [\ 00000; 01101; 11010; 10111]$

As a result, this polynomial multiplication creates a simple means of maintaining a specific Hamming distance between all the bit combinations which represents information. There several possible ways of interpreting the Hamming distances, but for the purpose of this dissertation, the four different bit combinations from the polynomial multiplication can be arranged in two pair to indicate the transmission of a ‘0’ or a ‘1’. Such as:

TRANSMITTING A ‘**0**’	TRASNMITTING A ‘**1**’
00000	11010
01101	10111

This makes it easier to detect an error at the receiver side because all the four different bit combinations have hamming distance of 3 which means the 5-tuples in either column of the table has a weight of 3. The chance of receiving 3 bits in error at all 3 different bit positions is unlikely.

4.0 THE APPLICATION OF CDMA FOR SIMULTANEOUSE READING OF MULTIPLE RFID TAGS

4.1 INTRODUCTION

The technique of Spread Spectrum (SS) is necessary to implement code division multiple access which is one of the fundamental concepts of this dissertation. Spread Spectrum has been known to provide excellent immunity to interference and detection that may result from intentional jamming by allowing a transmission to be hidden in background noise. Recently, SS has been adapted in the field of wireless telephony as a means of solving the interference problem providing effective multiple accesses to multiple users and bandwidth efficiency. There are three primary approaches to implementing SS systems: Direct Sequence Spread Spectrum (DSSS), Frequency-Hoping Spread Spectrum (FHSS), and Time-Hoping Spread Spectrum (THSS).

The code division multiple access (CDMA) technique is used in wireless communication to distinguish information from different devices within the same proximate area or cell. In addition, it makes it possible also to spread information symbols over a wide frequency bandwidth. In this part of the dissertation, the application of CDMA for the simultaneous reading of multiple RFID tags will be studied and analyzed. Thereby the problem of collisions and multiple access interference otherwise encountered when multiple tags communicate simultaneously to a common receiver can be solved. In particular, CDMA greatly reduces the time required for multiple transmissions while avoiding the complications of hardware required to overcome collisions using multiple transmissions.

4.2 SPREAD SPECTRUM

As indicated previously, there are three approaches to implementing SS system; direct sequence spread spectrum (DSSS), frequency-hopping spread spectrum (FHSS), and time-hopped spread spectrum (THSS).

4.2.1 Direct Sequence Spread Spectrum (DSSS)

Here, a carrier is modulated by a digital code with bit rate considerably larger than the information signal bit rate. Pseudo-noise sequences are also used to implement this system [1] while providing information security.

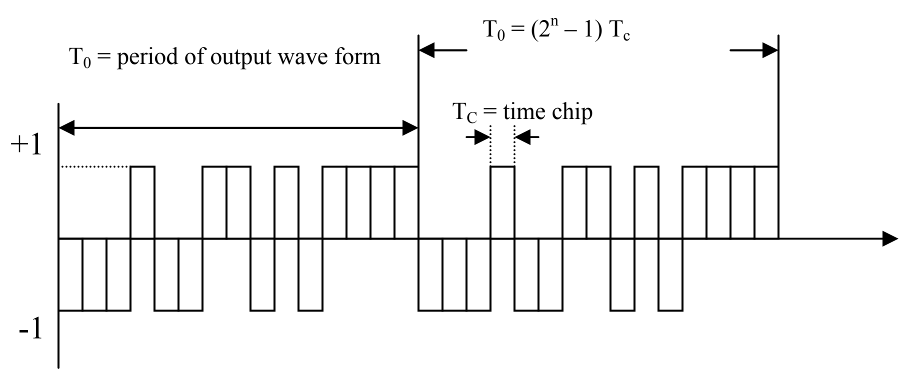

Figure 4.1: Direct sequence spread spectrum approach

4.2.2 Frequency-Hopping Spread Spectrum (FHSS)

The code sequence generates a pattern in which the frequency is shifted in discrete increments. In a FHSS system, the signal frequency remains constant for specified time duration, referred to as a time chip T_c [1]. The FHSS system can be a fast-hop system where the frequency hopping occurs at a rate greater than the message bit rate, or slow-hop system where the hop rate is slower than the message bit rate.

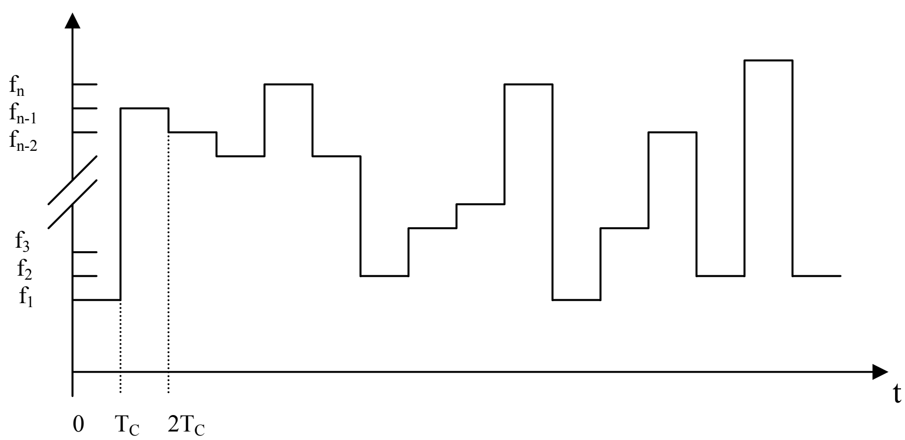

Figure 4.2: Frequency-hopping spread spectrum approach

4.2.3 Time-Hopped (TH) Spread Spectrum

The transmission time is divided into intervals called frames with each frame further being divided into time slots. During each frame, only one time slot is modulated with a message.

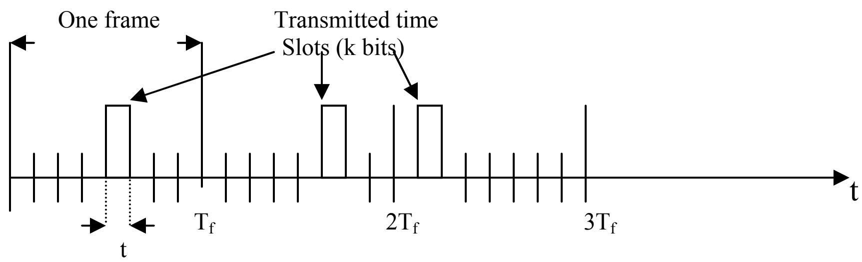

Figure 4.3: Time-hopping spread spectrum approach

4.3 CODE DIVISION MULTIPLE ACCESS (CDMA)

Code Division Multiple Access (CDMA) was developed by Qualcomm for digital cellular phone applications. The CDMA system reuses the same frequency within a cell to increase the capacity where capacity is the total number of active users in an area with many cells. In CDMA the uplink (from mobile station to base station) uses the band 869 to 894 MHz and downlink (from base station to mobile station) uses the band 824 to 849 MHz. The CDMA channels are defined in terms of an RF frequency and code sequence [1].

4.3.1 Orthogonal Functions in CDMA

The bandwidth efficiency of a spread spectrum system can be improved using orthogonal functions. In mobile systems, each user employs one member of a set of orthogonal functions representing the set of symbols used for transmission. The Walsh and Hadamard sequences are the functions or symbols used in CDMA. For the modulation of the orthogonal functions into an information stream for CDMA, signals in most cases use one of two different methods. The orthogonal set of functions can simply be used as a spreading code, or it can be used to form the modulation symbols that are orthogonal.

In orthogonal symbol modulation, the information bit stream is divided into blocks such that each block represents a nonbinary information symbol associated with a particular transmitted code sequence. Suppose there are *b* bits per block, one of the set of k = 2^b functions is transmitted in each symbol interval. The signal at the receiver is correlated with a set of k-matched filters, with each matched to the code function of one symbol. The symbol with the largest output is considered to be the transmitted symbol after comparing all the outputs.

Taking into consideration interference due to multipath, multiple users, and the decision process of the correlators, then

$$\frac{E_b}{N_0} \approx \frac{G_p}{(M-1)+(k-1)} \tag{4.1}$$

Where M =number of mobile users

G_p =processing gain of the system

K-1 =noise from the outputs of correlators other than the one corresponding to the correct symbol.

Equation (4.2) can be written as

$$M = \frac{G_p}{E_b / N_0} - k + 2 \tag{4.2}$$

Typically, one of the 64 possible modulation symbols is transmitted for each group of six code symbols. The modulation symbol is one member of the set of 64 mutually orthogonal functions, and the orthogonal functions have the following characteristic:

$$\sum_{k=0}^{M-1} \phi_i(\kappa\tau)\phi_j(\kappa\tau) = 0 \qquad i \neq j \tag{4.3}$$

where $\phi_i(\kappa\tau)$ and $\phi_i(\kappa\tau)$ =*i*th and *j*th orthogonal members of an orthogonal set, respectively, and M = length of the set, τ = Symbol duration.

4.3.2 Walsh Function

A Walsh function can be constructed for block length $N=2^j$, where j is an integer [1].

CDMA normally uses a set of 64 orthogonal functions generated by using Walsh functions. The Walsh 64x64 matrix can be generated using the following recursive procedure:

$$H_1 = [0] \qquad H_2 = \begin{bmatrix} 00 \\ 01 \end{bmatrix} \qquad H_4 = \begin{bmatrix} 0000 \\ 0101 \\ 0011 \\ 0110 \end{bmatrix} \qquad H_{2n} = \begin{bmatrix} H_N H_N \\ H_N \overline{H}_N \end{bmatrix}$$

Here, N is a power of 2 and $\overline{H}_N$ is the transformation of H_N such that each 0 becomes a 1 and each 1 becomes a 0, i.e., each bit is inverted.

The Walsh function is used to eliminate multiple access interference among users in the same cell in the forward channel. To correlate the Walsh code at the receiver, the receiver needs to be synchronized with the transmitter. In the forward direction the base station transmits a pilot signal to enable the transmitter and receiver to maintain synchronization. From the mobile station to the base station, the Walsh symbol modulation is used.

The Walsh function forms an ordered set of rectangular waveforms that are defined over a limited time interval T called the time base. For example, the situation where 8 chips per bit are used to generate the Walsh functions will be of the form below [1].

$$H_8 = \begin{bmatrix} 00000000 \\ 01010101 \\ 00110011 \\ 01100110 \\ 00001111 \\ 01011010 \\ 00111100 \\ 01101001 \end{bmatrix} = \begin{bmatrix} \phi_1 \\ \phi_2 \\ \phi_3 \\ \phi_4 \\ \phi_5 \\ \phi_6 \\ \phi_7 \\ \phi_8 \end{bmatrix}$$

Consider for example having five stations, A, B, C, D, and E with chip sequence, 01010101, 00110011, 01100110, 00001111, and 01011010, respectively. Each station uses the chip sequence to send a '1' and uses a negative chip sequence to send a '0'. Below is a table of chip sequences with the corresponding binary value of the chip sequence.

Table 4.1: Example of 8 chips per bit used to generate Walsh function

Chip sequence	Binary values of the chip sequence
A: 01010101	A: (-1+1-1+1-1+1-1+1)
B: 00110011	B: (-1-1+1+1-1-1+1+1)
C: 01100110	C: (-1+1+1-1-1+1+1-1)
D: 00001111	D: (-1-1-1-1+1+1+1+1)
E: 01011010	E: (-1+1-1+1+1-1+1-1)

It can be shown that the receiver recovers the bit stream of any of the stations, say A, by computing the normalized inner product of the received sequences with the chip sequence of the particular station, in this case station A.

Table 4.2: Five cases when one or more stations transmit

Stations (ABCDE)	Transmitting	Received chip sequence
1 - - - -	A	$S_1 = (-1+1-1+1-1+1-1+1)$
1 - - - 1	A+E	$S_2 = (-2+2-2+2\ 0\ \ 0\ \ 0\ \ 0)$
- - 1 1 -	C+D	$S_3 = (-2\ \ 0\ 0\ –2\ 0+2\ +2\ 0)$
1 1 1 1 1	A+B+C+D+E	$S_4 = (-5+1-1+1-1+1+3+1)$

Calculating the normalized inner products:

$S_1.A/8 = 1+1+1+1+1+1+1+1/8 =1$

$S_2.A/8 = 2+2+2+2+0+0+0+0/8 =1$

$S_3.A/8 = 2+0-0-2-0+2-2+0/8 =0$

$S_4.A/8 = 5+1+1+1+1+1-3+1/8 =1$

From the received chip sequence power level, it is possible to determine the number of stations transmitting, and from the normalized inner products, it is possible to determine the exact stations transmitting.

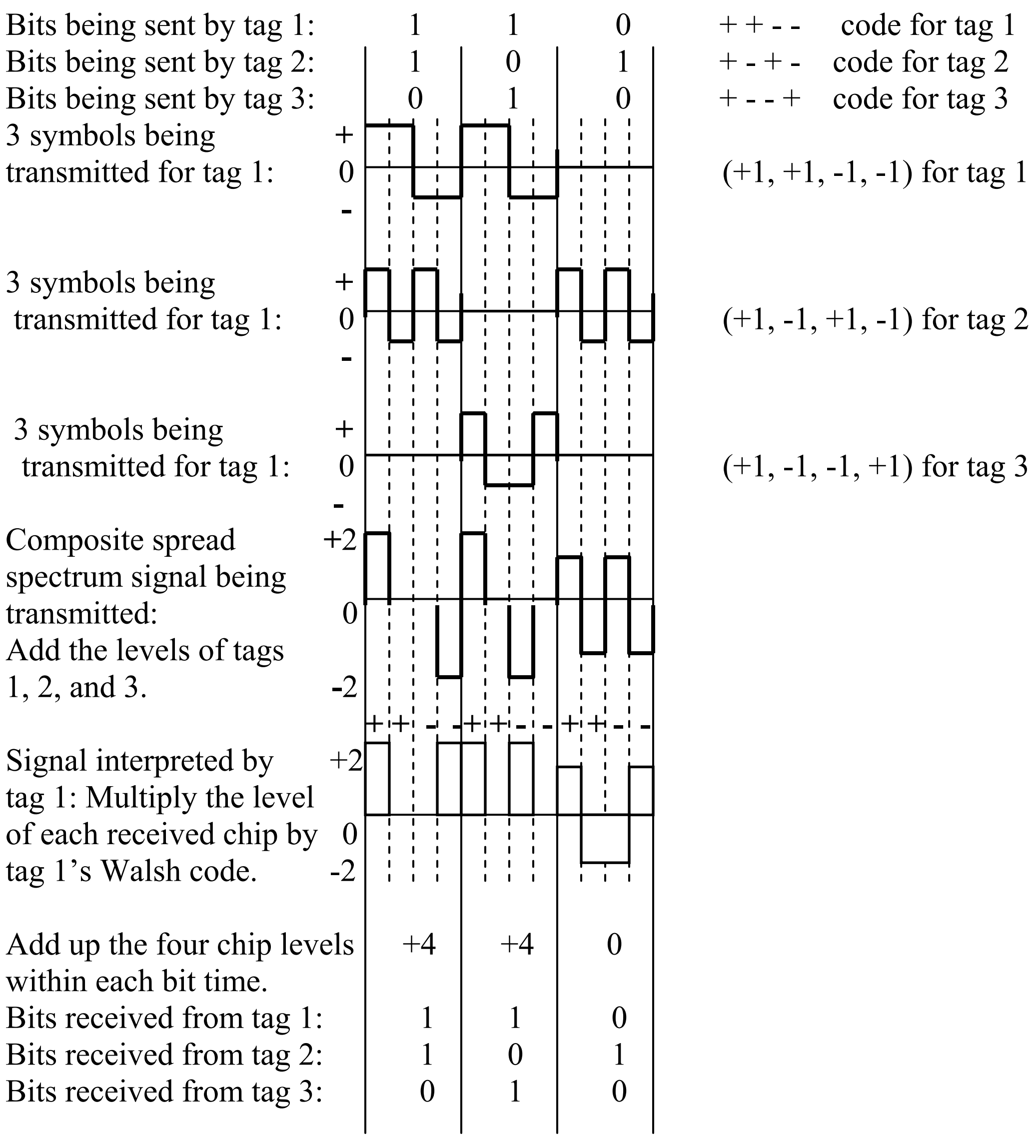

Figure 4.4: Transmission for three users being sent over one carrier and how user 1 interprets it's transmission to be "110."The codes for each user are shown in the inset[1].

4.4 POWER CONTROL IN CDMA

In the typical cellular telephone CDMA implementation, the power output of every user must be maintained at essentially equal levels regardless of the proximity of the user to the base station. Without power level management, it might result to what is referred to as *near-far interference*.

"Near-far" refers to the ratio of signal strength from a near user to the signal strength of a user that is far away. This is especially critical for the CDMA implementation because multiple users share the same frequencies. Near-far interference degrades performance, reduces capacity and causes loss of RF links. The ratio of received signals at the base station is given by [24]

$$\frac{RSSI_1}{RSSI_2} = \left(\frac{d_2}{d_1}\right)^{\gamma} \tag{4.4}$$

where

$RSSI_1$ = received signal from user 1

$RSSI_2$ = received signal from user 2

d_1 = distance between user 1 and base station

d_2 = distance between user 2 and base station

γ = path-loss slope

This simply means that if d_1 and d_2 are not the same, the received signal will be different depending on the propagation environment and the respective distances. For example, if $d_2 = 4d_1$ and $\gamma = 4$ (a typical dense urban environment), the received signal from user 1 will be 256 times (24 dB) stronger than the received signal from user 2, and the base station will be unable to recover the signal from user 2. Hence, there is a need to constantly control the power level from every mobile transmitter.

4.4.1 Multiple Access CDMA

The main characteristic of multiple access CDMA is that the codes assigned to each user are orthogonal, which means the multiple users do not interfere with each other transmitting in the same medium. The receiver does not receive the individual transmitted signal from each user rather it receives the composite of the signals from all of the users. The unique code from each user is used to multiply the composite signal in order to recover information. The power control process from the previous section makes the recovery of individual messages from the composite possible.

In mobile applications, the power level of each mobile station (MS) is adjusted to maintain power equality, when viewed from the receiver, with the remainder of the MSs in the same cell. This is done by increasing or decreasing the power of the MS every few seconds. A similar process is implemented in this work where the power level of each transmitter is adjusted by position such that essentially equal power (viewed from the receiver) is transmitted among all transmitters to avoid multiple access interference (MAI) among transmitters grouped by a logical methodology. In an RFID checkout application, only the items in the cutomer's cart are to be read. Figure 4.10 is a setup for multiple transmitters transmitting different codes to a common receiver. It is possible to recover information from each transmitter within the appropriate logical group because of the unique code. The proper control of the power levels of each transmitter avoids reading from the improper logical group. A typical cart and aisle scenario is shown in the Figure 4.7, and the idea is for the correct information to be read even when a signal from adjacent aisle may typically be reaching the reader. An appropriate tolerance is given for the total power received at the reader for a near cart so as not to be distorted by signal from a far cart.

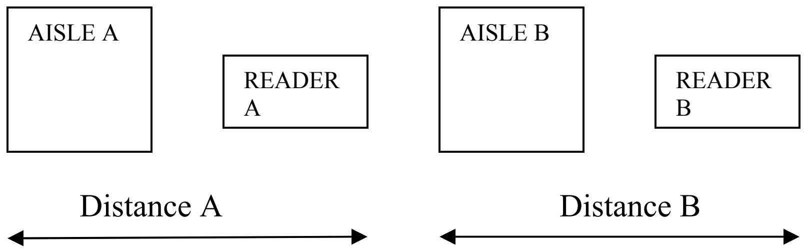

Figure 4.7: Showing a typical aisle arrangement

4.5 CDMA PRODUCT IDENTIFICATION

Human creativity and inventions through numerous innovative ideas has resulted in to an amazingly large number of "objects" in almost every environment, from plants and animals tagged in the forests and seas to the homes, offices, stores and industries in the most advanced cities. These all together create a very large inventory to keep track of which calls for a better and more effective way of accomplishing this goal, by way of proper record keeping and speedy information retrieval. For this purpose, open standards, protocols and languages are being created to facilitate the formation of a new "Internet of Things". This is envisioned to be an intelligent infrastructure which automatically and seamlessly links physical objects to the global internet. This intelligent infrastructure has four major components: (1) Electronic Tags, (2) Electronic Product Code (EPC), (3) Physical Markup Language (PML) and (4) Object Name Service (ONS).

This section of the dissertation is directed toward how the effective implementation of a system capable of simultaneously reading multiple RFID tags can play a significant roll in accomplishing this vision.

4.5.1 The Electronic Product Code (EPC)

A product numbering scheme is required that can provide unique identification for physical objects, assemblies and systems. Information is not stored directly within the code, but rather the code serves as a reference for networked (or internet-based) information. The code is an address that tells a computer where it should go to find information on the internet.

The EPC is an extension of the existing Universal Product Code (UPC) or European Article Number (EAN), currently used by manufacturers to identify products [11].

The UPC and EAN codes are both made up of two components parts:

A manufacturer identifier

A product identifier

The EPC is made up of:

A manufacturer identifier

A product identifier

An item serial number

Scientists at The MIT Auto ID center have proposed a 96 bit numbering scheme including an 8 bit header and three data partitions, as shown below

X.XXX.XXX.XXXXX

HEADER.MANUFACTURER.PRODUCT(SKU).SERIAL NUMBER

Header: 8 bits

Manufacturer: 24 bits or 16 million+ unique IDs

Product(SKU): 24 bits or 16 million+ unique IDs

Serial Number: 40 bits or 1 trillion+ unique IDs

The sizes for partitions are clearly depiction of the large number of manufacturers, products, and items that can be addressed. By interpretation, we can assert that for every one of the 16 million + unique manufacturers there are the possibility of 16 million + unique products and for each of the 16 million + unique products there are possibly 1 trillion + addressable items. This is good indication of large addressable inventory which currently there doesn't seem yet to be enough items to exhaust the size.

4.5.2 Size

The number of bits in the EPC determines the theoretical upper bound on identifiable objects. This upper bound is given by

$$N = 2^n \tag{4.5}$$

where, N is the total address space, and n is the number of bits in the code.

Partitions in the EPC reduce the practical address space because under utilized segments produce gaps in the subsequent section. Assuming a uniform utilization rate within each partition, the total address space is [11]

$$N = f_1 2^{n1} * f_2 2^{n2} * \ldots * f_m 2^{nm} \tag{4.6}$$

where,

f_I is the utilization rate

n_i is the number of bits for partition i

m is the number of partitions

For uniform utilization over uniform partition, the reduction in address space is

$$R = f^{m} \tag{4.7}$$

Address space is thus reduced exponentially by the number of partitions, and therefore the partition count should be minimized

Table 4.3: Seven Varieties of EPC^{TM}

EPC^{TM} TYPE	**VERSION SIZE**	**VERSION NUMBER**	**DOMAIN MANAGER**	**OBJECT CLASS**	**SERIAL NUMBER**	**TOTAL**
EPC-64- TYPE I	2	01	21	17	24	64
EPC-64- TYPE II	2	10	15	13	34	64
EPC-64- TYPE III	2	11	26	13	23	64
EPC-96- TYPE I	8	0010 0001	28	24	36	96
EPC-256- TYPE I	8	0000 1001	32	56	192	256
EPC-256- TYPE II	8	0000 1010	64	56	128	256
EPC-256- TYPE III	8	0000 1011	128	56	64	256

From Table 4.3 we can draw the simple conclusion that EPC-64-TYPE I, II, and III can be implemented using the current 64 bit Walsh code. Figure 4.8 gives a pictorial illustration of the bit distribution into four partitions.

96 bits

8	24	24	40

64 bits type I

2	21	17	24

64 bits type II

2	15	13	34

64 bits type III

2	26	13	23

Figure 4.8: The Code Structure Showing; Version – Domain manager – Object class – Serial number

The number of bits in each of the last three of the partitions in Figure 4.8 may be set to accommodate different distributions of inventory. In other words, for example to cater to more manufacturers with lesser products *type III* becomes more suitable. To address lesser number of manufacturers having larger number of product lines *type I* at this instance becomes more suitable. For fewer manufactures and fewer products having larger items *type II* at this point becomes the partitions of choice. These multiple partition types give the EPC much flexibility and the header (first partition) also simplifies the implementation by defining the partition type at the beginning of every packet.

4.5.3 Partition

Partition reduces address space, yet greatly increases the efficiency of searching through the address space. Suppose we have catalog or cross reference of EPC and network information reference, such as uniform resource locators (URLs), the size of any given catalog is given by

$$C = 2^{ni} \tag{4.8}$$

where C is the catalog size and *ni* is the number of bits for each partition *i*.

4.6 ANTI-COLLISION METHOD

A greater part of the advantage of electronic product identification is hinged on the speed of reading, which in turn emanates from the ability to read multiple objects simultaneously. The Auto ID Lab implemented a binary tree scanning anti-collision protocol that is an implementation of a "reader talk first" methodology, where the simultaneous replies to a reader's interrogation represent a contention for reader attention (collision) yet need not represent a loss of information. The protocol is a contention-resolving and collision-free method for negotiating data from the multiple tags. The reader-to-tag communication is accomplished using an amplitude modulated (AM) carrier, and the tag-to-reader communication is accomplished through the passive backscatter of the tag-to-reader carrier to produce widely separated sub-carrier tones.

In this method a population of tags to be read by the reader is presented as a binary tree descending from the "root" at the top, with "branches" leading downwards to more "nodes". Through this procedure of scanning the tree from root to leaf fully defines an EPC™, and hence a particular item, terminating nodes at the bottom represents leaves where products may be present. In this method the MSB of the EPC^{TM} is placed adjacent to the root of the tree. The LSB by default is considered to be at the leaf of the tree. We can see in Figure 4.9 how a unique path through the tree defined by the EPC^{TM} of a particular product.

This technique regards a node as *populated* if there are branches from the node descending to a product or it is a bottom node corresponding to a product, otherwise the node is described as *unpopulated*. A populated node is further classified as *singly populated* if only a single branch leading to a product descends from it, or *multiply populated* if more than one branch descending from it leads to a product.

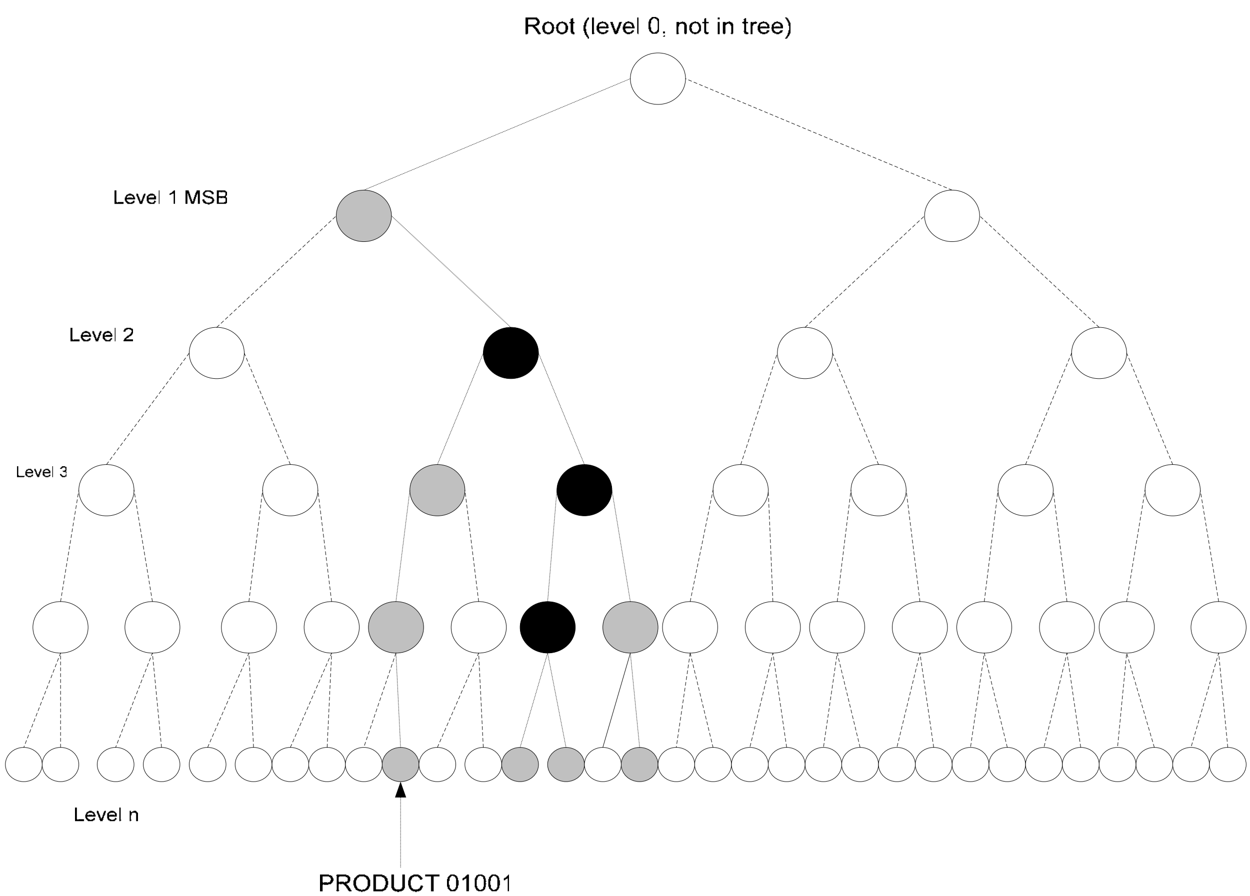

Figure 4.9: Representation of an EPC^{TM} as a Tree

It is assumed here that there is one reader in communication with all the tags of the population and interference among tags, or "masking" or "cloaking", is possible but highly unlikely to occur. The masking of weak tags-to-reader signals by strong tag-to-reader signals is avoided completely in the subcarrier tone encoding method employed, but destructive interference between tags of equal strength can occur, but only with low probability[30]. Although destructive interference may occur in the tag-to-reader data link, it can only be intermittent as changes in the reader-to-tag carrier frequency, and drift in the internal tag subcarrier tones, can always be counted on to eliminate destructive interference masking[30]. The operation of multiple readers may jam both the reader-to-tag and tag-to-reader data links, but proper reader design and the speed of the protocol can mitigate these inherent problems.

The multiple access CDMA technique provides an efficient and effective way of resolving both "masking" in the reader-to-tags and tags-to-reader cases, and the multiple reader cases. This is possible because of the inherent interference rejection characteristics of CDMA systems.

4.7 CDMA REDUCING MULTIPLE READ TIME

The read time sequence for the current reader to tag dialog can be illustrated as follows:

Consider an 8 tags 3 levels binary tree reading system.

To read the first tag

Reader Transmits – (Respond if you are out there)

8 tags respond – (Collision occurs)

Reader Transmits – (All 0s at level 1 don't respond)

4 tags respond (Collision occurs)

Reader Transmits – (All 0s at levels 1 & 2 don't respond)

2 tags respond – (Collision occurs)

Reader Transmits – (All 0s at levels 1, 2, and 3 don't respond)

1 tag responds – (No collision)

This illustrates the number of reader transmission and tag transmission involved in the dialog to read just one tag. To read the eight tags in this example a total of 32 transmissions from the reader and a total of 32 responses from the tags is required. Applying the CDMA RFID methodology to the same 8 tags scenario the following is the result:

Reader Transmits – (Respond if you are out there)

8 tags respond – (No Collision)

The result is 1 reader transmission and 1 simultaneous 8 tags response compared to 32 reader transmissions and 32 tag responses.

When the number of tags grows very large there is a good possibility that it might not be possible to read all tags at once using the CDMA RFID methodology. Under such a condition, multiple reading of different sets of the tags becomes necessary. However, the total number of reads is drastically reduced. The example below gives an illustration of the CDMA reducing multiple read time sequence.

0 0 0 0 0 0 0 0
1 1 0 1 0 1 0 1
1 0 1 1 0 0 1 1
0 1 1 0 0 1 1 0
1 0 0 0 1 1 1 1
0 1 0 1 1 0 1 0
0 0 1 1 1 1 0 0
1 1 1 0 1 0 0 1

From the above eight chip sequence, one way to create a multiple read sequence is to switch OFF all tags whose first chip, 2^7, is a “0”. This will leave only 4 tags out of 8 tags responding. Using the 8 chip example, any of the chips 2^0 to 2^7 can be used to switch OFF a set until all possible number of sets are read.

However, this concept can be extended in general to the situation illustrated below

$$\left|2^{m+2^3}...2^{m+1}2^m\right\|...\left\|2^{23}...2^{17}2^{16}\right\|2^{15}...2^9 2^8\left\|2^7...2^1 2^0\right|$$

By fixing and sequencing bits 2^{m+2^3} through 2^3, in the worst case, eight tags can be read simultaneously. Next, fix 2^{m+2^3} through 2^{16} and 2^7 through 2^0, again eight tags can be read simultaneously, etc.

Given a full binary tree, the number of reads can be drastically reduced. For example, assume a full tree of 24 bits. The maximum number of required reads is 2^{24}. However, with a 2^3 CDMA slice of simultaneous reads only on the least 8 significant bits, the maximum number of reads is 2^{16}. With a 2^4 CDMA slice, the maximum total number of reads is 2^8.

Thus, the maximum number of reads is reduced by $2^n / 2^S$

Where S is the number of CDMA codes within the CDMA slice. Thus the maximum number of reads with a CDMA slice of S bits is given by

Maximum number of reads = 2^{n-S}

4.8 CDMA RFID HARDWARE DEMONSTRATION

In order to demonstrate the concept developed in this dissertation, a hardware tag simulator has been designed as shown in Figure 4.10. Each group of transmitters can be output directly to an antenna. This simulates the tag from the logical group to be read in the proper aisle. Each group of transmitters can have the power to the antenna attenuated so as to simulate a cart in the next aisle that may be triggered by a transmitter in another aisle.

In Figure 4.10 switches SW1 to SW8 are used to select one of two paths. The first path is a short circuit path that connects the RF output pin of the transmitter directly to the antenna thus transmitting at a full power level. The second path connects the RF out pin of the transmitter to potentiometers R1 to R8 for the purpose of adjusting the output power of the transmitter. This power adjustment simulates the weaker signal coming from a more distant cart where the purpose is to demonstrate the situation of reading the correct information without influence from the weaker signal.

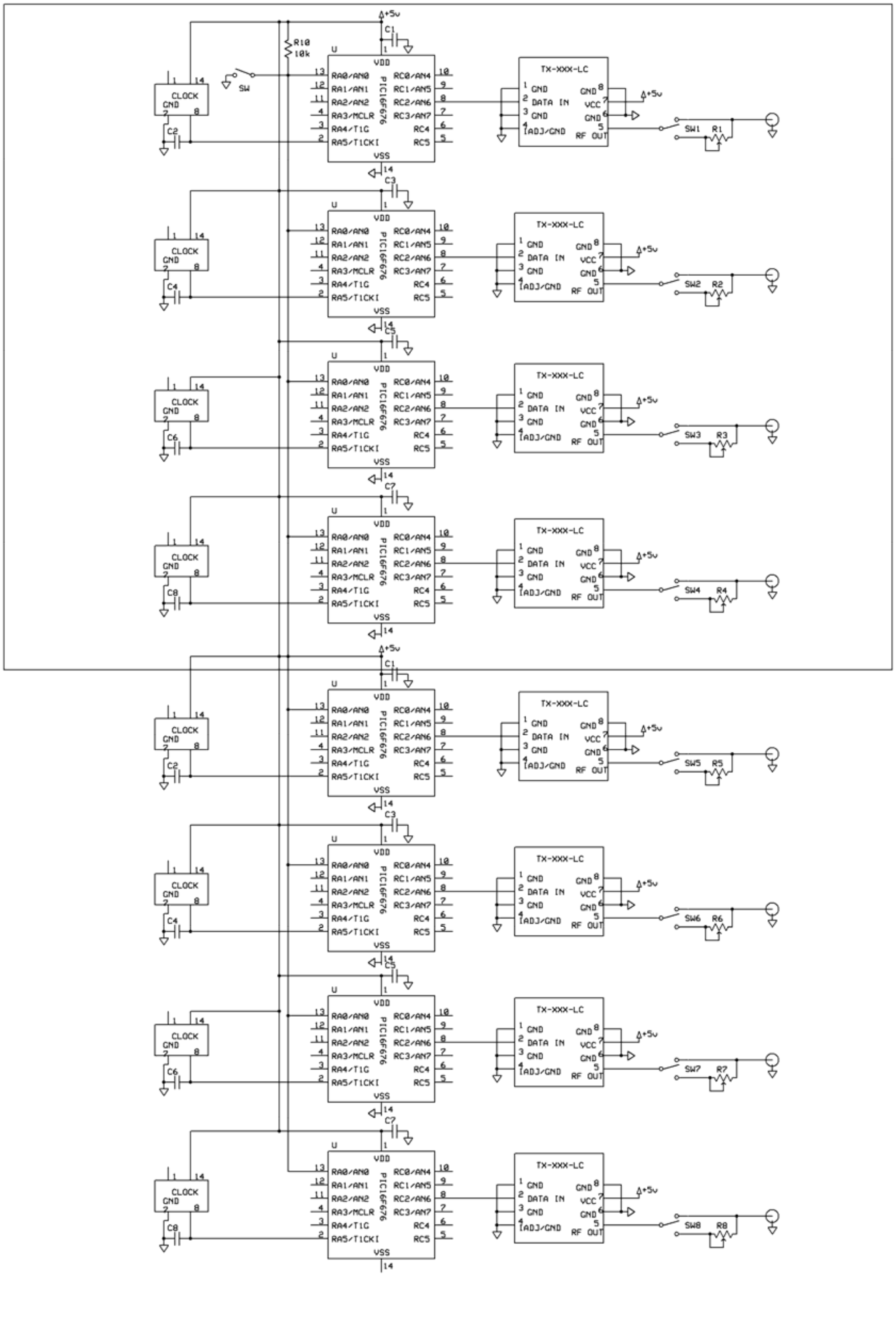

Figure 4.10: Multiple transmitters with unique codes to transmit simultaneously

5.0 RADIO FREQUENCY PRODUCT IDENTIFICATION

5.1 RADIO FREQUENCY IDENTIFICATION (RFID)

A basic radio frequency identification (RFID) system consists of three components, an antenna or coil, a transceiver, and a transponder or RF tag electronically programmed with unique information. Data within the tag provides identity for an item in manufacture, goods in transit, a location, the identity of a vehicle, even plants, animals or human. A system requires a transceiver for reading or interrogating the tags and a means of communicating data to a host computer or information management system.

There are two types of RFID systems based on their operations; passive powered and active powered.

5.1.1 Passive Power

The passive RFID does not have an internal power source, but instead relies solely on the energy from the electromagnetic field created by the propagating RF signal from a reader. This has positive implication on cost, lifetime and the environmental situation. Passive RFID either (1) reflects energy from the reader or (2) absorbs and temporarily stores a very small amount of energy from the reader's signal to generate its own quick response. In either case, passive RFID operation requires relatively strong signals from the reader, and the signal strength returned from the tag is constrained to relatively low levels by the limited energy.

5.1.2 Active Power

Active RFID uses an internal power source (battery) within the tag to power the tag and the RF communication circuitry. This provides a higher operational range and extended functionality. Active RFID allows relatively low-level signals to be received by the tag (because the reader does not need to power the tag), and the tag can generate high-level signals back to the reader, driving from its internal power source.

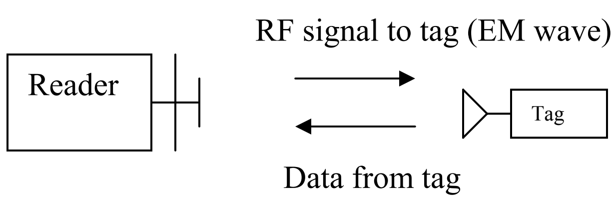

Figure 5.1: Basic principle of RFID system

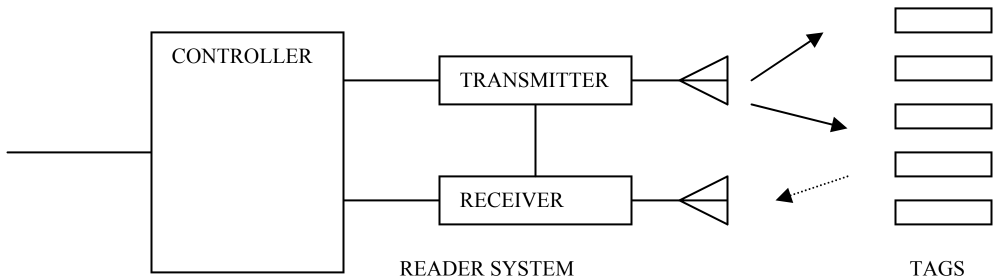

Figure 5.2: Illustration of a Multiple Tag Reading System

5.2 RFID OPERATING PRINCIPLE

The reader transmits an electromagnetic wave (EM), which propagates towards the tag at an appropriate distance. The tag is then immersed in the propagating wave and collects some of the energy as it passes or is reflected. The amount of energy available at any particular point is related to the distance from the transmitter and may be expressed as being proportional to $1/d^2$ where d is the distance from the transmitter. The amount of energy collected is a function of the aperture of the tag antenna, which is related to the wavelength of the received signal [10].

Compared to other identification technologies like the barcode and smart card, RFID is gaining popularity due to its promising features, which includes embeddable, remote read/write, and multiple reading capabilities.

5.2.1 Embeddable

Line of sight is not necessarily required for the RFID reader to read the tags. RFID tags can be embedded in non-metallic items like wood and concrete blocks. One of the major areas of the application of RFID tag is the replacement of the bar codes currently used to identify items, type and manufacturers. The bar code as it is now often suffers physical and mechanical wear and tear which renders it unreadable and useless. The RFID tag because of its embed-ability can survive all the transit and warehouse environments that goods and merchandise normally encounter.

5.2.2 Remote Read/Write

The RFID tag system does eliminate distance between the tag and the remote reader that might be within the *readable distance* but beyond the envelope of influence because of its utilization of the RF medium of communication. Besides reading capabilities, information can be written remotely onto the tags. Tags that are built with the processor programmed to have inherent intelligence can be instructed to either transmit and or store data as required by individual applications. The read/write capability provides more flexibility as the tag can be instructed to perform multiple functions at different moments.

5.2.3 Multiple Reading

Some classes of RFID systems have anti-collision software in them, and this means that a number of tags can be read at the same time. Without any anti-collision, multiple tags attempting to transmit simultaneously will have all of their receive information corrupted and the reader will not be able to decode the various tag trasmitted information. Collision has been a major obstacle in the implementation of simultaneous multiple reads of the RFID tag system, and this is the reason why one of the contributions in this dissertation is the application of CDMA to RFID for the simultaneous reading of multiple tags. The multiple reading also enhances the speed of the system particularly in the case of the CDMA because the same amount of time needed for reading a single tag is used to read multiple tags when read simultaneously. For example, if it takes i seconds to read 1 tag, then in a simultaneous mode it should take the same i seconds to read k tags, where k is any number greater the (>) 1.

5.3 RFID CLASSICIFICATIONS

There are two broad categories of RFID systems, namely nearfield RFID and farfield RFID. When a reader emits a radio frequency (RF) wave by creating an electromagnetic field in the air, nearfield occurs at a distance less than $l/2\pi$ (the radian sphere), where the magnetic field is dominant. Other definitions on the nearfield/farfield boundary are possible. The *l* is wavelength of the RF wave which is frequency dependent [13]. Farfield occurs at a distance greater than *l/2π*, where the electric field is dominant. The antenna used in the nearfield RFID tag is a coil whose physical size has little dependence on the RF energy used. It can be as smaller than 1 cm in diameter. The farfield RFID tag antenna is usually a dipole that idealy is half a wavelength long and is thus dependent on the frequency used. The size of the farfield RFID tag antenna can become smaller with higher frequencies. This becomes important to application engineers in choosing which class to use in specific applications.

Note: It is necessary at this juncture to emphasize the difference between the *nearfield/farfield* described in Section 5.3 and the *near-far interference (effect)* described in Section 4.4. The former is simply a means of classifying the RFID tags using the type of antenna on the tag because of the electromagnetic characteristics of the antenna with respect to proximity to the reader. This classification can be deemed general to the RFID systems. The former refers to the ratio of power from a nearer transmitter (in this case tag) to the power from a more distant transmitter (in this case tag). In the CDMA technique used in this research this is extremely important because the power levels of the tags must be maintained at approximately the same level for all tags to be read simultaneously without inter tag interference.

5.4 CDMA APPLICATION TO READING MULTIPLE RFID TAGS

A major problem with current RFID applications is the reading of multiple tags where only one tag can be read at a time as discussed previously. However, all tags respond when energized unless explicitly told to not respond. The resulting necessary communications between reader and tags consumes a considerable amount of time until the reader protocol completes its service of exchanges with the tags in the tags in the field of influence.

The contribution of this dissertation in this area of research is the ability to read multiple RFID tags simultaneously using CDMA as is done in wireless communication with minimal modification in the typical operation of the overall system. The passive tags are assumed in this case, which means the reader must generate the EM wave with enough energy to activate the tags within distance sufficient to transmit valid tag data to the reader.

Active tags do not typically need the CDMA methodology due to the protocols used where the tags do not depend upon the reader as a source of power. The results of this research may also apply to the active RFID tags with proper measures taken with respect to synchronization, but is not a part of this dissertation.

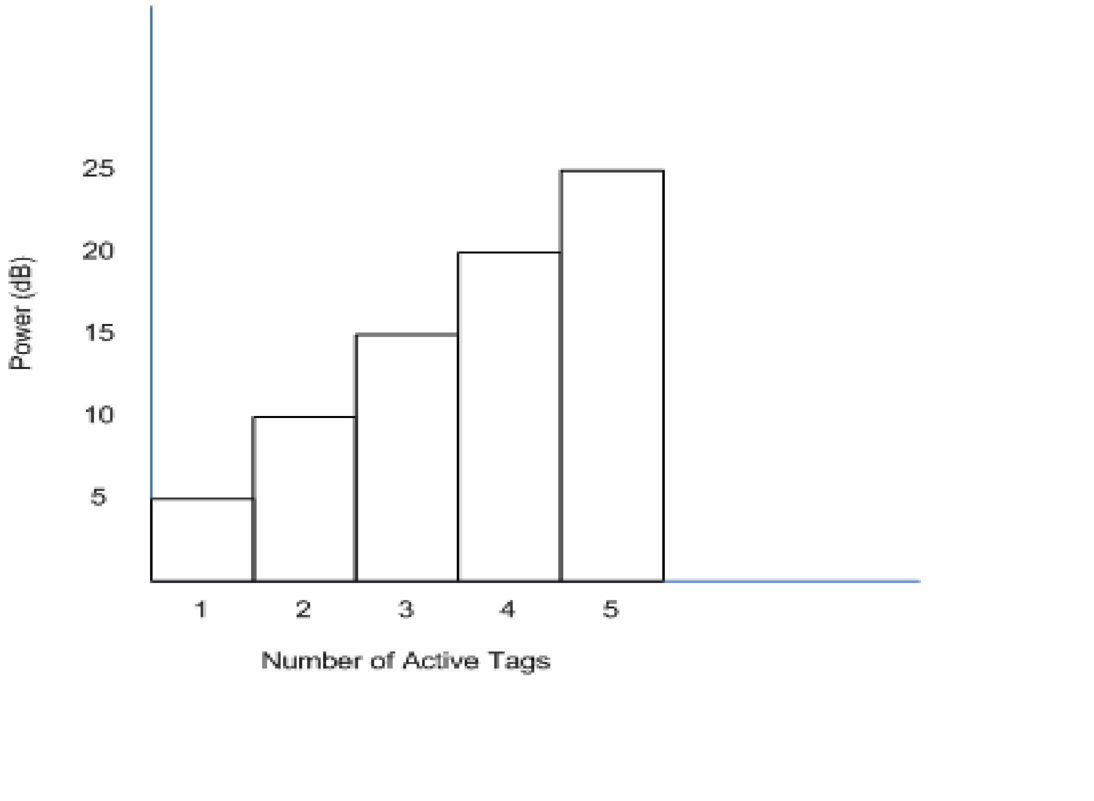

Figure 5.3: Multiple tags combining power while sharing the same frequency bands

Figure 5.3 is an illustration of all tags sharing the same frequency band, the tags are separated by an orthogonal code not a timeslot or frequency. Each tag's communication is spread in the frequency domain, and at the receiver end the tags are de-spread using their own unique codes. The Walsh sequence explained in Section 4.3.2 is used to generate the unique code for each tag. The tag axis indicates the cumulative addition of signals transmitted by all tags.

Figure 5.4 represents symbols each made up of eight chip sequence and the composite level received by the reader. The code symbols for each of the three tags can be written as;

Tag 1 - - - - + + + + and sending "111"

Tag 2 - - + + - - + + and sending “101”

Tag 3 - - + + + + - - and sending “010”

In this example, the negative signs represent a certain power level per chip at the particular point; the positive signs also represent another power level per chip at that specific point. For tag 1 in this instance a bit “1” is sent by transmitting energy level representing the negative sign for the first four consecutive chip times and immediately followed by transmitting energy level representing the positive sign for the next four consecutive times. The eight chips make up the symbol and the detection of the eight chips (symbol) in the combination: - - - - + + + + by the receiver suggests to the receiver that a bit “1” is being transmitted. Leaving the eight chip positions at zero level indicates the transmission of bit “0”. For tag 2 the energy levels representing the symbol - - + + - - + + is transmitted to indicate bit “1” and zero levels for the eight chip time to represent bit “0”. Transmitting energy levels representing the symbol - - + + + + - - for tag 3 suggests that bit “1” has been transmitted and zero energy level for the eight chip times suggests bit “0”.

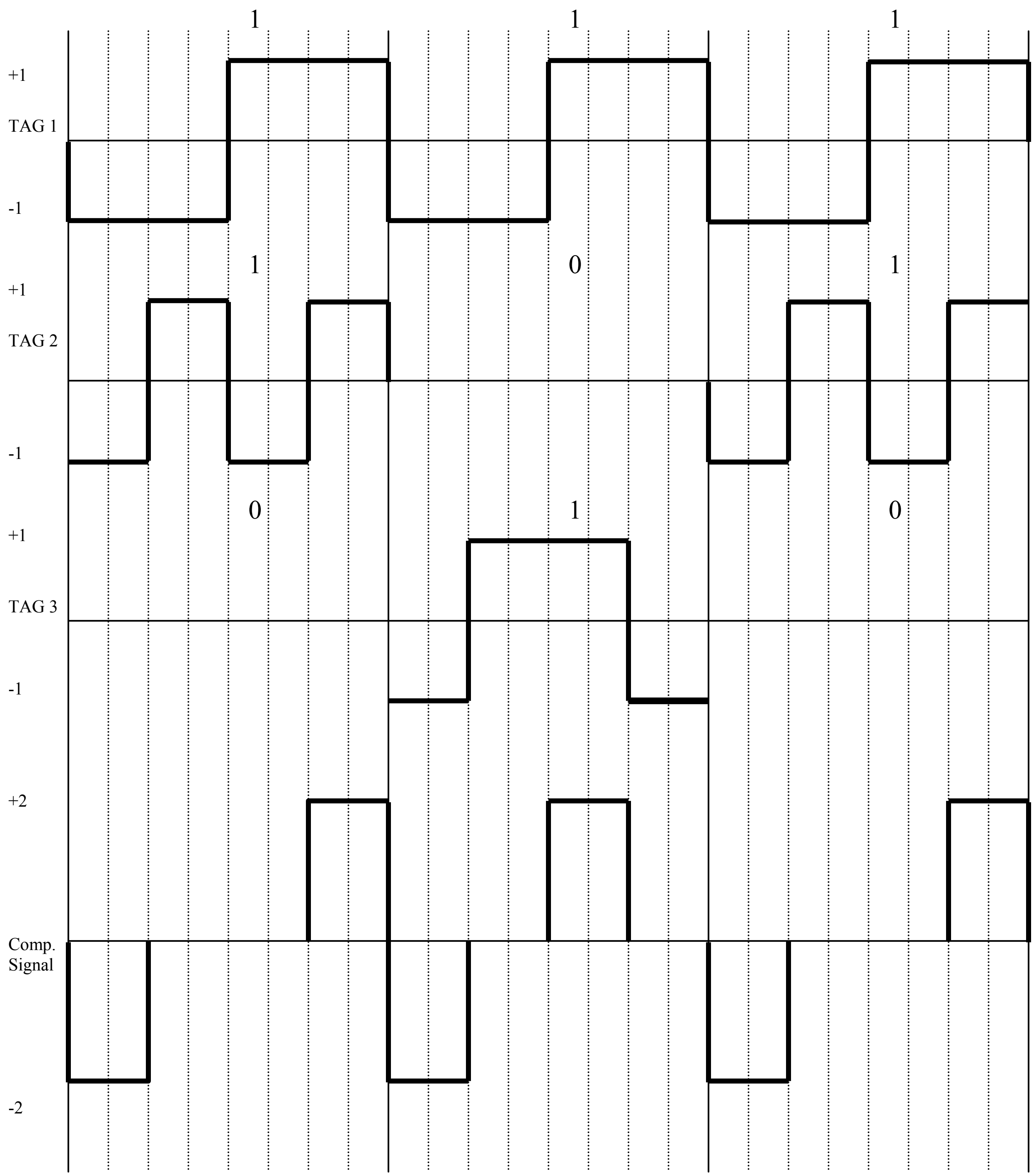

Figure 5.4: Illustration of Composite Energy Levels of Three Tags Communicating Simultaneously

5.5 IMPLEMENTATION

The corresponding EPC code is now encoded using this CDMA coding technique as described in Section 4.6. The CDMA coding technique described in the earlier section is the Walsh code, which is comprised of 64 chips per symbol. It is expected that as the number of users increases the number of chips per symbol will also increase to accommodate more users as needed.

Figure 4.8 in the earlier section is a diagram of the various packet sizes for the numbering system, 64 bits and 96 bits are two of the frequently used sizes currently. For the RFID implementation of the EPC code it is necessary to take into consideration the possible error in the reception of the transmitted information especially due to interference. In the wireless communication systems one of the ways loss of information is minimized is by transmitting fewer bits of information at a time. For the CDMA system interference can also cause the loss of synchronization during transmission.

In this dissertation, we are proposing the division of the packets into smaller 1 byte (8 bits) packets to be transmitted at a time upon an interrogation. This implies that the tags will need reactivation after transmitting every 8 bits until the entire packet is transmitted. This keeps the tags in sync because the probability of interference for short transmissions is relatively low. This opens the possibility of having multiple packet sizes, for example having both 64 bit type and 96 bit type. In this case, the 64 bit type will complete transmission after the 8^{th} interrogation, but the 96 bit type will have to respond up to the 12^{th} interrogation. This arrangement is meant to minimize the chances of loss of synchronization in the simultaneous reading multiple tags, transmission error, while at the same time giving room for flexibility in the sizes of packets being implemented.

Packet 1	Packet 2	Packet 3	Packet 4	Packet 5	Packet 6	Packet 7	Packet 8

Figure 5.5: A diagram of eight separate packets of 8 bits each totaling 64 bits from a single tag

5.6 RFID CHECK OUT AND OTHER DIFFICULTIES

The stores and supply chains represent one of the largest potential areas for the deployment of RFID technology. With most stores demarcated into numerous aisles for overlapping common classes of products with carts being used to move items around and the warehouses segregated into lots with pallets to load products of similar category, it has become very important in this research to analyze the implementation of the technique of CDMA for the simultaneous reading of multiple tags in the cart aisle scenario.

One problem that has not been addressed in the open literature is the lack of a demarcation of read and no read zones in free space for an accurate scanning of an individual cart without placing the cart in a specifically designed RF environment with specially designed RF barriers. In short, if RFID tags work really great, how do you keep a customer in one aisle from paying for items in a cart in a neighboring aisle? One solution is the separation of the aisles by an adequate distance for standard reading scenarios. This is a major flaw in implementing the current level of RFID technology using the existing store layouts of aisle and customer flow.

A typical read range for a passive RFID system is less than 10-20 feet [31]. However, some passive tags can be read at a distance of 35 feet. Read range in this analysis stands for maximum distance within which the transmitted energy of the reader is still strong enough to activate a tag, and the receiver is sensitive enough to read the activated tag. Hence, the read range can be utilized as the first line of demarcation in determining which cart and its contents communicate with the interrogating reader in a given aisle. Assuming the maximum read rage in this case is x feet, we denote any distance greater than x feet ($> x'$) as D_{OR} (distance out of range) and denote any distance equal to or less than x feet ($\leq x'$) as D_{IR} (distance in range). By this definition, it implies that tags on any cart at the range D_{OR} from the reader will not be activated or readable when the reader of interest performs an interrogation. All tags in the cart at the distance D_{IR} from the reader will be activated simultaneously (with the CDMA implementation) and all activated tags will respond simultaneously by transmitting their unique number (ID).

With conventional tags, a relatively small amount of energy can allow the reader to read the tag. With conventional RFID tags, there is no differentiation of signal strength other than read or no read. Thus, there is a wide range of energies all of which are read when interrogated.

Inter tag interference has been one of the persistent problems in most techniques encountered with the simultaneous reading of multiple tags. Multiple access CDMA is a technique that remedies this problem because of its orthogonal coding scheme. The CDMA technique also provides the means of distinguishing tags from two different carts which may be within the D_{IR} distance. The CDMA technique makes this possible without requiring a demarcation of the true/false (1/0) for the vagaries of RF energy. Instead, it introduces a range of discernable energy that can be seen by a receiver and yet not included in the read envelope of influence.

As an example of the concept involved, consider Figure 5.6 that shows a diagram of the voltage ranges representing logical values in the RS232 electrical standard. The range from -3v to +3v is referred to as *transition region*, which means voltage levels within this region will be ignored, and as such will not create any form of interference. In a similar manner in this tag system the distinction is made from their respective energy levels with the ability to receive energy and still differentiate tags accurately without triggering a false read. Thus, it can be "seen" but "seen" under a threshold. The energy level of the most distant tag being lower allows the establishment of a threshold. For the purpose of this work, we set the desired condition of having only one cart within the D_{IR} range. There now exists the potential solution of the problem of the interference from items in carts in adjacent aisles, which may have been activated by either the reader in question or a different reader on an adjacent aisle. Thus, a proper tolerance or threshold is needed to accommodate the additional weaker energy from a far cart that may add to the energy of the cart being read without compromising the reading integrity of the input information. A tag activated by a second reader may introduce too much energy for a threshold established by the first reader in the envelope of influence. Thus, either a more robust threshold must be applied or the reader can be sequenced on a rotating basis, i.e., one reader active at a time. This second alternative is preferred for simplicity and is practical due to the CDMA short read time. This capability is what differentiates CDMA from classical RFID. This tolerance is possible because of the fading effect of the RF signal as it travels a distance. While it is known that several factors contribute to the fading effect, the “Inverse Square Distance Law” among these factors has the most dramatic effect on the strength of the propagated signal. Therefore, in this analysis we will consider only the inverse square distance effect. Other effects will only act to strengthen the result that is obtained. The square distance effect can be seen in Table 5.1, which contains the received signal strength when devices at different distances from the reader all transmit at a 1 Watt power level.

Table 5.1: Illustration of Received Signal at the Reader when Multiple Tags Transmit the Same Power from Different Distances

Distance from Reader	**Transmitted Power**	**Received Power**
2 feet (2′)	1 Watt	0.2500 Watt
3 feet (3′)	1 Watt	0.1100 Watt
4 feet (4′)	1 Watt	0.0625 Watt
5 feet (5′)	1 Watt	0.0400 Watt
6 feet (6′)	1 Watt	0.0278 Watt
7 feet (7′)	1 Watt	0.0204 Watt
8 feet (8′)	1 Watt	0.0156 Watt
9 feet (9′)	1 Watt	0.0123 Watt
10 feet (10′)	1 Watt	0.0100 Watt

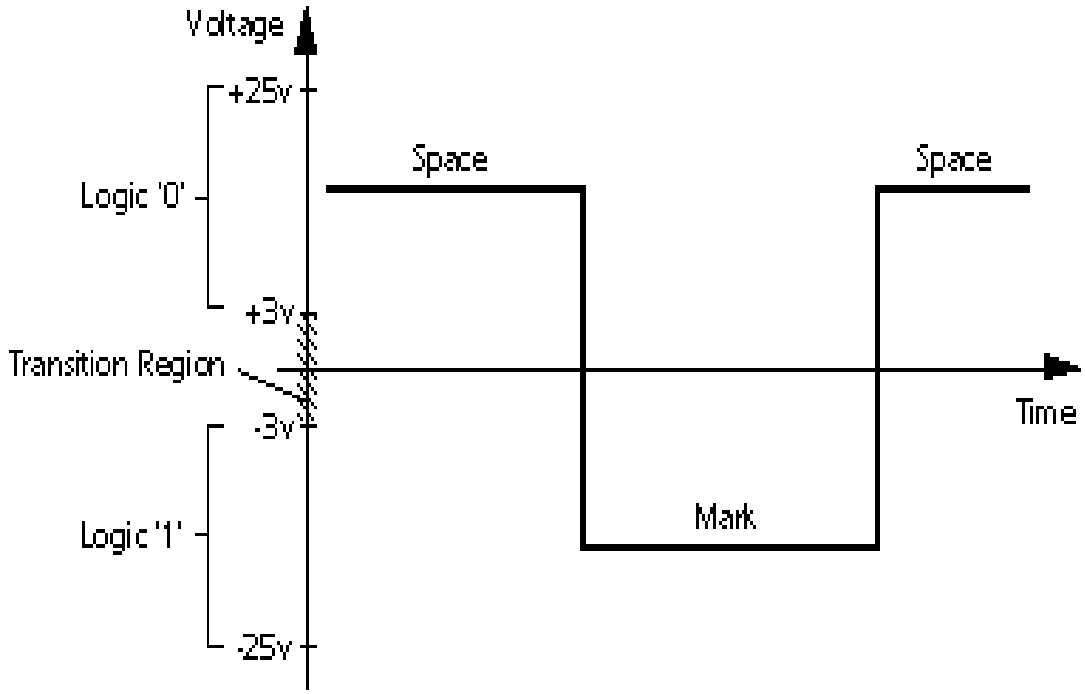

Figure 5.6: Voltage ranges representing logic states in the RS232 electrical standards

5.6.1 Power Spreading

The Walsh code is one of the coding schemes used among others for the spreading of the information energy in the multiple access CDMA technique. Therefore, it is important for reading the correct information in the cart-aisle scenario to understand the spreading process. Hence, it is important to understand the spreading process as shown in Figure 5.7 where one bit is discretized into 8 chips (as an example) and the chips are used to form a communications symbol which represents one bit of information.

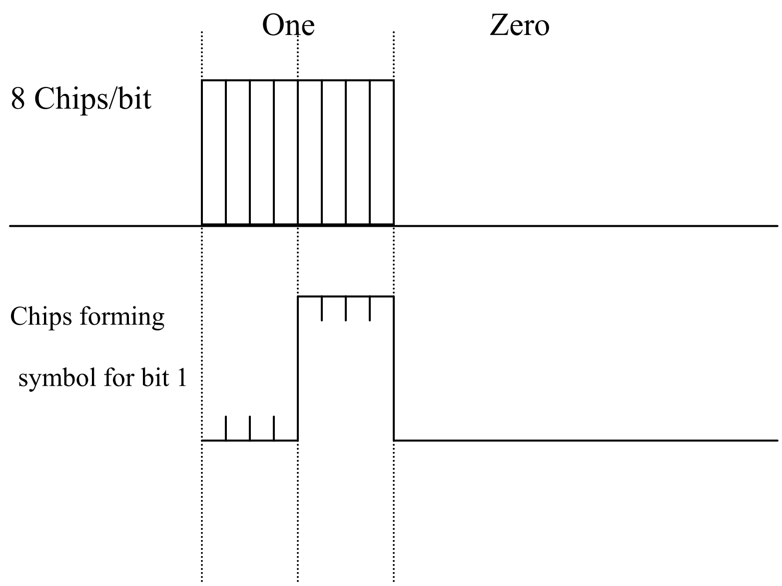

Figure 5.7: The spreading of the energy of a bit into chips for the code - - - -+ + + +

The energy per bit, E_b, can be determined by dividing the carrier power by the bit rate. Using the same approach, the energy per chip, E_c, can be determined by dividing the bit power by the chip rate. Equation 5.1 provides relations between the energy per bit and energy per chip.

$$E_c = \frac{E_b}{N_c} \tag{5.1}$$

where, N_c is the number of chips per symbol. For the EPC code, which we are considering in this work, N_c is 64 and if E_b is 1 watt then

$$E_c = \frac{1}{64} = 0.015625 watt$$

In order to accomplish the implementation of RFID EPCglobal for general RFID applications, it is inevitable that the possibility of interference from an adjacent aisle be not only considered but also be carefully analyzed for total performance. From Table 5.1 we have seen the effect of the "inverse square distance law" on signals transmitted at 1 watt of power, similarly, the effect of distance traveled on the energy level of a single chip can also be seen as tabulated in Table 5.2

Table 5.2: Illustration of Received Signal at the Reader when a Single Chip is transmitted

Distance from Reader	**Transmitted Power(mW) per Chip**	**Received Power(mW)**
2 feet (2′)	15.625	3.9063
3 feet (3′)	15.625	1.7361
4 feet (4′)	15.625	0.9766
5 feet (5′)	15.625	0.6250
6 feet (6′)	15.625	0.4340
7 feet (7′)	15.625	0.3189
8 feet (8′)	15.625	0.2441
9 feet (9′)	15.625	0.1929
10 feet (10′)	15.625	0.1563

5.6 PREVENTING ADJACENT AISLE INTERFERENCE

The previous sections present an analytic approach to adjacent aisles. Interference in terms of received energy from a cart in an adjacent aisle can be eliminated by maintaining a "clear" distance between aisles. Clear distance in this instance simply means any distance at which signal from any aisle does not interfere with reading process at any of the aisles next to it. There are several possible ways to accomplish the non interference among aisles, but in this analysis we will look at two scenarios. The first is the *clear distance technique* and secondly the *directed signal technique*.

5.6.1 Clear Distance Technique

In this method, the transmitted energy per bit E_b is used to determine the transmitted energy per chip E_c because it is the chip sequence that is used to formulate the transmission symbol for each tag. The power per chip can further be divided by the number of simultaneously transmitting tags which in this instance is 64, so

$$E_s = \frac{E_c}{64} \tag{5.2}$$

where, E_s is the safe power. Using Equation 5.2 and the calculated energy per chip of 15.625 mW, we now have

$$E_s = \frac{15.625mW}{64} = 0.2441mW$$

as safe power to be received at any adjacent aisle. This means that if all 64 tags from an adjacent aisle transmit all 1s simultaneously at the same chip point the cumulative energy received at the adjacent reader will be seen as a single tag transmitting rather than the actual 64 tags because the energy adds algebraically to give 15.625 mW which is the energy of a single chip. From Table

5.2, we see such a safe distance to be at distances ≥ 8 feet, when the fading effect of the inverse square law is used because at 8 feet and over the energy level of the signal in this example is at a level equal to or less the energy of one chip divided by 64. Therefore, the spacing between aisles will be assumed to be ≥ 8 feet.

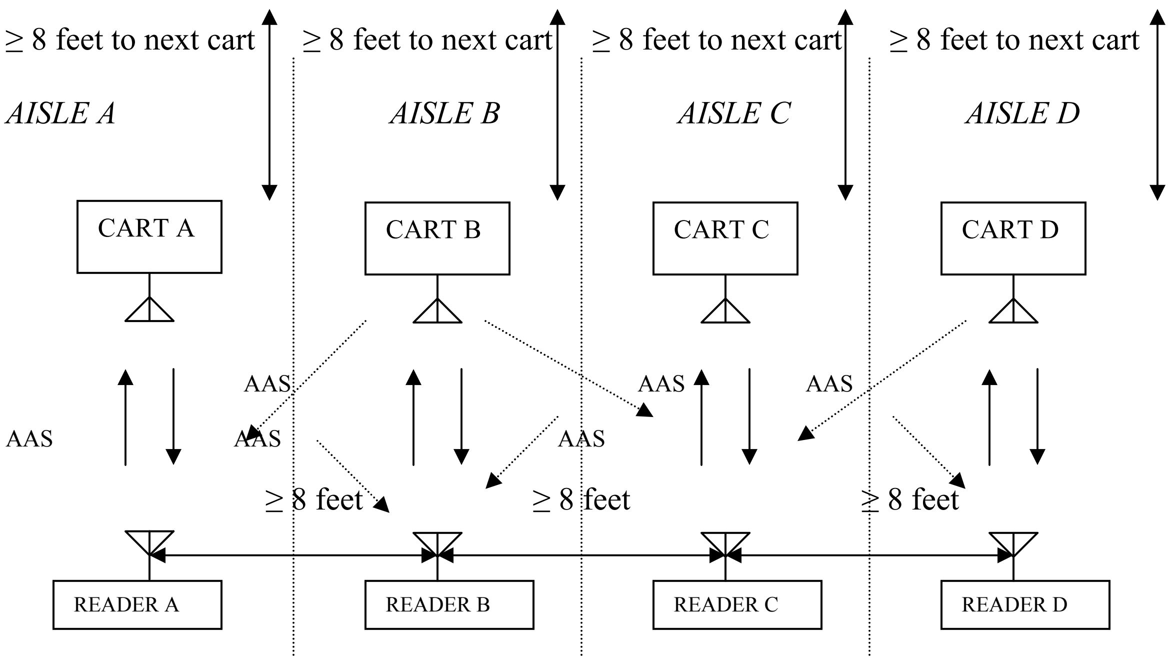

Note: AAS = Adjacent Aisle Signal

Figure 5.8: A Diagram of the Clear Distance Aisle Scenario

5.6.2 Directed Signal Technique

In this section, the signals from both the reader and the tag could be assumed to be both focused ahead in only one direction rather than being isotropic. Designing the system to transmit uni-directionally ensures the tag and reader signals to ideally travel parallel to the other and that eliminates interference among adjacent aisles. Unfortunately uni-directional flow of signal is not feasible in the aisle case because under normal circumstances customers will not and should not be expected to perform checking and aligning the tag antenna orientations in any particular direction. Therefore, it is safe to assume that in a typical cart containing multiple items that some of the signals will definitely travel in the direction of the adjacent aisles. Hence this needs to be addressed in this consideration.

One of the means for resolving the problem under consideration in this dissertation is to implement *readers to synchronize* by simply time multiplexing the reader in all the aisles. This means that at any instant, only the reader in one aisle is reading and sequentially the next reader from the next aisle commences reading the next clock cycle after the previous reader. Another consideration that must be taken into account in a cart is the tag orientation with respect to the reader antenna of interest with the possibility of some of the items in the cart being perpendicular to the reader at such instance the reader might not be able to reader from such item. As a solution to this problem an array of cooperating readers is formed using three readers with one placed at the front of the aisle (or overhead) and two placed one each at the two adjacent walls of the aisle. The three readers are connected together such that they function as one reader, hence the term cooperating readers.

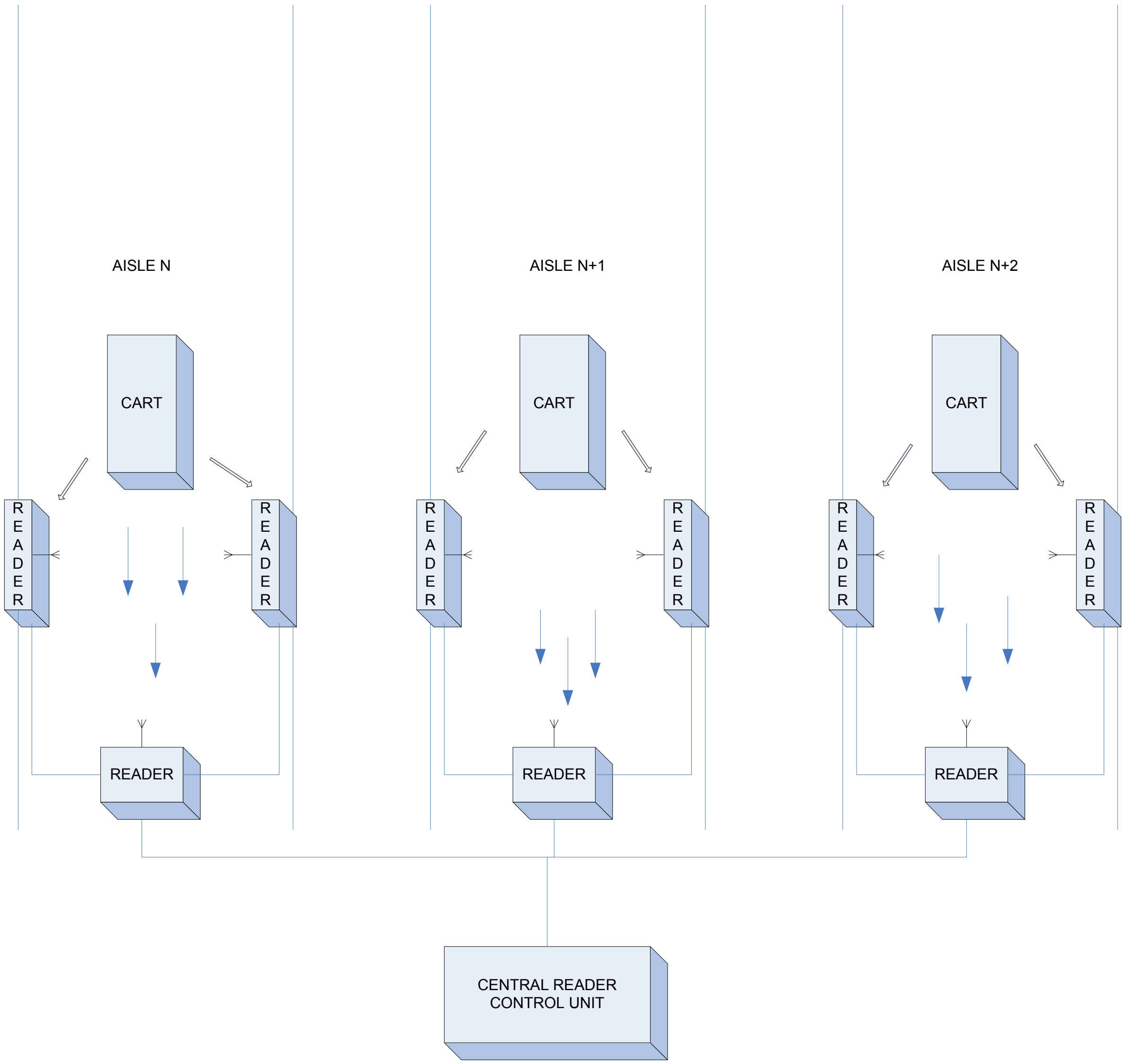

Figure 5.9: A diagram of the directed signal technique

Figure 5.9 illustrates the arrangement with one central reader control unit (CRCU) which performs the duty of synchronizing the readers from all the aisles such that no two readers (two adjacent aisles) function simultaneously. By this method any signal from an adjacent aisle, even if detectable, will arrive when the reader has been momentarily switched off by the CRCU, thereby rendering the signal from the adjacent aisle to be non-interfering.

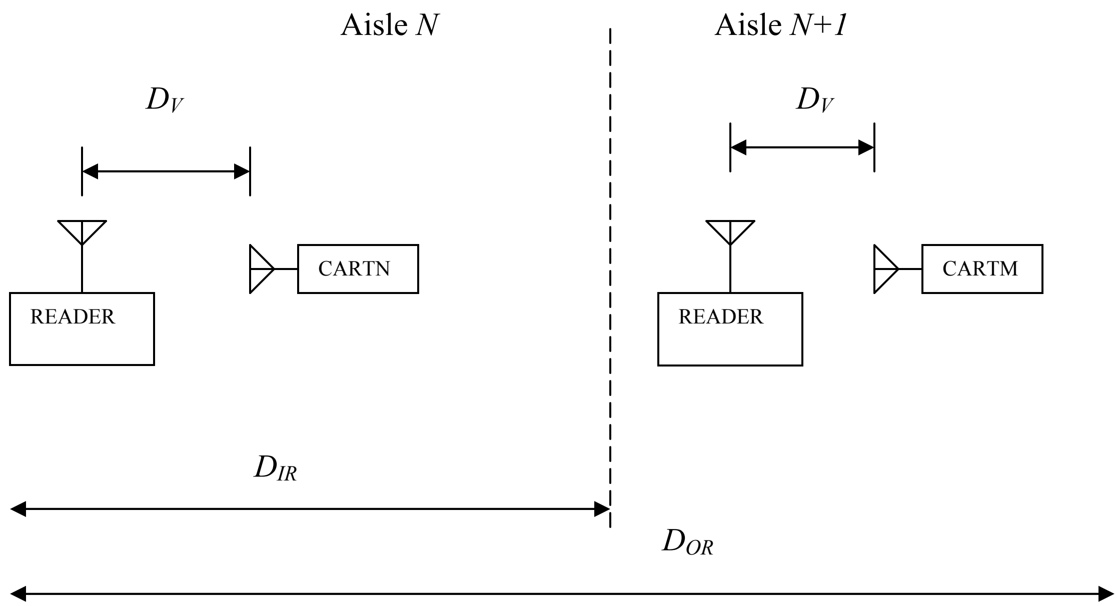

Figure 5.10: An illustration of reading distances from multiple aisles to avoid interference from adjacent aisles

A cart in the checkout location of a store contains numerous items that need to be read rapidly which implies simultaneous reading either as the cart passes the reading location (station) or being read with a handheld scanner. However, it must be kept in mind that the primary value of the CDMA implementation is the ability to overcome the problem of the integrity of the zone of influence (read space) from overscanning, i.e., reading unintended RFID tags. The proposed RFID implementation of CDMA is so far the only known technology that can read individual items simultaneously. Through the process of correlation, the reader systematically connects to the tags within the read range, D_{IR}. As we have seen in Section 5.4, the Walsh code provides excellent separation of transmitted channels. A CDMA reader to which a particular Walsh code was assigned, is able to pick out the data signal that was intended for it. This phenomenon is called auto-correlation [32, 33]. The reader is also able to reject signals which were not intended for it; this is called cross-correlation [32, 33]. This correlation process through the process of normalization, that is, taking the product of the unit code of the respective tag with the composite received sequence. When the unique code is not part of the composite sequence the product give a zero, but if the unique code is part of the composite received sequence then a one or a higher order of one is the result.

The Walsh code requires very precise synchronization among all the transmitted channels. Hence, it is the best candidate for implementing simultaneous reads of multiple "passive RFID tags". Thus, the simultaneous powering of the multiple passive tags provides an inherent and convenient control of synchronization of their transmitted channels.

5.7 PHYSICAL CONCEPT

An analysis of some of the problems that may be encountered in a typical store implementation of RFID technology is presented in this section. While it may not be practical to solve every possible scenario at this moment and in this work, it is feasible to look at a *worst case scenario* that may enhance the appreciation of the problem. An in-depth analysis of the chip energy of the items in a cart is carried out in this section. The result of this analysis facilitates the proper and reliable means of establishing adequate read range between reader and cart and also the inter aisle distance which enhances the ability to avoid the erroneous charging of customers.

CDMA provides a feasible method of reading tags from one cart without the problem of reading tags from a cart in an adjacent aisle. Examples of some of the likely scenarios are depicted in figures 5.11, 5.12, and 5.13. Figure 5.11 illustrating an instance in which cart *A* from aisle *A* contains eight items placed at eight different positions horizontally in succession creating eight different distances from the reader antenna. Because of the different positions of the items in cart *A*, eight different energy levels will be received by the reader whenever each one of the eight transmits separately. At the same time, items from cart *B* from the next aisle *B* might have been turned on and are simultaneously transmitting their required information. The goal of this part of the research is to insure the act of reading involves (identifies) items from only the intended (correct) cart without the mistake of reading tags and adding charges from a cart in a nearby aisle.

First, we investigate the relationship among the energy levels of the items in cart *A* of aisle *A*, in this example, eight items are placed at eight different positions horizontally (perpendicular) in relation to the reader antenna. As such, eight different energy levels are produced with the highest level coming from the item (tag) nearest to the antenna and the lowest energy level coming from the item (tag) farthest from the reader antenna. The difference in energy levels can be explained by the fading effect of the radiated signal which in turn is given by the inverse square law (distance) and/or the radar equation. The received power is expressed as in equation 5.3 which is the radar equation.

$$P_R = P_T \left[\frac{\lambda}{4\pi D} \right]^2 G_T G_R \tag{5.3}$$

In equation 5.3, P_T and P_R are transmitted and received power respectively, and G_T and G_R are transmitter and receiver gain respectively.

Figure 5.11 is a diagram of eight items in a cart communicating with the interrogator. It also indicates the various energy levels, starting from instances when single items are communicating with the reader to the instances when multiple items are simultaneously communicating with the reader. The energy levels in figure 5.11 each represent the energy of a single RFID tag.

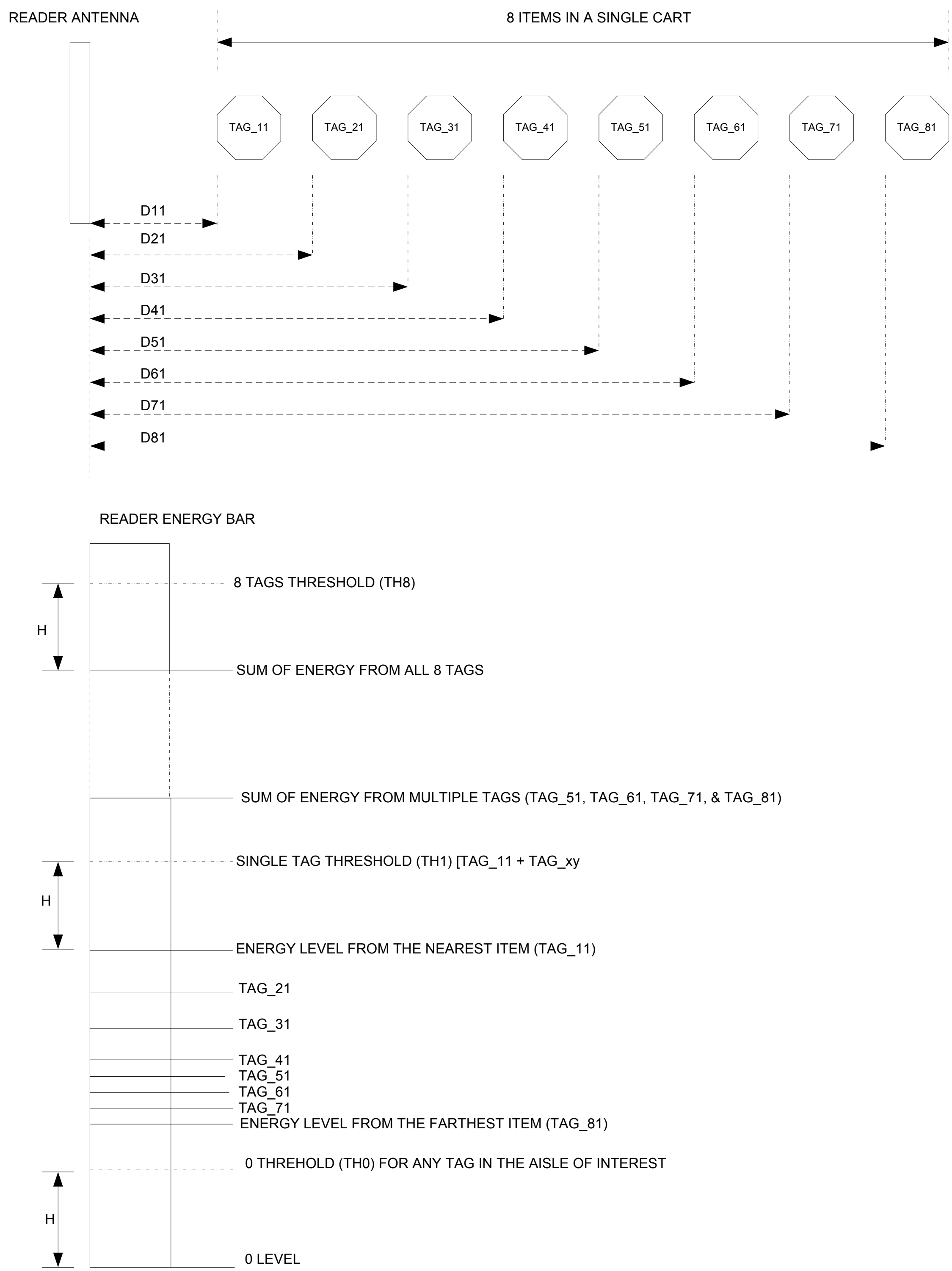

Figure 5.11: Illustration of Eight Tags in the Same Cart at Eight Different Distances to the Reader Antenna, and the Energy Level of the Closest and Farthest Item

One of the assumptions is that all tags transmit at the same power level; therefore for the eight items in figure 5.11 the power received by the reader at the same chip position for each item is expressed as follows

$$\left.\begin{aligned} P_{R11} &= \frac{P_{TAG\_11}}{D_{11}^{\;2}} \\ P_{R21} &= \frac{P_{TAG\_21}}{D_{21}^{\;2}} \\ P_{R31} &= \frac{P_{TAG\_31}}{D_{31}^{\;2}} \\ P_{R41} &= \frac{P_{TAG\_41}}{D_{41}^{\;2}} \\ P_{R51} &= \frac{P_{TAG\_51}}{D_{51}^{\;2}} \\ P_{R61} &= \frac{P_{TAG\_61}}{D_{61}^{\;2}} \\ P_{R71} &= \frac{P_{TAG\_71}}{D_{71}^{\;2}} \\ P_{R81} &= \frac{P_{TAG\_81}}{D_{81}^{\;2}} \end{aligned}\right\} \tag{5.4}$$

This assumption is based on the fact that the energy level from the reader is much greater than the reflected (backscatter) energy from the tags. Thus, the loss of energy from the reader across the field of tags read is minimal. In addition, any loss of energy due to distance can be accounted for in the reduction of energy from the tags distributed across the aisle.

From equation 5.4, it is clear that the only variable is the distance from each item to the reader antenna. If TAG_11 and TAG_81 are considered to be at the nearest and most distant ends of the cart respectively, with the subsequent spacing between items being essencially equal, then an expression can be derived in terms of the spacing. Let *S* be the spacing between items. Then the distances between each of the eight items to the reader can be expressed with respect to the distance of the closest item to the reader which is D_{11}.

$$\left.\begin{aligned} D_{21} &= D_{11} + S \\ D_{31} &= D_{11} + 2*S \\ D_{41} &= D_{11} + 3*S \\ D_{51} &= D_{11} + 4*S \\ D_{61} &= D_{11} + 5*S \\ D_{71} &= D_{11} + 6*S \\ D_{81} &= D_{11} + 7*S \end{aligned}\right\} \tag{5.5}$$

The CDMA facilitates a non interference capability in a multiple access environment that received power must exceed a given *threshold* for it to be treated as authentic information from a relevant tag. The given threshold is set such that if items from a cart in a nearby aisle are all transmitting '1's at the same chip position, the sum of their energy must be below the threshold in order for it not to interfere with the on going communication. The value of the threshold is set with reference to the energy level of the most distant item in a cart; in this example *TAG_81* is the most distant tag (item) with the received power of P_{R81} at the reader. There is a single tag threshold (*TH1*) (indicated in figure 5.11) which represents the level at which the total power received from a single item (tag) transmitting a "1" simultaneously at the same chip position with all the items from the adjacent aisle. The nearby (next aisle) tag responses must stay below this level. In section 5.5.2 the *clear distance technique* was explained, which simply means maintaining an *inter aisle distance (IAD)* that allows for sufficient fading of all adjacent aisle signals such that the sum satisfies the following condition.

$$H > \Sigma TAG\_xy \tag{5.6}$$

Here, x and y represent the horizontal and vertical position of items in a given cart on an aisle. It is important to note that this condition greatly relaxes the simple condition of requiring the threshold, H, to be the level at which the reader can no longer detect (read) the tag. The CDMA methodology is the mechanism as developed in this dissertation that allows the reader to establish a minimum threshold with non-zero measure as opposed to a simple read no read condition with a single line of no thickness.

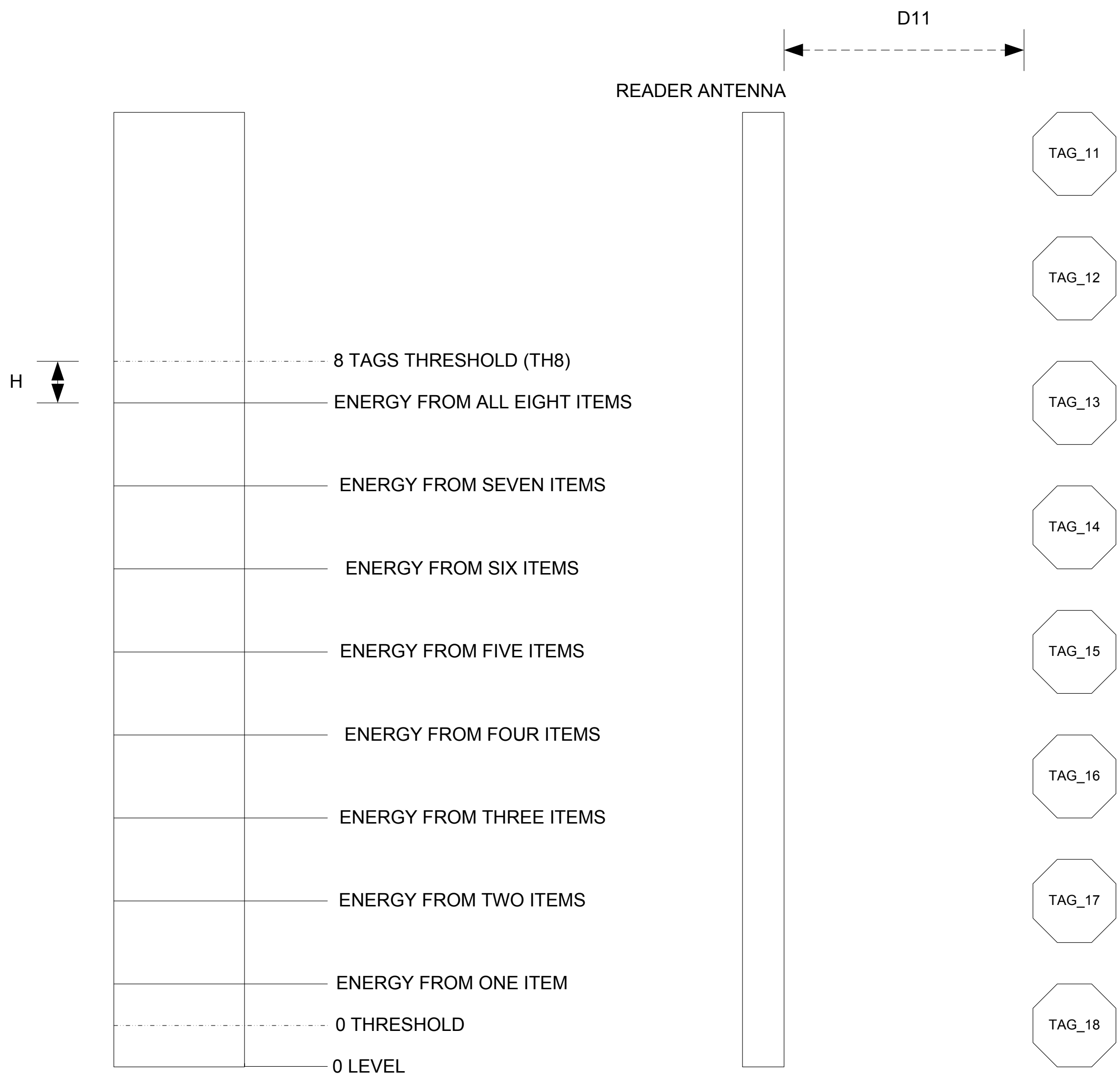

Figure 5.12: Illustration of Eight Items at the Same Distance to the Reader Antenna

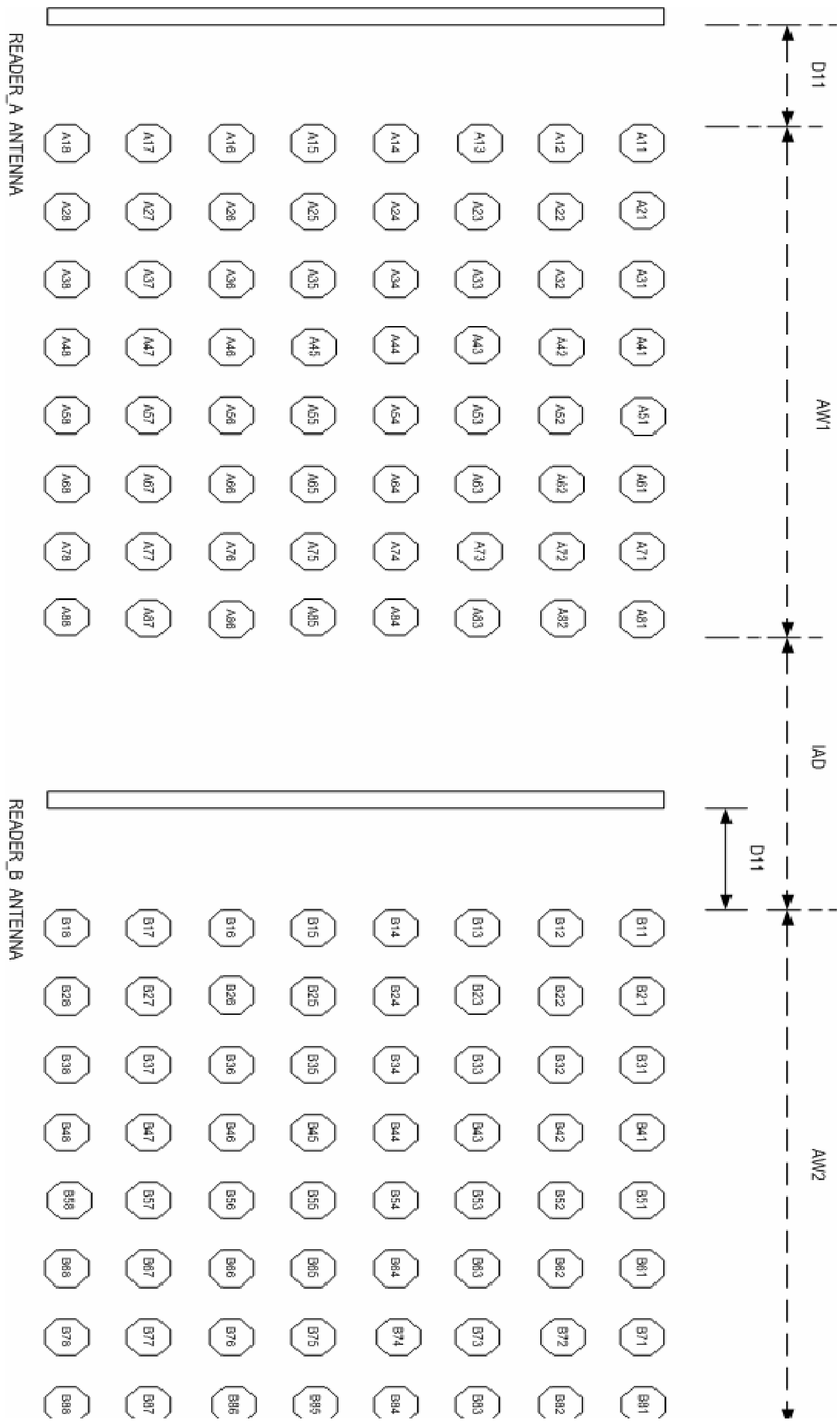

Figure 5.13: An Example of a Two Aisle Scenario with each Cart containing 64 Items

A different possible scenario is pictured in figure 5.13 showing two adjacent aisles each having a single cart with 64 items spread within the carts. Several instances can be illustrated in this setup which includes a possible situation in which all 64 items from both carts transmit a "1" at the same chip position. The main objective is to read only the 64 items from cart *A* without the erroneous addition of any item from cart *B*. But a possible worst case scenario is have a single item say *A88* in cart *A* transmitting a "1" at the same chip position simultaneously with all 64 items from cart *B*. For an error free reading to take place, the total power level of all 64 items in cart *B* must satisfy equation 5.6, where in this case both x and y range from 1 to 64 inclusive.

Figure 5.14 is the energy representation of a worst case instance of *TAG_88* transmitting a "1" simultaneously at the same chip position with the 64 items in the adjacent aisle. It is important that the sum of power from the 64 adjacent items be less than a single item from the 8th column of the cart in question (most distant position from the reader antenna). Because it is necessary to be able to distinguish between two items in the same column (in this case the same most distant position from the reader antenna), and one item plus dispersed signal from adjacent aisles. In figure 5.13 the power level of any two most distant items from the cart in question is distinct from the sum of energy of one farthest item plus the sum of all 64 items from the adjacent aisle. This ensures the elimination of interference or corruption from other carts thereby protecting customers from paying for extra items not contained in their carts.

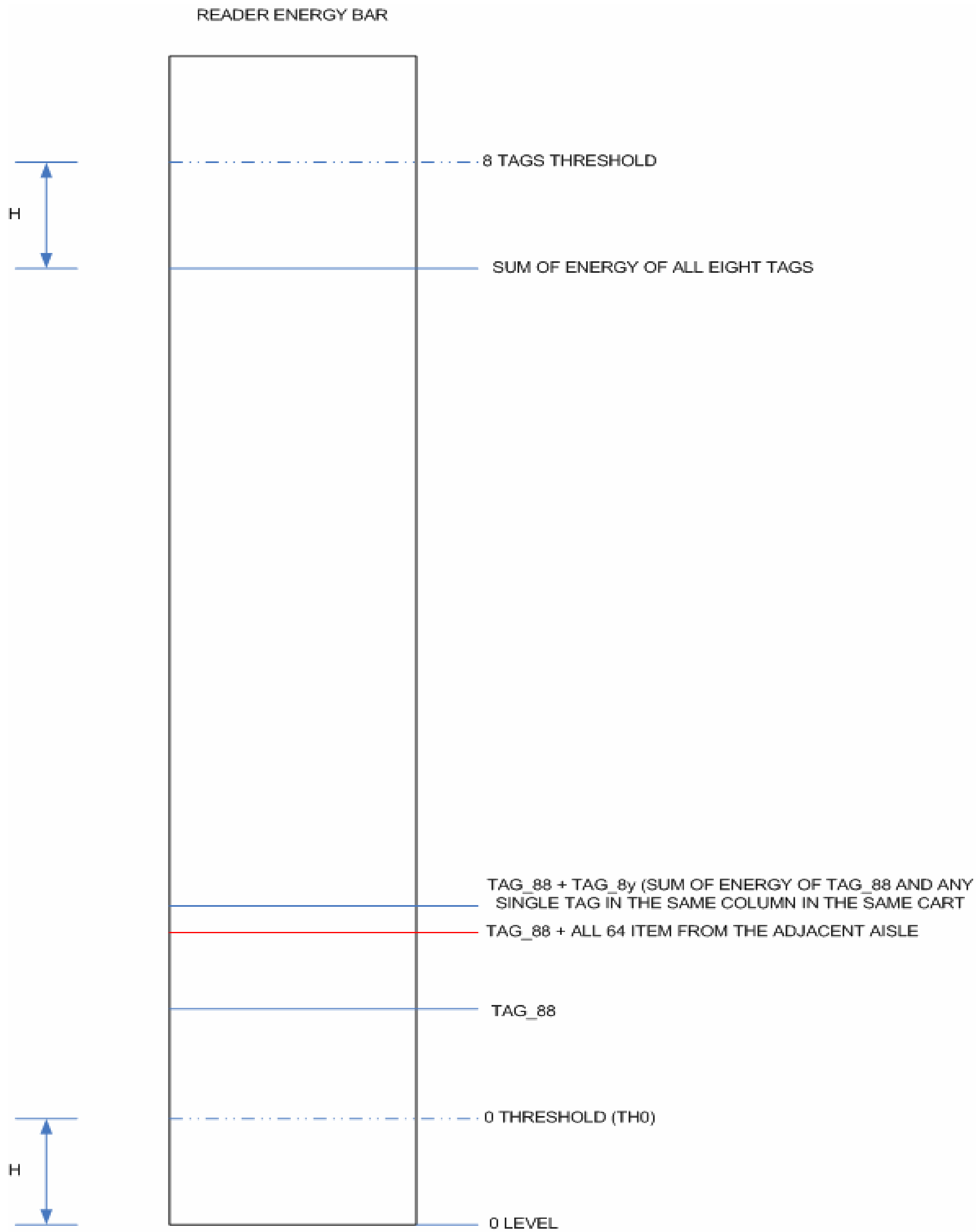

Figure 5.14: Power Level of a Single Item in a Cart with the Faded Power of 64 Items from a Cart on an Adjacent Aisle

6.0 RANDOM MULTIPLE ACCESS COMMUNICATIONS WITHOUT FEEDBACK

This chapter is important to the results of this dissertation because it presents a specific alternative coding scheme or method of approaching the issues of multiple access in the RFID tag communication systems, and a technique for the analysis of performance of the systems. In addition, this section presents one of the numerous methods being implemented in the zest to solving the problem of collision in the current RFID multiple access systems.

6.1 INTRODUCTION

When multiple users share a common communication resource using techniques such as time-division multiple-access (TDMA) the user with less frequent and shorter transmission may experience delay in gaining medium access. This problem is addressed normally using "*random accessing*". The random accessing method on the other hand leads to the inevitable problem of "*collision*" which occurs when multiple senders transmit simultaneously. In most communications systems prone to collision problems, feedback is incorporated to facilitate the resend of messages according to specified rules in the event of any collision [29].

This part of the dissertation explores a specific alternative multiple access method; in particular the technique of *Random Multiple Access without Feedback,* by analyzing the loss or potential loss of transmission capacity when *M* users (in particular *M* RFID *tags)* use random accessing when they are compelled to transmit without synchronization.

6.2 THE CHANNEL MODEL

In constructing the channel model for analyzing this technique, two distinct constraints are taken into consideration:

1. A conditional probability law (or deterministic rule) is specified for the channel outputs for given channel inputs.
2. Constraints are specified for the channel usage.

It is important to note that the channel model is not complete, and in particular the capacity is not *computable* without specifying the constraints on the channel usage.

6.2.1 The Basic Channel Model

Figure 6.1 is a model of the situation of M tags sharing the same channel with each occasionally sending a "packet" of fixed duration, say T seconds, and silent when not sending. Thus, $x_i(t)$ is the input signal from tag i as shown in figure 6.1, with the exception of those intervals where $x_i(t)$ is zero. It is assumed that $x_i(t)$ is some waveform recognizable to the receiver. Assuming the packet has Q possible values for some fixed integer Q, with $Q \geq 2$ a packet of information is defined as $log_2 Q$ bits [29].

As one of the criteria in the model, there are no time references between or among the users or the receiver. The *time offsets* $\delta_1, \delta_2, ..., \delta_M$ as shown in figure 6.1 are used to offset all the users to make sure there is no time reference. While $x_i(t)$ indicates user i transmitting in it's own local time t, $y(t)$ denotes the received signal at the receivers local time t. It can be deduced from the model that the difference between the transmitter local time and receiver local time is $(t - \delta)$. The data from tag i received by the receiver at time t was actually sent at time $(t-\delta_i)$ on tag i's clock. This situation is only possible when the user and receiver clocks are completely synchronized.

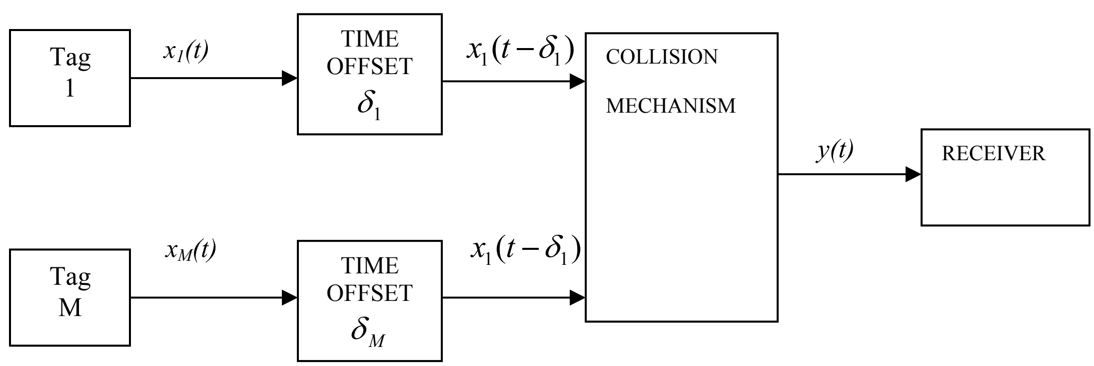

Figure 6.1: Basic Model for Random Multiple Access Channel without Feedback

Packets received at the receiver without collision are considered error free, while completely or partially collided packets are discarded. Therefore, in the event of a collision, a packet sent by tag i starting at time t_a will be assumed to collide with a packet sent by tag j starting at time t_b if and only if

$$\left|(t_a-\delta_i)-(t_b-\delta_j)\right|<T \tag{1}$$

This is true, if and only if the difference between the times of receipt of their leading edges is less than T, the packet duration. Here we assume that the received signal $y(t)$ at the output of the "collision mechanism" in figure 6.1 is given the following interpretations:

1. Coincides with the corresponding recognizable packet waveform during receipt of a non-collided packet
2. Is recognizable as "garbage" (and nothing more) during receipt of any collided packets

3. Is recognized as “silence” during periods when no packet (either collided or not) is received.

There are two cases of the unknown time offset considered in this analysis.

The slot-synchronized case in which the time offsets $\delta_1, \delta_2, ..., \delta_M$ are arbitrary integer multiple of T

The synchronized case where the time offsets $\delta_1, \delta_2, ..., \delta_M$ are arbitrary real numbers.

If we define *time slot n* to be the semi-open interval $nN \leq t < (n+1)T$, with a clear understanding of local time, then in the slot-synchronized case, tag i sends a packet precisely within the receiver’s time slot $n + \delta_i / T$. Thus, if all tags align their packet transmissions within time slots, a collision will result only when received packets completely overlap. In the unsynchronized case, however, the tags have no way to avoid collisions that result from only partial overlapping of packets.

Hence, the slot-synchronized case clearly gives a more favorable way of executing a multiple access operation with an appreciable reduction of inter-tag collision and read time for the reader.

6.2.2 Constraints on Channel Usage

There are simply boundaries put in place to facilitate the quantification of the channel performance when multiple tags transmit at the same time. Figure 6.2 shows the mechanism a tag is permitted to use the basic channel of figure 6.1. Each tag is assumed to have an independent, on demand source producing Q-ary symbols for transmission. The statistical nature of the information does not determine the transmission times because each tag has a *protocol* *signal generator* which generates a periodic signal that completely specifies the transmission initiation time and duration for the tag.

The protocol signal for tag i is $s_i(t)$ with a period τ_i, and having a value of either zero or one for all times t. It assumes the value one only over semi-open intervals whose length are integer multiple of T. Thus, the encoder for tag i will transmit packets only when $s_i(t) = 1$ and is expected to be silent (i.e., emit zero waveform) whenever $s_i(t) = 0$. The assumption is made that the receiver knows the choice of protocol [29].

This channel model is aimed primarily at determining how much loss is encountered when M senders (in this case RFID tags) share a common channel with absolutely no time-sharing due to prohibitions to have any time reference between tags and or receiver. The random process controlling the transmission is not dependent on the information source.

The output of a Q-ary source is encoded into packets for transmission so the receiver will be able to reconstruct the output of this source from the received signal $y(t)$ with acceptably small error probability.

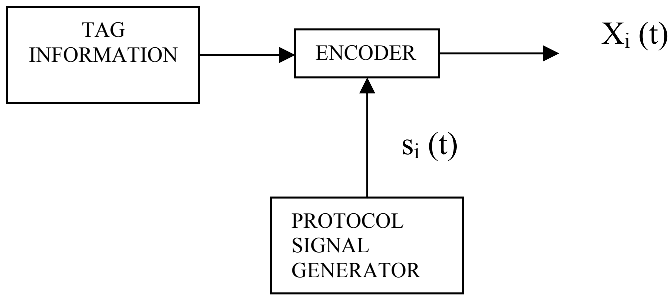

Figure 6.2: Constraint on Channel Usage for Random Multiple Access without Feedback

6.3 CAPACITY REGION AND MAIN RESULTS

Suppose the "on demand" information from the *i* tags is in the form of a Q-ary symmetric source (QSS), which means the next output digit is equally likely to be any of Q possible values, independent of it's past history. The QSS has an information rate of $\log_2 Q$ bits per symbol or, equivalently, one packet per symbol [29]. For the *random multiple access without feedback*, the period of time when the output of the protocol signal $s_i(t)$ is non zero is known as the *duty factor* p_i for user *i*, this is the fraction of time during which tag *i* is actually transmitting packets. From this, we deduce that for a tag *i* transmitting information from it's QSS at a rate R_i packets/slot, then it is actually transmitting information at a rate R_i/p_i packets/slot during those times that it is actively using the channel [29].

In a multi user channel "capacity region" means the set of all simultaneous user rates such that it is possible to communicate with arbitrarily small (positive) error probability at any joint rate within this set, but is impossible outside this set. The multiple simultaneous rates region where "zero-error" probability is possible is termed "zero-error capacity region".

In this analysis the *capacity region* ξ can be defined as either "unsynchronized" or "slot-synchronized".

The *capacity region* ξ_u of M tags unsynchronized is the set of all rate vectors $R = (R_1, R_2, \ldots, R_M)$, with $R_i \geq 0$ for $1 \leq i \leq M$, that are approachable in the sense that, for some positive numbers δ and Є there is a protocol signal $s_i(t)$ and a block code of length n_i packets for each tag i such that:

QSS for tag i are segregated into blocks of $(R_i / p_i - \delta)n_i$ packets which are then encoded into blocks of n_i packets for transmission during the time when tag i is actually using the channel.

A decoder using the channel output signal can reconstruct the output sequence of tag i's QSS with an average packet error probability at most Є, regardless of the values of the chosen time offsets $\delta_1, \delta_2, \ldots, \delta_M$.

The zero-error capacity region, ξ_{u0}, of the unsynchronized *random multiple access without feedback* has the same definition as ξ_u except the error probability Є = 0 is specified. The capacity region and zero-error capacity region or in other terms, the slot-synchronized RMAWF, ξ_s and ξ_{s0}, respectively, are defined similarly.

The regions described in all the preceding sections can only be distinct if there are some boundaries defining these regions. Therefore, any point R in any of the capacity (or zero-error capacity) regions defined in the previous sections satisfies the relation $R \geq 0$, where 0 denotes the all-zero vector with M components. Suppose R and R^* are two different vectors with the following corresponding inequality $R^* \leq R$, then if R is in a capacity (or zero-error capacity) region and $0 \le R^* \le R$, then R^* is also in this capacity (or zero-error capacity) region. Thus, from this we can define the "outer boundary" of a capacity (or zero-error capacity) region as a set of all points R of this region such that there is no other point $R^{'}$ in this region for which $R \le R^*$.

From this concept, it can be derived that the capacity region of a single-sender single-receiver discrete memoryless channel (DMC) with capacity C is the closed interval [0, C] and its outer boundary is the singleton set $\{C\}$. Because the outer boundary of a capacity (or zero-error capacity) region for a multi-user channel is the natural generalization of the capacity (or zero-error capacity) of a DMC, we shall denote points on the outer boundary of such a region by $C = (C_1, C_2, ..., C_M)$ [29].

The inclusions:

$$\xi_{u0} \subset \xi_u \subset \xi_s \tag{6.2a}$$

$$\xi_{u0} \subset \xi_{s0} \subset \xi_s \tag{6.2b}$$

define the corresponding regions and the fact that the allowable *time offset* $\delta = (\delta_1, \delta_2, ..., \delta_M)$ for the slot-synchronized RMAWF are a subset of those for the unsynchronized RMAWF. The inclusions indicate that the regions coincide. Theorems promulgated by Massey and Mathys et al. 1985 [29], presents proof for the coincidence of the regions as recorded in Appendix D of this dissertation.

6.4 NON-APPROACHABILITY OF RATES OUTSIDE ξ

In this section, we show that rates outside the region ξ, as defined in theorem 1, cannot be approached for the RAMWF in either the slot-synchronized or unsynchronized case and for either error probability criterion. From equation (6.2), we see that points outside ξ can not be approached with arbitrarily small positive error probability in the slot-synchronized case. For this reason, we will consider only the synchronized case.

For any choice of protocol signals and codes for the tags, we may assume that the period τ_i of the protocol signal $s_i(t)$ is a rational multiple of the slot length T, for $1 \leq i \leq M$. Thus, we can write $\tau = (m_i / m)T$ where m_i and τ_i are integers. Then NT, where $N = m_1 m_2 ... m_M$ is an integer multiple of each τ_i. Thus, for all t,

$$s_i(t + NT) = s_i(t) \tag{6.7}$$

for $1 \leq i \leq M$.

We now impose a fictitious probability distribution on the time offsets $\delta_1, \delta_2, ..., \delta_M$; namely, we specify that these are independent and identically distributed (IID) random variables that are equally likely to take on any of the N values $0, T, ..., (N-1)T$. It therefore follows from equation (6.7), from the definition of the duty factor p_i, and from the fact that $s_i(t)$ is nonzero only over the semi-open interval of lengths which are integer multiples of T, that

$$E[s_i(t - \delta_i)] = p_i \tag{6.8}$$

for every time instant t.

Tag i will be the only tag in the act of transmission at any given time t on the receiver clock if and only if

$$s_i(t - \delta_i) \prod_{j \neq i} [1 - s_j(t - \delta_j)] = 1; \tag{6.9}$$

Moreover, the left side of equation (6.9) will be zero. Hence, with a receiver clock of length *NT* during, and T_i being the time within an arbitrary semi-open interval, $[t_0, t_0 + NT)$, during which the receiver is receiving non-collided packets from tag *i*, we have

$$T_i \leq \int_{t_0}^{t_0+NT} s_i(t-\delta_i)\prod_{j\neq i}[1-s_j(t-\delta_i)]dt\,; \tag{6.10}$$

The inequality in equation (6.10) means the mere fact that equation (6.9) is satisfied for some *t* does not guarantee that packets sent at receiver time *t* by tag *i* will not experience partial collision. Now, taking the expectations of equation (6.9) making use of equation (6.8) and the independence of $\delta_1, \delta_2, ..., \delta_M$ gives

$$E\left[s_i(t-\delta_i)\prod_{j\neq i}[1-s_j(t-\delta_j)]\right] = p_i\prod_{j\neq i}(1-p_i) \tag{6.11}$$

Now taking expectations in equation (6.10) and using equation (6.11) gives

$$E[T_i] \leq NTp_i\prod_{j\neq i}(1-p_j) \tag{6.12}$$

For any given *i*, it follows from equation (6.12) that there must be some specific choice of $\delta_1, \delta_2, ..., \delta_M$ such that

$$T_i \leq NTp_i\prod_{j\neq i}(1-p_j) \tag{6.13}$$

and, indeed, it was only to arrive at this conclusion that we introduce the fictitious probability distribution on $\delta_1, \delta_2, ..., \delta_M$.

Equation (6.12) shows that, given *i,* there is a specific choice of $\delta_1, \delta_2, ..., \delta_M$ such that the receiver receives non-collided packets from tag *i* at a rate of at most $p_i\prod_{j\neq i}(1-p_j)$ packets/slot. Suppose there is a way of finding out in advance, for both tag *i* and the receiver, each interval in which tag *I* can send a non-collided packet. Along with the non-collided packets, if tag *i* has a noiseless Q-ary DMC to the receiver with capacity of one packet per use and with at most $p_i \prod_{j \neq i} (1 - p_j)$ tags per slot. Thus, based on the usual coding theorem for a DMC, tag *i* cannot send information from his QSS at a rate R_i with arbitrarily small positive error probability, regardless of the values $\delta_1, \delta_2, ..., \delta_M$, unless

$$R_i \leq p_i \prod_{j \neq i} (1 - p_i) \text{ packets/slot.} \tag{6.14}$$

It follows that $R = (R_1, R_2, ..., R_M)$ cannot be approached with arbitrarily small positive error probability, independent of δ, unless equation (6.14) is satisfied for $i = 1, 2, ..., M$ [29].

In order to complete the proof that points outside ξ cannot be achieved, we need only show that every $R \geq 0$ that satisfies equation (6.14) for $1 \leq i \leq M$ lies in the region ξ defined in Theorem 1, i.e., that if *R* satisfies equation (6.14) for $1 \leq i \leq M$ for some duty factor *p*, then *R* also satisfies equation (6.14) for $1 \leq i \leq M$ for some probability factor *p*.

6.5 THE PRELIMINARIES

In this section we concentrate solely on the slot-synchronized case. Because we are dealing with a constructive scheme, we impose the restriction that all tags align their packet transmissions to fall within time slots on their local clocks, and hence also within time slots of the receiver's clock, because time offsets are integer multiple of the slot length *T*. We take *T* = 1 so that each time offset δ_i is an integer. The period of each protocol sequence is now also an integer, and denoted by N_i for user *i*, and we write *N* for the least common multiple of $N_1, N_2, ..., N_M$.

We can now equivalently describe the protocol signal $s_i(t)$ by the protocol sequence $s_i = [s_{i1}, s_{i2}, ..., s_{iN}]$ in the manner that s_{in} is the value of $s_i(t)$ in the n^{th} time slot $n \leq t < n + 1$. We also assume that the transmitted packets take values in the set {0, 1, 2,…,Q-1}. The symbol Λ is written to denote the silent signal ("idle") in a slot. Therefore, the transmitted signal from tag i in it's own n^{th} time slot by the discrete random variable $X_i(n)$ in the manner that [29]

$$\begin{aligned}
&X_i(n) = \Lambda, \qquad if \quad s_{in} = 0 \\
&X_i(n) \in \{0,1,...,Q-1\}, \qquad if \quad s_{in} = 1
\end{aligned}$$

Similarly the received signal in the n^{th} time slot is denoted by the discrete random variable $Y(n)$ in the manner that

$$\begin{aligned}
&Y(n) = \Lambda, \qquad if \quad X_i(n-\delta_i) = \Lambda \quad for \quad 1 \leq i \leq M \\
&Y(n) = X_i(n-\delta_i), \qquad if \quad X_j(n-\delta_i) = \Lambda \quad for \quad all \quad j \neq i \\
&Y(n) = \Delta, \quad otherwise,
\end{aligned}$$

where Δ denotes a collision of two or more packets. In this manner, we obtain a fully discrete representation for the slot-synchronized RAMWF. The channel input alphabet of each tag contains Q + 1 letters and the channel output alphabet contains Q + 2 letters.

For the sake of convenience we assume that the output alphabet of the QSS of each tag is also the set {0,1,…,Q-1}. We then choose a protocol sequence and block code for each user that, regardless of the value of the time offsets, the receiver can reconstruct each output sequence without error. Moreover, we must show that the joint rates R that can be achieved are dense on the outer boundary of the region ξ defined in Theorem 1 (appendix D).

6.5.1 Protocol Matrices

Here, we define the *protocol matrix S* as the M x N binary matrix whose ith row is the protocol sequence s_i of tag i. For instance, with $M = 2$ tags, and protocol sequence period $N_1 = 2$ and $N_2 = 4$ with least common multiple $N = 4$, we could choose

$$S = \begin{bmatrix} 1010 \\ 1100 \end{bmatrix} \tag{6.15}$$

We shall be interested in the received sequence over a span of N consecutive time instants, which, we can take to be time instants 1,2,…,N. We write

$$Y = [Y_1, Y_2, ..., Y_N]$$

to denote this received N-tuple. From equation (6.15) if the time offsets are $\delta_1 = \delta_2 = 0$, then

$$Y = [\Delta, P_A, P_B, \Lambda],$$

i.e., slot 1 is a collision slot, slot 4 is idle, and that slots 2 and 3 contain packets. From equation (6.15), we see that packet P_A was sent by tag 2 whereas packet P_B was sent by tag 1.

Suppose that $\delta_1 = 5$, the periodic protocol sequence of tag 1 will be delayed by 5 slots, so that it will appear to the receiver that tag 1 is actually using the protocol sequence [0, 1, 0, 1] in slots 1 through 4. Similarly, if $\delta_2 = 3$, it will appear to the receiver that tag 2 is actually using the protocol sequence [1, 0, 0, 1]. Thus, it will appear to the receiver as if the modified protocol matrix

$$S[\delta] = \begin{bmatrix} 0101 \\ 1001 \end{bmatrix} \tag{6.16}$$

is actually in use. In particular we then see that

$$Y = [P_A, P_B, \Lambda, \Delta]$$

where the packets P_A and P_B are from tags 2 and 1, respectively.

From the above example, a time offset (or "delay") of δ_i slot corresponds to δ_i right cyclic shifts of the protocol sequence s_i. We write $s_i[\delta_i]$ to denote the sequence obtained from s_i after δ_i right cyclic shifts and, as we have already done in equation (6.16), we write $S[\delta]$ for the *effective protocol matrix* whose ith row is $s_i[\delta_i]$. Note that $S = S[0]$. Because $s_{in} = s_{i,n+N}$ for all i and n, it follows that $s_i[\delta_i] = s_i[\delta_i + N]$. Thus, given N, we can do hereafter restrict ourselves to the condition [29]

$$0 \le \delta_i < N \tag{6.17}$$

Because of equation (6.17), we see that there are only N^M values of $\delta = [\delta_1, \delta_2, ..., \delta_M]$ to be considered, and hence at most this many distinct effective protocol matrices.

From the protocol matrix S of equation (6.15), it can be determined that all 16 choices of δ result in an $S[\delta]$ such that the resulting $Y = [Y_1, Y_2, Y_3, Y_4]$ always contain one collision slot, one idle slot, and one packet from each of the two tags. Moreover, the packet from tag 2 is always adjacent to a collision slot [provided we count slot 1 as adjacent to slot N] whereas the packet from tag 1 is never adjacent to a collision slot. Thus, the receiver can, from examination of $Y = [Y_1, Y_2, Y_3, Y_4]$, uniquely identify the sender of each of the successfully received packets in this sequence regardless of the values time offsets. Suppose further more that each tag employs the simple rate r = ½ packets/slot repeat code in which each information packet from its QSS is sent twice. Precisely one of the two packets will be correctly received, and its sender identified, as the other packet will be lost in a collision. Hence, the receiver can perfectly reconstruct the output sequence from each of the two QSS's.

6.6 APPROACHABILITY OF RATES IN ξ

In proving the direct part of Theorem 1 (appendix D), equation (6.2) can be used to show that any rate vector R in the region ξ defined in Theorem 1 can be approached without error for the unsynchronized RMAWF. Here, we first show that such R can be approached without error for the slot-synchronized RMAWF, and then give a simple argument that reduces the unsynchronized case to the slot-synchronized case.

6.6.1 The Slot-synchronized Case

Consider R to be any vector in ξ as defined in Theorem 1 (appendix D). R can be on the boundary or even on the outer boundary of ξ. Therefore, there must exist a point $C^{'}$ (possibly R itself) on the outer boundary of ξ such that $R \leq C^{'}$. Hence, for any positive δ, $R - \delta 1 < C^{'}$. It now follows from Theorem 2 (appendix D) that there is a point C on the outer boundary of ξ that is achievable with zero error in the slot-synchronized case and for which $R - \delta 1 < C$. Therefore, R is indeed approachable in the slot-synchronized case.

6.6.2 The Unsynchronized Case

This constructive coding scheme enforces the provision that all tags must align their packet transmissions to fall within time slots on their local clocks, and this includes the unsynchronized case being considered in this section. In the unsynchronized case, because the components of δ are arbitrary real numbers, the received packets in general will not fall into time slots on the receiver's clock.

Due to the restriction on the packet transmission, we can describe the protocol signals in the unsynchronized case by protocol sequences and protocol matrices as in section 6.4.2. Again taking the slot length for convenience to be $T = 1$. Because of the arbitrariness of m, the following result shows that any rate approachable without error in the slot-synchronized case is also approachable without error in the unsynchronized case. We write 0^m and 1^{m-1} to denote, respectively, a string of m zeros and a string of $m-1$ ones.

6.7 CDMA RFID SYSTEM AND RMAWF SYSTEM

The CDMA RFID technique and the RMAWF technique both have the commonality of sharing a single channel among multiple tags. There is also a fundamental difference between the two techniques in the fashion by which communication is initiated between readers and tags. For the CDMA RFID system the reader/receiver initiates the communication process, whereas in the RMAWF system the tag initiates the communication process. The significance of this difference ensues in the process of synchronization. Ideally, the CDMA RFID system is expected to always be in sync. The RMAWF on the other hand operates without synchronization among the tags and with the reader. The only synchronization that takes place in the case of the RMAWF is between the specific tag communicating at any instance with the reader.

The philosophy behind the RMAWF method of multiple access was to eliminate the problem of media access plaguing the time division multiplexing (TDMA) type communication systems. But by making the media access easier the problem of collision was introduced because the tags individually generate the protocol without any peer consultation. The CDMA systems inherently are in sync because these tags are simultaneously activated by the same reader. The orthogonal coding scheme in the CDMA type system resolves the problem of collision which plagues the RMAWF type system.

The RMAWF does introduce an important phenomenon which is the *capacity region*, this is measured by the sum of the rates of all simultaneous users with fairly small positive probability of error. The capacity region also is categorized into either *unsynchronized* or *slot-synchronized*. The chances of collision appear to be greater in the unsynchronized case even though the region under certain conditions may coincide. In the case of the CDMA system because of the spread spectrum nature of the technique the wide bandwidth provides for a greater number of simultaneous multiple users. Also by creating a higher chip energy to noise spectral ratio, the theoretical Shannon's limit shows that CDMA systems can have more users per cell (region) than traditional narrowband systems that are limited by number of dimensions [1].

The CDMA RFID system at this moment is the only system that actually does the simultaneous reading of multiple tags. The other techniques are most either TDMA or some derivatives of the TDMA type system.

7.0 CONCLUSIONS

There are three main contributions in this dissertation:

1. The demonstration of the use of the Ultra Wide Band concept of forming a complex RF pulse for communication using the coefficients conceptually derived to be analogous to the discrete Fourier transform. The pulses constitute a *virtual pulse train*. In addition, a technique of AM type pulse width modulation was developed as a part of this particular pulse forming technique.
2. The second contribution is the application of multiple access CDMA for the reading of RFID tags. This contribution makes possible the simultaneous reading of multiple RFID tags without inter-tag interference or collisions while using a single reader. This technique can also be applied to the current logical tree technique to reduce the total number of reads required for a given ensemble of tags.
3. Relaxed restrictions for the typical cart aisle implementations (specified distance) providing a band of discernment for reading or ignoring tags that should or should not be read in an error proof multiple access CDMA RFID technique in particular for a grocery store checkout system.

7.1 RF PULSE COMMUNICATIONS

A method of complex RF pulse formation has been developed to form a *virtual pulse train* using the ISM (or other user selected) frequencies within the radiation levels allowed by the FCC and other regulating bodies. This technique stems from the need to implement multiple frequency communications as a form of ultra wide band for the purpose of communications security.

It has been shown in this dissertation that two sets of coefficients can be obtained analogous to the discrete Fourier transform of rectangular pulse train forming two different pulse widths that produce a method of 0/1 modulation. Associated with each of these coefficients is the corresponding frequency component which provides the differentiation as a result of the two distinct virtual pulse widths.

The ISM frequencies were used as the primary example for the pulse formation because they are available for the purposes of Industrial Scientific and Medical use without requiring a license. This also makes the ISM frequencies available for academic research and development purposes. The technique is not restricted to ISM frequencies. However, this restriction does make the technique legal with respect to the FCC. This is a technique of customizing an analogy of the discrete Fourier transform to modulate the pulse width of the *virtual pulse train*.

Incorporated in the pulse width modulation is the classical fading effect of the individual frequencies causing each frequency to arrive at the same distance at different relative energy level thus facilitating a method of secure communications based on a *priori* known distances.

This technique also has been shown to be implemented in order to take advantage of the hamming distance for error correction.

7.2 CDMA RFID COMMUNICATIONS

The second contribution of this dissertation has been the use of the Walsh coding scheme to implement the CDMA technique for simultaneously reading multiple RFID tags. The orthogonal characteristics of the Walsh code have been used to determine codes and eliminating inter tag collisions.

RF transmitters driven by microcontrollers have been used to provide an excellent demonstration of the received cumulative (composite) energy from the multiple tags. By using the code for each individual transmitter, the correct information is decoded to confirm the implementation of a CDMA implementation of simultaneously reading multiple RFID tags without collisions among the tags.

Also demonstrated in the CDMA technique is the power control among tags within the same proximity. This was carried out by simply setting the power levels of some of the tags such that they are of sufficient magnitude to demonstrate the ability to differentiate reading the messages from tags that are readable, but out of range.

An implementation procedure for the EPC global numbering system for identifying manufacturers, product type, and product serial number has been demonstrated using 64 chips with the corresponding Walsh code. This procedure automatically allows for a larger number of addressable products and items.

7.3 CART AISLE CDMA RFID IMPLEMENTATIONS

Another CDMA contribution has been the incorporation of a guard band of power in the receiver detection of RFID tag energy to remove the single demarcation line (zero guard band width) to distinguish between valid tag reads and non-related tag reads. This is necessary to eliminate the possibility of a customer wrongly paying for an item in a nearby aisle.

CDMA energy levels with respect to distance between the cart and reader provide greatly reduced stipulated distances between aisles to accommodate existing aisle configurations in commercial stores.

The increased speed of reading through the use of the CDMA technique allows synchronization of the readers to be used as a means of simplifying the multiple reader scenario. The technique thus becomes non-interfering with only one reader active (per aisle) at the time of transmission.

7.4 ALTERNATIVE TECHNIQUE

The alternative technique considered in comparison with the CDMA RFID system is the method of *random multiple access without feedback* (RMAWF). The main concept in this technique involves deliberately randomizing the tags using time offsets such that the tags do not access the medium in a time multiplexing manner. It has been observed that this in turn introduces greater possibilities of collision which are taken care of to some degree by generating the time offsets in a slot form. The slots have the same duty cycle as the packet time in the system thereby cutting down the probability of collisions.

The analysis of this alternative technique in comparison to the work in this dissertation (CDMA RFID), did confirm the assertion that the proposed technique of using CDMA for RFID is much more favorable when compared to other methodologies.

8.0 SUGGESTIONS FOR FUTURE RESEARCH

Complex Pulse Formation

The complex pulse in this dissertation has been implemented using multiple ISM frequencies because of FCC regulations and licensing restrictions within the RF spectrum. This opens numerous research possibilities in the area of bandwidth reuse by researching possible ways of implementing similar pulse formation using non-ISM frequencies.

With the ultra wide nature of the pulse forming technique, numerous modulation techniques are possible. Research into the new techniques can be channeled specifically to enhance certain aspects of the communications while forfeiting others. For example, techniques allowing for higher bandwidth for short range transmission, and complexity in communication protocol for more security compared to simple protocols.

This pulse forming technique can be applied to the RFID technology, and because of its wide bandwidth with multiple access, it can also be implemented making it applicable to the problem of read time in the RFID applications.

CDMA RFID

Other coding schemes need to be researched in comparison to the Walsh (Hadamard) orthogonal coding implemented in this research work taking into consideration the possibility of enlarging the chip size for the anticipated drastic growth in the application of RFID. In addition, power balancing among tags to reduce aisle distances creates another area of potential research.

Cart Aisle CDMA RFID

There is a need for a full scale mathematical model for the implementation of the CDMA RFID system in the store and warehouse scenario which provides an excellent area of research. The actual integration of the CDMA RFID system to the organizational data base and security system can also be researched.

APPENDIX A

FOURIER COEFFICIENTS

The following example illustrates the concept of multiple frequencies, and coherent transmission.

A periodic signal *x(t)* can be described by an harmonic series expressed in exponential form as [4]

$$x(t) = \sum_{n=-\infty}^{\infty} X_n e^{jnw_0 t} \tag{a.1}$$

where

w_0 is the fundamental frequency

X_n is the complex amplitude

The signal can also be expressed in amplitude-phase form as

$$x(t) = \sum_{n=0}^{\infty} A_n \cos(nw_0 t + \theta_n) \tag{a.2}$$

where

$$A_n = \begin{cases} |X_0| & n=0 \\ 2|X_n| & n\neq 0 \end{cases} \qquad \theta_n = \angle X_n \tag{a.3}$$

Because the period of the series must equal the period of the signal represented by the series, the fundamental frequency of the harmonic series describing a signal *x(t)* is given by

$$f_0 = 1/T \qquad (a.4)$$

where, T is the period of the signal.

The complex amplitude of the series can be derived by multiplying (a.1) by e^{-jkw0t} and integrating the product over a period say from $t = t_0$ to $t = t_0 + T$. This gives

$$\int_{t_0}^{t_0+T} x(t)e^{-jkw_0t}dt = \int_{t_0}^{t_0+T} \sum_{n=-\infty}^{\infty} X_n e^{j(n-k)w_0t}dt$$

where $w_0 = 2\pi/T$

$$\int_{t_0}^{t_0+T} x(t)e^{-jkw_0t}dt = \sum_{n=-\infty}^{\infty} X_n \int_{t_0}^{t_0+T} e^{j(n-k)w_0t}dt$$

$$\int_{t_0}^{t_0+T} e^{j(n-k)w_0t}dt = \begin{cases} T & n=k \\ 0 & n\neq k \end{cases} \qquad (a.5)$$

This result shows the only nonzero term in the sum above is the one for $n = k$, which equals, TX_k

$$X_k = \frac{1}{T}\int_{t_0}^{t_0+T} e^{j(n-k)w_0t}dt \qquad k=0, \pm 1, \pm 2 \ldots \qquad (a.6)$$

The complex amplitude obtained from (a.6) for a signal *x(t)* generates *FOURIER COEFFICIENTS* for the signal *x(t)*. The complex spectrum of a signal *x(t)* described by the exponential Fourier series of (a.1) is given by[4]

$$C_x(f) = \begin{cases} f=kf_0 \\ f\neq kf_0 \end{cases} k = 0,\pm 1,\pm 2,...$$

Equations (a.4) and (a.6) provide a path from the *time-domain* description (the waveform) of the periodic signal to the *frequency-domain* description (the spectrum) of the signal. Equation (a.1) provides the path from the frequency domain to the time-domain.

For the purpose of example, we will now apply the above technique to a rectangular pulse train representing data as shown in figure a.1

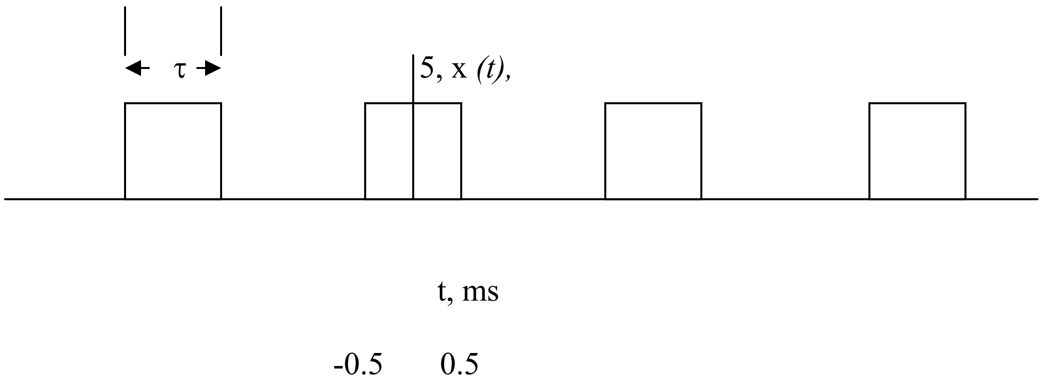

Figure a.1: Rectangular Pulse Train Example

The period of the signal *x(t)* is T = 2 ms. The fundamental frequency of the Fourier series for *x(t)* is:

$$f_0 = \frac{1}{0.002} = 500Hz$$

The Fourier coefficients are given by (a.6) where T = 2 ms, $w_0 = \pi\, k\, rad/2$ t_0 is arbitrary (t_0 = -T/2 = -1 ms in which case $t_0 + T$ = 1 ms)

$$X_k = \frac{1}{T}\int_{-T/2}^{T/2} x(t)e^{-jw_0 t}\,dt$$

$$x(t) = \begin{cases} 0 & -T/2 < t \le -\tau/2 \\ x_0 & -\tau/2 < t \le T/2 \\ 0 & \tau/2 < t \le T/2 \end{cases}$$

with x_0 = 5V and τ = 500uS; thus

$$X_k = \frac{1}{T}\int_{-\tau/2}^{\tau/2} x_0 e^{-jkw_0 t}\,dt$$

Performing integration yields

$$X_k = \begin{cases} \dfrac{x_0\tau}{T} & k=0 \\ \dfrac{x_0(e^{-jkw_0t\tau/2} - e^{jkw_0t\tau/2})}{-jkw_0T} = \dfrac{2x_0}{T}\sin\dfrac{(kw_0T/2)}{kw_0} & k \neq 0 \end{cases}$$

This can be written compactly as

$$X_K = \frac{x_0\tau}{T} sa\,\frac{kw_0\tau}{2} = \frac{x_0\tau}{T} sa\,\frac{k\pi\tau}{2}$$

Where sa $\propto$ denotes the sampling function, defined by

$$sa\alpha = \begin{cases} 1 & \alpha = 0 \\ \dfrac{\sin\alpha}{\alpha} & \alpha \neq 0 \end{cases}$$

The exponential form of the Fourier series for the above rectangular pulse train is

$$x(t) = \sum_{n=-\infty}^{\infty} \frac{x_0\tau}{T} sa\,\frac{n\pi\tau}{T} e^{jnw_0t}$$

where x_0 = 5v, T = 2ms, τ = 500 us, and $w_0 = \pi$ k rad/s

APPENDIX B

THE CONCEPT OF SPREAD SPECTRUM SYSTEM

The C. E. Shannon channel capacity formula defines the theoretical capacity of any communications channel [1], as

$$C = B_w \log_2 \left[1 + \frac{S}{N} \right] \tag{b.1}$$

Where:

B_w = bandwidth in Herz,

C = channel capacity in bits per second,

S = signal power,

N = noise power

Equation (b.1) provides the relationship between the theoretical ability of a channel to transmit information without errors for a given signal-to-noise (S/N) ratio and a given bandwidth on a channel. Increasing the channel bandwidth, the transmitted power, or both increases the channel capacity. Equation (b.1) is applicable to a radio frequency (RF) channel by assuming that the intermediate frequency (IF) filter has an ideal (flat) bandpass response with a bandwidth that is at least $2B_w$.

An analog cellular system is typically engineered to have an S/N ratio of 17 dB or more[1]. CDMA can be engineered to operate at much lower S/N ratios because the extra channel bandwidth can be used to achieve improve performance at a very low signal-to-noise ratio. Equation (b.1) can be rewritten as

$$\frac{C}{B_w} = 1.44 \log_e \left[1 + \frac{S}{N} \right] \tag{b.2}$$

since

$$\log_e \left(1 + \frac{S}{N} \right) = \frac{S}{N} - \frac{1}{2}\left(\frac{S}{N}\right)^2 + \frac{1}{3}\left(\frac{S}{N}\right)^3 - \frac{1}{4}\left(\frac{S}{N}\right)^4 + \ldots \tag{b.3}$$

The algorithmic expression is used with the assumption that the S/N ration is small (example, $S/N \leq 0.1$). Therefore, the higher order terms can be neglected to rewrite equation (b.2) as

$$B_w \approx \frac{C}{1.44} * \frac{N}{S} \tag{b.4}$$

A low information error rate can be achieved by increasing the bandwidth used for transmission for any given S/N ratio.

Modulating information into a spread spectrum signal can be performed using several mathematical methods. The most common method is to add the information to the spectrum spreading code before it is used for modulating the carrier frequency. Spread Spectrum systems that use a code sequence to determine RF bandwidth apply this technique. In spread spectrum, the system processing gain G_p quantifies the degree of interference rejection. The ratio of RF bandwidth to the information rate gives the system processing gain.

$$G_p = \frac{B_w}{R} \qquad \text{(b.5)}$$

In spread spectrum system, the noise level is determined both by the thermal noise and interference. The interference is processed as noise for a user, and the input and output S/N ratios are related as

$$\left(\frac{S}{N}\right)_0 = G_P\left(\frac{S}{N}\right)_i \qquad \text{(b.6)}$$

It is instructive to relate the S/N ratio to the E_b/N_0 ratio where, E_b is the energy per bit and N_0 is the noise power spectral density:

$$\left(\frac{S}{N}\right)_i = \frac{E_b * R}{N_0 * B} = \frac{E_b}{R} * \frac{1}{G_P} \qquad \text{(b.7)}$$

From equation (b.6), E_b/N_0 can be expressed as

$$\frac{E_b}{N_0} = G_P * \left(\frac{S}{N}\right)_i = \left(\frac{S}{N}\right)_0 \qquad \text{(b.8)}$$

APPENDIX C

CDMA TRAFFIC CHANNELS

A CDMA system has two types of downlink channels and two types of uplink channels. Traffic and broadcast channels make up the downlink; and traffic and access channels make up the uplink. The downlink channels are separated using Walsh codes. The broadcast channels consist of pilot, sync, and paging channels. The pilot channel provides initial synchronization, the sync channel provides base station (BS) identification, and the paging channels connect incoming calls to the correct mobile stations (MSs) to make out going calls [2].

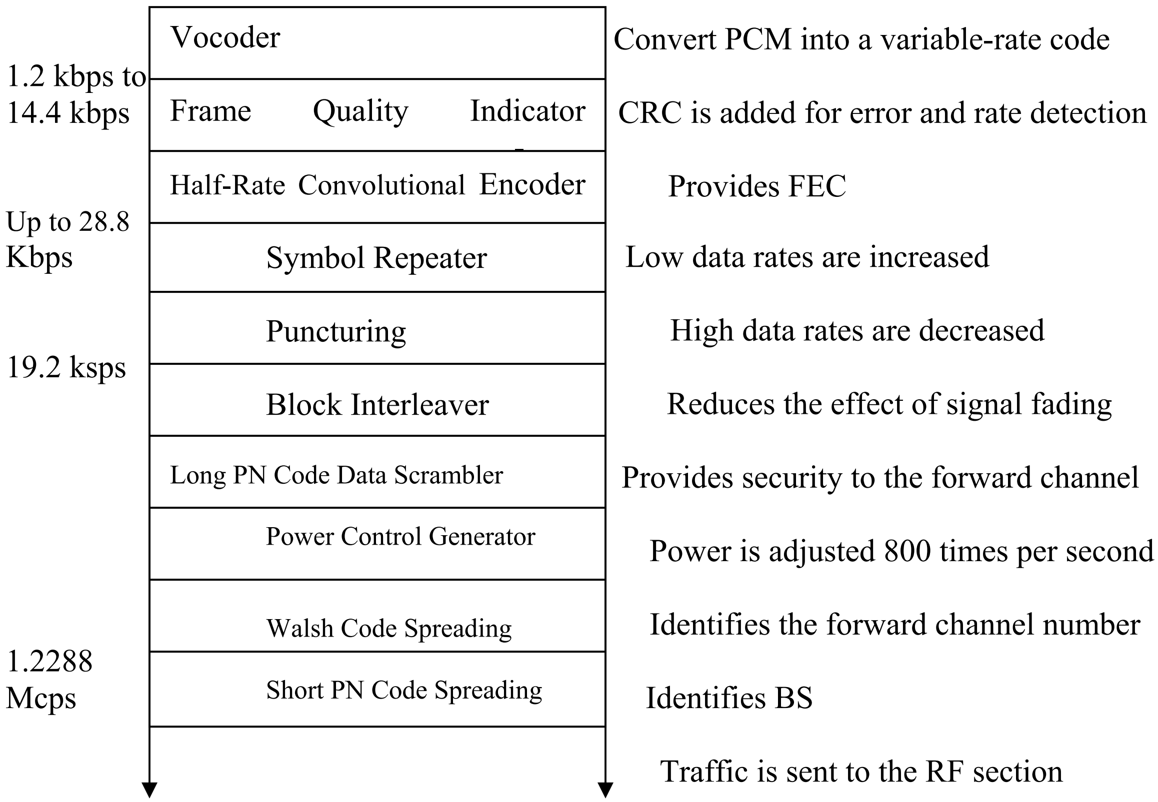

Figure C.1: The functional Diagram of the Forward, Downlink Traffic Channel

The vocoder indicator in figure 4.5 has two sets:

Rate set 1 vocoder will reduce the voice rate down to 1.2 kbps, 2.4 kbps, 4.8 kbps, and 9.6 kbps.

Rate set 2 provides higher quality signal at 1.8 kbps, 3.6 kbps, 7.2 kbps, and 14.4 kbps.

Next is the CRC which allows the receiver to detect errored frames and also determines the rate of the voice signal. The half-rate convolutional encoder doubles the number of bits. The symbol repeater increases the rate of the low-rate signals to the appropriate rate. Here, all rate 1 signals are adjusted to 19.2 ksps and all rate 2 signals are adjusted to 28.8 ksps. The puncturing stage is active only if the rate 2 vocoder is being used. After puncturing, then comes the block interleaver, then the long code, Walsh code, and the short code spreading of this signal. There is also power control generator placed in here. It sends a single bit 800 times per second pre-empting the data stream bits. Depending on the value on this bit, the receiver will either reduce or increase it's transmitted power by 1dB.

The basic operation of the uplink traffic channel is shown in figure 4.6. A 1/2-rate convolutional coder is used for rate set 2 vocoder and 1/3-rate for rate set 1 vocoder. Because rate set 2 has a better voice-quality signal it is not hampered by the lower-quality, 1/2-rate convolutional coder. The Walsh code in this case does not provide any spreading, separation of channels, or identifications as it does in CDMA. It substitutes every 6th symbol with a corresponding 64-bit Walsh code. All 64-bit Walsh codes appear in the bit stream, and the purpose of this processing is to add additional forward error correction. There are 2^{64} possible combinations, and due to error in the air interface, all of these combinations may occur. However, only 64 of those codes are valid combinations. This provides another level of forward error correction. The randomizer compensates for variable-rate transmissions.

	Vocoder	Convert PCM into a variable-rate code.
1.2 kbps to 14.4 kbps	Frame Quality Indicator	CRC is added for error and rate detection.
	Convolutional Encoder	(1/2 or 1/3 rate) Provides FEC.
Up to 28.8 Ksps	Symbol Repeater	Low data rates are increased.
	Block Interleaver	Reduces the effect of signal fading.
28.2 ksps	Walsh Code	Every 6 bits are substituted by 64 bits.
307.2 kcps	Data Burst Randomizer	Provides variable rate transmission.
	Long PN Code Data Scrambler	Identifies the MS.
1.2288 Mpcs	Short PN Code Spreading	Lock the BS to the MS.

Figure C.2: The Functional Diagram of the Reverse, Uplink Traffic Channel.

APPENDIX D

THEOREM 1

For the *M* user RMAWF,

$$\xi_{u0} = \xi_u = \xi_{s0} = \xi_s$$

This equality expression defines the common capacity region and zero-error capacity region ξ as the set of all points $C = (C_1, C_2, ..., C_M)$ such that

$$C_i = p_i \prod_{\substack{j=1 \\ j \neq i}}^{M} (1 - p_j) \qquad (6.3)$$

where $p = (p_1, p_2, ..., p_M)$ is a vector satisfying

$$p \geq 0 \qquad (6.4a)$$

and

$$\sum_{i=1}^{M} p_i = 1 \qquad (6.4b)$$

where each such *C* is determined by a unique such *p*. We remark that conditions (6.4a) and (6.4b) are equivalent to saying that *p* is a *probability vector*. Thus, theorem 1 states that there is a simple one-to-one correspondence between probability vector and points on the outer boundary of ξ.

Region ξ for the *M* = 2 user RMAWF is shown in figure 6.3. For *M* = 2, the probability vector has the form $p = (\gamma, 1-\gamma)$ where $0 \leq \gamma \leq 1$. Equation (6.3) then gives $C_1 = \gamma^2$ and $C_2 = (1-\gamma)^2$.

This shows that the outer boundary of ξ is just the set of all points $C = (C_1, C_2)$ such that $C \geq 0$ and $\sqrt{C_1} + \sqrt{C_2} = 1$.

THEOREM 2

Every open neighborhood of every point on the boundary of the capacity region ξ_s and ξ_{s0} contains achievable rates that also lie on the outer boundary.

It is appropriate to define the symmetric capacity C_{sym} because in a random-access system usually the "symmetric case" raises most interest. For the *M*-user RMAWF it is the maximum rate *r* such that $R = (r/M, r/M, ..., r/M)$ is in ξ. If there is an *r* such that $C = (r/M, r/M, ..., r/M)$ is on the outer boundary of ξ, then $C_{sym} = r$. But, from (6.3) and (6.4), we see that the choice $p = (1/M, 1/M, ..., 1/M)$ gives such a *C*. This proves all but the final part of the following corollary.

COROLLARY TO THEOREM 1

The symmetric capacity of the *M*-user RMAWF with $M \geq 2$ (whether unsynchronized or slot-synchronized and whether for arbitrarily small positive error probability or for zero-error probability) is

$$C_{sym} = (1 - \frac{1}{M})^{M-1} \quad \text{packets/slot} \tag{6.5}$$

Moreover, the rate point $(C_{sym}/M, C_{sym}/M, ..., C_{sym}/M)$ is achieved in the slot – synchronized case. For instance we can calculate:

$$C_{sym} = \begin{cases} 1/2 & M = 2 \\ 4/9 \quad \approx 0.444, & M = 3 \\ \quad\quad \approx 0.3874, & M = 10 \\ \quad\quad \approx 0.3678, & M = 100 \end{cases}$$

Moreover, C_{sym} decreases monotonically as M increases and

$$C_{sym} \to 1/e, \text{as } M \to \infty \tag{6.6}$$

The quantity 1/e is, of course, the well known maximum throughput of the slotted ALOHA algorithm [29] for finitely many identical users. Therefore, (6.6) could perhaps be expected for the slot-synchronized case, although the ALOHA algorithm makes essential use of the feedback that is not present in this model. That (6.6) holds for the unsynchronized case seems truly surprising because the maximum throughput of the "pure" ALOHA algorithm is only ½ e.

We remark here that C_{sym} is also the minimum of $C_1 + C_2 + ... + C_M$ for any point $C = (C_1, C_2, ..., C_M)$ on the outer boundary of ξ. This confirms the intuition about random-access systems which claims that a given total amount of traffic is most difficult to serve when it is equally apportioned among the M tags.

BIBLIOGRAPHY

[1] V. K. Garg, K. Smolik, J. E. Wilkes, Applications of CDMA in Wireless/Personal Communications, Prentice Hall PTR, New Jersey,1997.

[2] T. S. Ramteke, Networks, Prentice Hall, New Jersey, 2001.

[3] M. K. Simon, J. K. Omura, R. A. Scholtz, B. K. Levitt, Spread Spectrum Communications Handbook, McGraw-Hill, Inc., New York, 1994.

[4] T. H. Glisson, Introduction to System Analysis, McGraw-Hill, New York, 1985.

[5] S. D. Senturia, B. D. Wedlock, Electronic Circuits and Applications, John Wiley & Sons, Inc., New York, 1975.

[6] PulsON Technology, "Time Modulated Ultra-Wideband For Wireless Applications", Time Domain Corporation, 2000.

[7] J. Bardwell, "Converting Signal Strength Percentage to dBm Values", WildPackets, Inc., 2002.

[8] R. Bridgelall, "Bluetooth/802.11 Protocol Adaptation for RFID Tags", Symbol Technologies, Research & Development, New York.

[9] M. Loy, "Understanding and Enhancing Sensitivity in Receiver for Wireless Applications", Texas Instruments, 1999.

[10] The Association of the Automatic Identification and Data Capture Industry (AIM), "The Characteristic of RFID-Systems", AIM Frequency Forums, 2000.

[11] MIT Auto-ID Center, "The Electronic Product Code (EPC)", www.eretailnews.com/Features/epc.htm.

[12] Hyperphysics, "Inverse Square, Law", Department of Physics and Astronomy, Georgia State University, Atlanta, Georgia.

[13] www.smartid.com.sg/RFID.htm

[14] H. Vogt, "Multiple Object Identification with Passive RFID Tags", Department of Computer Science Swiss Federal Institute of Technology, Switzerland.

[15] H. Vogt, "Effective Object Identification with Passive RFID Tags", Department of Computer Science Swiss Federal Institute of Technology, Switzerland.

[16] A. Juels[1], R. L. Rivest[2], M. Szydlo[1], "The Blocker Tag: Selective Blocking of RFID Tags for Consumer Privacy", [1]RSA Laboratories, Bedford, [2]Laboratory for Computer Science, MIT Cambridge, USA.

[17] R. Chatterjee, P. Wolfe, S. Park, J. Choi, "Evaluation of using RFID Passive Tags for Monitoring Product Location/Ownership", Arizona State University, Tempe, USA.

[18] Benetton undecided on use of 'smart tags'. Associate Press, 8 April 2003.

[19] R. Shim, "Benetton to Track Clothing with ID Chips", CNET, 11 March 2003. URL: http://news.com.com/2100-1019-992131.html.

[20] J. D. Lindsay, W. Reade, "Cascading RFID Tags", http://www.jefflindsay.com/rfid3.shtml

[21] S. C. Q. Chen[1], V. Thomas[2], "Optimization of Inductive RFID Technology", [1]Department of Electrical Engineering and [2]Center for Energy and Environmental Studies, Princeton University, Princeton, New Jersey, IEEE 2001.

[22] MicroID 13.56 MHz System Design Guide, Microchip Technology Inc. 2001.

[23] P. Lafrance, Fundamental Concepts in Communication, Prentice-Hall, Inc. 1990.

[24] F. Saleh, Cellular Mobile Systems Engineering, Northwood, MA Artech House. 1996.

[25] G. Roberto Aiello, Minnie Ho and Jim Lovette, "*Ultra-Wideband: An emerging technology for wireless communications",* Fantasma Networks, Inc. Paco Alto, U.S.A.

[26] U.S. Patent No. 2,671,896, filed Dec 15, 1942

[27] U.S. Patent No. 3,728632, issued April 17, 1973

[28] R. A. Scholtz, "*Multiple Access with Time-Hopping Impulse Modulation",* (invited paper), MILCOM'93, Bedford, MA, Oct. 11-14, 1993.

[29] J. L. Massey, P. Matthys, "*The Collision Channel Without Feedback",* IEEE Transaction on Information Theory, Vol. IT-31, NO. 2, March 1985

[30] Auto-ID Center "Technical Report 860MHz-930MHz Class 0 Radio Frequency Identification Tag Protocol Specification Candidate Recommendation, Version 1.0.0", Published June 1, 2003.

[31] http://www.rfidjournal.com/

[32] P. Castoldi, Multiuser Detection in CDMA Mobile Terminals, Artech House, Inc., Norwood, MA, 2002.

[33] B. J. Wysocki, T. A. Wysocki, "*Orthogonal Binary Sequence with Wide Range of Correlation Properties*", University of Wollongong, Australia.